

# Dilatation versus self-intersection number for point-pushing pseudo-Anosov homeomorphisms

Spencer Dowdall

February 10, 2019

## Abstract

A filling curve  $\gamma$  on a based surface  $S$  determines a pseudo-Anosov homeomorphism  $\mathcal{P}(\gamma)$  of  $S$  via the process of “point-pushing along  $\gamma$ .” We consider the relationship between the self-intersection number  $i(\gamma)$  of  $\gamma$  and the dilatation  $\lambda_\gamma$  of  $\mathcal{P}(\gamma)$ ; our main result is that  $(i(\gamma) + 1)^{1/5} \leq \lambda_\gamma \leq 9^{i(\gamma)}$ . We also bound the least dilatation of any pseudo-Anosov in the point-pushing subgroup of a closed surface and prove that this number tends to infinity with genus. Lastly, we investigate the minimal entropy of any pseudo-Anosov homeomorphism obtained by pushing along a curve with self-intersection number  $k$  and show that, for a closed surface, this number grows like  $\log(k)$ .

## 1 Introduction

In this paper we consider the entropy generated by “stirring” a surface  $S$  in the following manner. Place a finger on a point  $p \in S$  and smoothly deform the surface by pushing  $p$  along a closed path  $\gamma: [0, 1] \rightarrow S$ ; the resulting homeomorphism of  $S$  mixes the surface just as one stirs a pot of soup. Certainly the amount of entropy introduced in this way depends entirely upon the stirring pattern: pushing along a simple path will have little effect, whereas following a complicated path that winds all over the surface will mix things up in short order. The goal of this paper is to understand *how* the entropy depends on the pushing path.

### Point-pushing homeomorphisms

We begin by formalizing the stirring procedure described above. Throughout,  $S = S_{g,n}$  will denote an oriented, genus  $g$  surface with  $n \geq 0$  punctures. A closed loop  $\gamma: [0, 1] \rightarrow S$  based at  $p = \gamma(0) = \gamma(1)$  defines an “isotopy of maps”  $f_t: \{p\} \rightarrow S$  given by  $f_t(p) = \gamma(t)$ ; this may be extended to an isotopy  $F_t: S \rightarrow S$  of the whole surface that effectively “pushes” the basepoint  $p$  along the path  $\gamma$  and drags the rest of the surface along. The resulting homeomorphism  $\varphi_\gamma = F_1$  is called the *point-pushing homeomorphism* corresponding to the

*pushing curve*  $\gamma$ ; see the discussion in Birman’s book [Bir], where such homeomorphisms are called “spin maps.”

As  $\varphi_\gamma$  is only well-defined up to isotopy, and is freely isotopic to the identity, we are led to consider its mapping class  $[\varphi_\gamma]$  in the *based mapping class group of  $S$* , that is, the group  $\text{Mod}(S, p)$  of  $p$ -fixing isotopy classes of orientation-preserving homeomorphisms of  $S$ . In fact, since this mapping class only depends on the homotopy class of  $\gamma$ , the assignment  $\gamma \mapsto [\varphi_\gamma]$  gives a well-defined, injective group homomorphism

$$\mathcal{P}: \pi_1(S, p) \rightarrow \text{Mod}(S, p) \tag{1.1}$$

called the *point-pushing homomorphism*. Note that when  $\gamma$  is *simple*, i.e., embedded,  $\mathcal{P}(\gamma)$  is just the composition of two Dehn twists (in opposite directions) about the boundary curves of a tubular neighborhood of  $\gamma$ . There is a natural surjection from  $\text{Mod}(S, p)$  onto the non-based mapping class group  $\text{Mod}(S)$  which simply “forgets” about the basepoint  $p$ . Together with  $\mathcal{P}$ , this forms the *Birman exact sequence* [Bir]:

$$1 \longrightarrow \pi_1(S, p) \xrightarrow{\mathcal{P}} \text{Mod}(S, p) \xrightarrow{\text{forget}} \text{Mod}(S) \longrightarrow 1$$

Thus the image of  $\mathcal{P}$  consists precisely of those mapping classes in  $\text{Mod}(S, p)$  that become trivial when one allows isotopies to move the basepoint. This subgroup is called the *point-pushing subgroup* and will be denoted by

$$\text{PP}(S) := \mathcal{P}(\pi_1(S, p)) \leq \text{Mod}(S, p).$$

### Pseudo-Anosov dilatation

A mapping class  $f \in \text{Mod}(S, p)$  exhibits the mixing behavior that interests us precisely if it is *pseudo-Anosov*, meaning that no iterate of  $f$  fixes the isotopy class of any essential 1-submanifold of the surface  $S$  with marked point  $p$ . This *marked surface* will be denoted by  $(S, p)$  to indicate that all isotopies are required to fix the marked point  $p$ . According to the Nielsen–Thurston classification [Thu], any pseudo-Anosov mapping class has a unique representative homeomorphism which respectively stretches and contracts a transverse pair of measured foliations on  $S$  by some stretching factor  $\lambda_f > 1$ ; see also [FLP], [Ber], or [FM]. This stretching factor  $\lambda_f$  is called the *dilatation* of  $f$ ; it is an algebraic integer and an important measure of the dynamical properties of  $f$ . For instance,

- $\log(\lambda_f)$  is the minimal topological entropy of any representative homeomorphism in the mapping class of  $f$ ,
- $\log(\lambda_f)$  is the translation length of the isometric action of  $f$  on the Teichmüller space of  $S$  equipped with the Teichmüller metric; thus  $\log(\lambda_f)$  also represents the length of the geodesic loop corresponding to  $[f]$  in moduli space of hyperbolic structures on  $S$ ,
- for any simple closed curve  $\alpha \subset S$  and any Riemannian metric  $g$  on  $S$ , the length of  $f^k(\alpha)$  grows like  $\lambda_f^k$ ; more precisely,  $\sqrt[k]{l_g(f^k(\alpha))} \rightarrow \lambda_f$  for all  $\alpha$  and  $g$ .

We refer the reader to [FLP] or [FM] for a more thorough discussion of the basic properties of pseudo-Anosov mapping classes.

## Dilatations in $\text{PP}(S)$

In the context of the point-pushing subgroup, there is a simple criterion, due to Kra, that determines whether a pushing loop defines a pseudo-Anosov mapping class. Recall that a closed curve  $\gamma \subset S$  *fills* the surface if every loop that is freely homotopic to  $\gamma$  cuts  $S$  into a union of (possibly punctured) disks. The following is taken from [Kra, Theorem 2’].

**Theorem 1.2** (Kra). *Let  $S = S_{g,n}$  be an orientable surface satisfying  $3g + n > 3$ , and let  $\gamma \in \pi_1(S, p)$  be a closed curve on  $S$ . Then the mapping class  $\mathcal{P}(\gamma) \in \text{Mod}(S, p)$  is pseudo-Anosov if and only if  $\gamma$  fills  $S$ .*

Kra’s theorem says that a pseudo-Anosov element of  $\text{PP}(S)$  must come from a sufficiently complicated pushing curve; an elementary proof of this result is given in §2.6 below. Each free homotopy class of closed curves on  $S$  corresponds to a conjugacy class in  $\pi_1(S, p)$ . As dilatation is a conjugacy invariant, it follows that to the free homotopy class of each filling curve  $\gamma \subset S$  we may assign a number

$$\lambda_\gamma := \text{the dilatation of } \mathcal{P}(\gamma)$$

whose logarithm measures the entropy introduced by stirring the surface along the path  $\gamma$ . We may now rephrase our motivating question as follows.

**Question 1.3.** *How does  $\lambda_\gamma$  depend on the complexity of the filling curve  $\gamma$ ?*

In order to answer Question 1.3, we need a quantitative measure of the complexity of a closed curve. The most natural choice seems to be self-intersection number.

**Definition 1.4** (Self-intersection number). If  $\gamma: S^1 \rightarrow S$  is a closed curve on the surface  $S$ , then the (*geometric*) *self-intersection number* of  $\gamma$  is defined to be the quantity

$$i(\gamma) := \min_{\mu \in [\gamma]} \frac{1}{2} |\{(x, y) \mid x, y \in S^1, x \neq y, \text{ and } \mu(x) = \mu(y)\}|,$$

where the minimum is taken over all closed curves  $\mu$  in the free homotopy class of  $\gamma$ .

Our goal is to relate  $\lambda_\gamma$  and  $i(\gamma)$ . A simple argument shows that, on a fixed surface  $S$ ,

$$\lambda_\gamma \text{ tends to infinity as } i(\gamma) \text{ increases.} \tag{1.5}$$

Indeed, since  $f\mathcal{P}(\gamma)f^{-1} = \mathcal{P}(f(\gamma))$ , we see that  $i(\gamma)$  is a conjugacy invariant of  $\mathcal{P}(\gamma)$  and that (1.5) is a consequence of the following well-known compactness property, which is due to Ivanov [Iva]: There are only finitely many conjugacy classes of pseudo-Anosov elements  $f \in \text{Mod}(S, p)$  with dilatation bounded above by any fixed constant. However, this does not explain *how*  $\lambda_\gamma$  depends on  $i(\gamma)$  nor at what rate  $\lambda_\gamma$  tends to infinity. Our main result addresses these issues by describing an explicit relationship between dilatation and self-intersection number.

**Theorem 1.6.** *Let  $S = S_{g,n}$  be a surface satisfying  $3g + n > 3$ . If  $\gamma: [0, 1] \rightarrow S$  is a filling curve on  $S$ , then the dilatation  $\lambda_\gamma$  of the mapping class  $\mathcal{P}(\gamma)$  satisfies the inequalities*

$$\sqrt[5]{i(\gamma) + 1} \leq \lambda_\gamma \leq 9^{i(\gamma)}$$

*with the following exceptions: If  $S = S_{0,4}$  or  $S_{1,2}$  and  $\gamma$  is the square of a primitive element in  $\pi_1(S)$ , then the lower bound is only  $\lambda_\gamma \geq \sqrt[5]{i(\gamma)}$ . If  $S = S_{1,1}$  and  $\gamma$  is the second, third, or fourth power of a primitive element, then the lower bound is only  $\lambda_\gamma \geq \sqrt[5]{(i(\gamma) + 1)/2}$ .*

We have chosen to work in the context of (possibly) punctured surfaces in order to ease the exposition. However, this result also holds for compact surfaces with boundary; see Remark 2.24.

Surprisingly, these bounds are independent of the surface—they only depend on the geometric complexity of the pushing curve  $\gamma$ . Recalling the context of stirring on a surface, this shows that any stirring path with many self-crossings is guaranteed to generate a lot of entropy and that, in a sense, the entropy is an actual consequence of the complexity of the stirring path.

It is also interesting to consider Question 1.3 in the context of other measures of complexity. For example, the *lower central series*  $\{G_i\}$  and the *derived series*  $\{G^{(i)}\}$  of a group  $G = G_1 = G^{(1)}$  are the recursively defined sequences

$$G_{k+1} = [G_k, G] \quad \text{and} \quad G^{(k+1)} = [G^{(k)}, G^{(k)}],$$

respectively. For non-abelian surface groups  $G = \pi_1(S, p)$ , Malestein and Putman [MP] have related the self-intersection number of a non-trivial element  $\gamma \in G$  to its depth in both the lower central series and the derived series of  $G$ . Combining their results with Theorem 1.6 immediately implies the following corollary.

**Corollary 1.7.** *Let  $S = S_{g,n}$  be a surface satisfying  $3g + n > 5$ , and let  $\gamma \in G = \pi_1(S, p)$  be a loop that fills  $S$ . The following implications hold. (Slightly weaker bounds hold for the three exceptional surfaces  $S_{0,4}$ ,  $S_{1,2}$  and  $S_{1,1}$  in Theorem 1.6.)*

- (1) *If  $\gamma \in G_k$ ,  $k \geq 1$ , then  $\lambda_\gamma \geq (\log_8(k))^{1/5}$ .*
- (2) *If  $\gamma \in G^{(k)}$ ,  $k \geq 3$ , then  $\lambda_\gamma \geq (2^{\lceil k/2 \rceil - 2} + 1)^{1/5} \geq 2^{\frac{k-4}{10}}$ .*
- (3) *Additionally, if  $\gamma \in G_k$ ,  $k \geq 3$ , and  $n \geq 1$ , then  $\lambda_\gamma \geq \left(\frac{k}{4g+n-1}\right)^{1/5}$ .*

## Least dilatations

In addition to studying the dilatation of individual elements, one may also consider the spectrum

$$\text{spec}(A) := \{\log(\lambda_f) \mid f \in A \text{ is pseudo-Anosov}\}$$

of all entropies attained in a particular subset  $A \subseteq \text{Mod}(S)$  (or  $A \subset \text{Mod}(S, p)$ ) of mapping classes. The aforementioned compactness property [Iva] implies that  $\text{spec}(A)$  is a discrete

subset of  $\mathbb{R}$ , a fact which was previously observed by Arnoux and Yoccoz [AY]. Consequently, this spectrum has a least element

$$L(A) := \inf \{\text{spec}(A)\}. \quad (1.8)$$

For example,  $\text{spec}(\text{Mod}(S))$  may be thought of as the length spectrum of closed Teichmüller geodesics in the moduli space of  $S$ , and its least element  $L(\text{Mod}(S))$  represents the minimum entropy of any pseudo-Anosov homeomorphism on  $S$ .

While explicit calculations of  $L(\text{Mod}(S))$  have only been made in a few low-genus examples (see, e.g., [LT] or [Hir]), its asymptotic behavior has been understood for some time. For real-valued functions  $f$  and  $h$ , we write  $f \asymp h$  if the quotient  $f(x)/h(x)$  is uniformly bounded between two positive numbers. For the closed surface  $S_g$  of genus  $g$ , Penner [Pen1] has shown that  $L(\text{Mod}(S_g)) \asymp 1/g$ . In particular, by increasing the genus, it is possible to find pseudo-Anosov elements of  $\text{Mod}(S_g)$  with dilatation arbitrarily close to 1.

Farb, Leininger, and Margalit [FLM] studied the spectrum of dilatations in the Torelli group  $\mathcal{I}_g$ , which is the subgroup of  $\text{Mod}(S_g)$  consisting of mapping classes that act trivially on  $H_1(S_g; \mathbb{Z})$ . Contrasting Penner's result, they proved that  $L(\mathcal{I}_g)$  is universally bounded between 0.197 and 4.127. Since these bounds are independent of genus, this shows that  $L(\mathcal{I}_g) \asymp 1$ .

In light of these results, it is natural to consider the asymptotics of  $L(\text{PP}(S_g))$ . Since point-pushing homeomorphisms act trivially on homology, it is apparent from [FLM] that  $L(\text{PP}(S_g))$  is universally bounded below away from zero. Furthermore, since the self-intersection number of any filling curve  $\gamma \subset S_g$  satisfies

$$i(\gamma) > -\chi(S_g) = 2g - 2, \quad (1.9)$$

one might be tempted to invoke the elementary observation (1.5) and conclude that  $L(\text{PP}(S_g))$  tends to infinity with  $g$ . While this reasoning is invalid, because Ivanov's compactness property only applies to one surface at a time, the following bounds on least dilatation show that the conclusion is nevertheless true.

**Theorem 1.10.** *For the closed surface  $S_g$  of genus  $g \geq 2$ , we have*

$$\frac{1}{5} \log(2g) \leq L(\text{PP}(S_g)) < g \log(11).$$

*In particular,  $L(\text{PP}(S_g))$  tends to infinity with  $g$ .*

Theorem 1.10 proves that the least dilatation in  $\text{PP}(S_g)$  exhibits drastically different behavior than that for the larger Torelli group—any point-pushing pseudo-Anosov on a high-genus surface must have huge dilatation. Interestingly, Theorem 1.10 has the following implication regarding the spectrum of all pseudo-Anosov dilatations of point-pushing homeomorphisms on all closed surfaces.

**Corollary 1.11.** *The infinite union  $\bigcup_{g \geq 2} \text{spec}(\text{PP}(S_g))$  is a discrete subset of  $\mathbb{R}$ .*

This is a marked contrast to the situation for the full mapping class group: although each spectrum  $\text{spec}(\text{Mod}(S_g))$  is discrete, Penner's above result [Pen1], for example, proves that the spectrum  $\bigcup_g \text{spec}(\text{Mod}(S_g))$  of all pseudo-Anosov dilatations contains convergent sequences.

We now consider the dependence of least dilatation on self-intersection number. For a nonnegative integer  $k$ , we define the subset

$$\text{PP}_k(S) := \{\mathcal{P}(\gamma) \mid \gamma \in \pi_1(S) \text{ with } i(\gamma) = k\}$$

of point-pushing homeomorphisms coming from pushing curves with self-intersection number  $k$ . Refining our investigation to this stratification of  $\text{PP}(S)$  leads to the following result, which completely describes the asymptotic dependence of least dilatation on self-intersection number.

**Theorem 1.12.** *Let  $S_g$  be a closed surface of genus  $g \geq 3$ . For any integer  $k \geq 3g - 1$ , we have that*

$$\frac{1}{5} \log(k + 1) \leq L(\text{PP}_k(S_g)) < \log(k) + g \log(11).$$

*In particular, for a closed surface  $S$  of genus at least 3, this shows that  $L(\text{PP}_k(S)) \asymp \log(k)$ .*

## Outline

The theory of train tracks provides a natural means of estimating pseudo-Anosov dilatations. This perspective is investigated in §3, where we describe a completely straightforward procedure to construct an invariant pretrack for any point-pushing homeomorphism; see Proposition 3.3. However, this approach is only partially successful because our methods do not produce a train track in general. Nevertheless, the pretrack  $\tau_\gamma$  is significant because it comes with an explicit incidence matrix  $M_\gamma$  that depends only on the combinatorial structure of  $\gamma$ . In §4, we use this matrix to establish the general upper bound in Theorem 1.6. In the case that  $\tau_\gamma$  is an actual train track, it provides a direct method for calculating the dilatation  $\lambda_\gamma$ . This framework is used in §5 to analyze concrete examples and prove the upper bounds on least dilatations in Theorems 1.10 and 1.12.

The pretrack  $\tau_\gamma$  is not able to provide a general lower bound on dilatation; see Remarks 3.5 and 4.7. Thus, in contrast to our other calculation-based results, the lower bound in Theorem 1.6 presents the primary theoretical difficulty. We prove this inequality in §2 by analyzing the action of  $\mathcal{P}(\gamma)$  on simple closed curves and counting the exponential growth rate of intersection numbers. The technique is to lift everything to the universal cover and control the images of paths by studying the motion of the marked points.

## Acknowledgements

The author would like to thank his advisor, Benson Farb, for suggesting this project and for many insightful conversations on the subject. The author is also grateful to Anna Marie Bohmann for her helpful comments on an earlier draft of this paper.

## 2 A lower bound on dilatation

Our first objective is to establish a general lower bound on the dilatation of a point-pushing pseudo-Anosov map; this will prove the lower bound in Theorem 1.6. The train track approach developed in §3 is inadequate for this purpose because it does not produce a train track in general, but only a pretrack. We instead estimate dilatations by examining the action on simple closed curves. Our primary tool in this endeavor is geometric intersection number.

**Definition 2.1** (Intersection number). Let  $a$  and  $b$  be simple closed curves on a marked surface  $(S, p)$ , and let  $\alpha$  and  $\beta$  denote their respective isotopy classes in  $(S, p)$ ; equivalently, these isotopy classes may be taken in  $S \setminus \{p\}$ . The (*geometric*) *intersection number* of  $a$  and  $b$  is then defined as

$$i(a, b) = \inf \{|a' \cap b'| : a' \in \alpha, b' \in \beta\}.$$

The connection between intersection number and pseudo-Anosov dilatation is made precise by the following theorem of Thurston; for a proof, see [FLP, Theorem 12.2].

**Theorem 2.2** (Thurston). *Let  $f$  be a pseudo-Anosov mapping class with dilatation  $\lambda_f > 1$ . For any two essential, simple closed curves  $a, b \subset (S, p)$ , there is a constant  $c \in (0, \infty)$  for which*

$$\lim_{k \rightarrow \infty} \frac{i(f^k(a), b)}{\lambda_f^k} = c.$$

This theorem says that we may estimate the dilatation of a pseudo-Anosov mapping class by understanding how intersection numbers grow under iteration.

**Assumptions 2.3.** For the remainder of this section, we fix a genus  $g$  surface  $S = S_{g,n}$  with  $n \geq 0$  punctures that satisfies  $3g + n > 3$ . We fix a complete hyperbolic metric on  $S$  and a filling curve  $\gamma \subset S$  that represents a primitive element of  $\pi_1(S)$ ; *primitive* here means that  $\gamma$  cannot be written as a nontrivial power  $\gamma = \mu^m$  in  $\pi_1(S)$ . Upon adjusting  $\gamma$  by a homotopy, we may assume that  $\gamma$  is geodesic and that it realizes the minimum self-intersection number  $i(\gamma) > 0$  in Definition 1.4. Lastly, we fix an essential, geodesic, simple closed curve  $\alpha \subset S$ . Since  $\gamma$  is filling, the curve  $\alpha$  necessarily intersects  $\gamma$  nontrivially.

Choose a basepoint  $p \in \gamma$  with  $p \notin \alpha$  and parameterize  $\gamma: [0, 1] \rightarrow S$  so that  $\gamma(0) = p = \gamma(1)$ . We then have the point-pushing homeomorphism  $\varphi_\gamma$ , which represents the mapping class  $\mathcal{P}(\gamma) \in \text{Mod}(S, p)$ , and we are interested in relating its dilatation  $\lambda_\gamma$  to the self-intersection number  $i(\gamma)$ . The hyperbolic metric gives a locally-isometric universal covering  $\pi: \mathbb{H}^2 \rightarrow S$ , and we fix a preimage  $p_0 \in \pi^{-1}(p)$  to serve as the basepoint of  $\mathbb{H}^2$ . This defines an isometric action by deck transformations of the fundamental group  $G = \pi_1(S, p)$  on  $\mathbb{H}^2$ .

**Strategy.** Our proof of the lower bound now proceeds in several steps. The ultimate goal is to study the images of  $\alpha$  under iteration by  $\varphi_\gamma$  and to count their intersection numbers with other curves on the marked surface  $(S, p)$ . Although it is relatively easy to describe

these iterates using, for instance, the train track theory developed in §3 and §4.1, such representative curves do not aid in calculating intersection numbers because they need not realize the infimum in Definition 2.1; see Remark 4.6.

To get around this difficulty, we lift everything to the universal cover  $\mathbb{H}^2$ , where it will be easier to understand the structure of  $\varphi_\gamma^k(\alpha)$ . As discussed in §2.1, the simple closed curves  $\varphi_\gamma^k(\alpha)$  lift to infinite paths  $\alpha_k$  in  $\mathbb{H}^2$ , and the process of point-pushing on  $S$  lifts to a procedure that we call “weaving” in hyperbolic space. In this setting, our goal is to study the paths  $\alpha_k$  obtained by weaving and to relate their complexity to the self-intersection number  $i(\gamma)$ .

Making these ideas precise involves many technical tools that we develop over the next several subsections. In §2.2 we introduce a tree  $\mathcal{T}$  that will serve as a sort of coordinate system for  $\mathbb{H}^2$ , and in §2.3 we develop the technical devices that will help us navigate through  $\mathcal{T}$ . As we will see in Observation 2.12, bounding the intersection numbers  $i(\varphi_\gamma^k(\alpha), \beta)$  on  $(S, p)$  roughly translates into showing that all paths in the isotopy class of  $\alpha_k$  must cross many edges of  $\mathcal{T}$ .

To prove that this is the case, we develop the notion of a constraint on  $\alpha_k$ ; this is essentially a marked point in  $\mathbb{H}^2$  that forces every path in the isotopy class of  $\alpha_k$  to visit a particular vertex of  $\mathcal{T}$ . The relevant machinery for working with constraints is developed in §2.4; we then give a recursive construction in §2.5 that identifies exponentially many of these points. Finally, in §2.6, we count intersection numbers and establish a lower bound on the dilatation  $\lambda_\gamma$ .

## 2.1 Setting the stage: weaving in hyperbolic space

The first step in our proof is to translate the idea of point-pushing on the surface  $S$  to its analogue in the universal cover  $\mathbb{H}^2$ ; it is in this setting that that we will ultimately be able to understand the iterates of  $\alpha$  and count their intersection numbers.

Recall the construction of  $\varphi_\gamma$  given in §1: the closed curve  $\gamma: [0, 1] \rightarrow S$  defines an isotopy of maps  $\{p\} \rightarrow S$  which we extend to an isotopy of the surface  $F_t: S \rightarrow S$  that “pushes” the marked point  $p$  around  $\gamma$ . At the end of this isotopy one obtains the point-pushing homeomorphism  $\varphi_\gamma = F_1$ . Since we are interested in iterating  $\varphi_\gamma$ , we extend the isotopy  $F_t$ , via the relation  $F_{t+1} = F_t \circ F_1$ , so as to be defined for all times  $t \in \mathbb{R}$ ; with this convention we have that  $\varphi_\gamma^k = F_k$  for all  $k \in \mathbb{Z}$ . We henceforth fix the isotopy  $F_t$  and homeomorphism  $\varphi_\gamma$  for the duration of §2.

Lifting this picture to the universal cover yields an isotopy  $\tilde{F}_t: \mathbb{H}^2 \rightarrow \mathbb{H}^2$  between the identity and a homeomorphism  $\tilde{\varphi}_\gamma$  which covers  $\varphi_\gamma$ . We think of  $\tilde{\varphi}_\gamma$  as a “weaving homeomorphism” for reasons which will soon be evident.

In attempts to avoid the confusing situation of “moving” the basepoint  $p$  throughout the point-pushing procedure, we introduce the notion of a dynamic marked point. The basepoint  $p \in S$  remains stationary while the isotopy  $F_t$  instead pushes the marked point around  $\gamma$ . Thus the marked point’s location at time  $t$  is given by  $F_t(p)$ , and this location agrees with the basepoint if and only if  $t$  is an integer.

Throughout we will suppress the distinction between a path  $\beta: [0, 1] \rightarrow S$  and its image  $\beta = \beta([0, 1]) \subset S$ ; paths that differ by a reparameterization will not be considered distinct.

A *lift* of a closed loop  $\beta: \mathbb{R}/\mathbb{Z} \rightarrow S$  is any path  $\tilde{\beta}: \mathbb{R} \rightarrow \mathbb{H}^2$  that cyclically covers  $\beta$ ; if  $\beta$  is a simple loop, then its lifts are exactly the connected components of  $\pi^{-1}(\beta)$ . We denote the set of lifts of  $\gamma$  by

$$\Gamma = \{\tilde{\gamma} \subset \mathbb{H}^2 \mid \tilde{\gamma}: \mathbb{R} \rightarrow \mathbb{H}^2 \text{ covers } \gamma: \mathbb{R}/\mathbb{Z} \rightarrow S\}. \quad (2.4)$$

Since  $\gamma$  is a geodesic loop, the elements of  $\Gamma$  are infinite geodesic lines. We will use the following notation to discuss lifts of paths to  $\mathbb{H}^2$ .

**Notation 2.5.** If  $\eta: [0, 1] \rightarrow S$  is a path in  $S$  starting at a point  $x_0 = \eta(0)$ , then for any preimage  $x \in \pi^{-1}(x_0)$  we let  ${}_x\eta$  denote the unique lift  $\tilde{\eta}: [0, 1] \rightarrow \mathbb{H}^2$  of  $\eta$  for which  $\tilde{\eta}(0) = x$ . Thus  ${}_x\eta$  is a path in  $\mathbb{H}^2$  which starts at  $x$  and goes to the point  ${}_x\eta(1)$ ; we denote this other endpoint by  $x \cdot \eta$ . A deck transformation  $g \in G$  acts on such a path by changing the starting point:  $g({}_x\eta) = {}_{gx}\eta$ .

If we consider loops based at  $x_0$ , then the pairing  $(x, \eta) \mapsto x \cdot \eta$  defines a right action of  $\pi_1(S, x_0)$  on the set  $\pi^{-1}(x_0)$ , that is,  $(x \cdot \eta) \cdot \mu = x \cdot (\eta\mu)$  for  $\eta, \mu \in \pi_1(S, x_0)$ . This right action commutes with the left action of  $g \in G$  in the sense that  $g(x \cdot \eta) = (gx) \cdot \eta$ . For a loop  $\eta \subset S$  without a natural basepoint,  ${}_x\eta$  is understood to mean  ${}_x\hat{\eta}$ , where  $\hat{\eta}: [0, 1] \rightarrow S$  is any parameterization of  $\eta$  based at  $\hat{\eta}(0) = \pi(x) \in \eta$ .

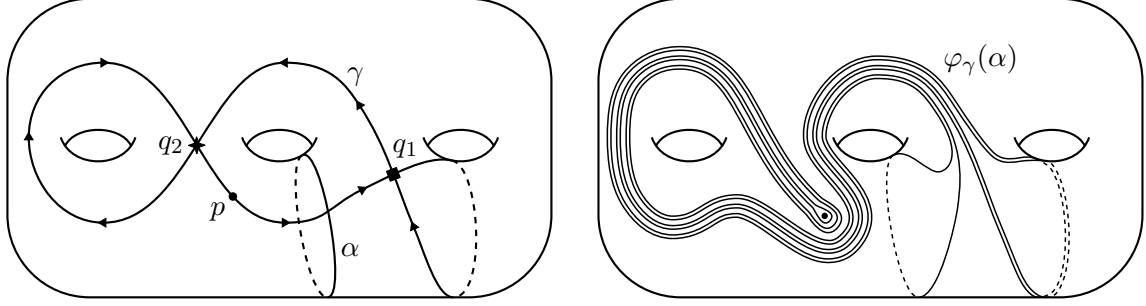
On the surface,  $F_t$  pushes the marked point  $p$  along the curve  $\gamma$ . Therefore, in the universal cover, we consider each preimage  $x \in \pi^{-1}(p)$  to be a marked point of  $\mathbb{H}^2$  and find that  $\tilde{F}_t$  has the effect of pushing  $x$  along the path  ${}_x\gamma$  to the point  $x \cdot \gamma$ . Since  $\gamma$  has self-intersections, each of its lifts  $l \in \Gamma$  intersects infinitely many other lifts. Thus the full preimage  $\pi^{-1}(\gamma)$  is an infinite grid of intersecting geodesics, and the isotopy  $\tilde{F}_t$  simultaneously pushes all of the marked points along their corresponding lifts in an intertwining pattern that resembles weaving on an infinite loom.

We are concerned with the images of our geodesic, simple closed curve  $\alpha \subset S$  under iteration by  $\varphi_\gamma$ . Since  $i(\alpha, \gamma) > 0$ , every lift of  $\alpha$  intersects some lift of  $\gamma$ , and we choose a particular lift  $\tilde{\alpha}$  that intersects the segment  ${}_{p_0}\gamma$ , where  $p_0$  is the chosen basepoint of  $\mathbb{H}^2$ . We denote this particular lift by  $\alpha_0$ , and denote its image under  $\tilde{F}_t$  by

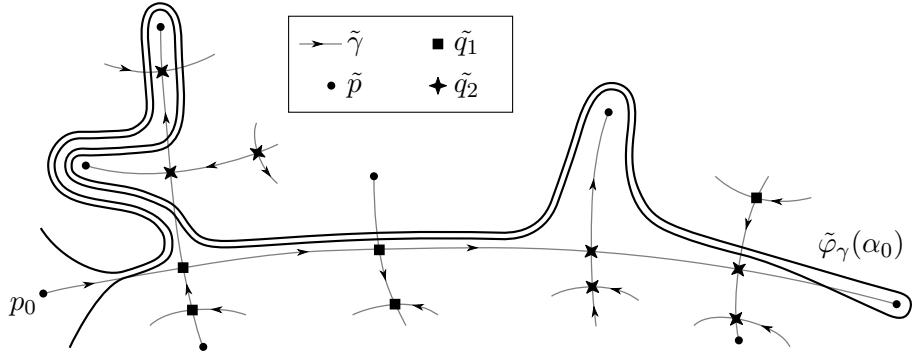
$$\alpha_t = \tilde{F}_t(\alpha_0).$$

The closed curves  $\varphi_\gamma^k(\alpha)$  naturally live in the marked surface  $(S, p)$ , and the paths  $\alpha_k$  naturally live in the marked space  $(\mathbb{H}^2, \pi^{-1}(p))$ . Throughout we will use this notation to indicate that all isotopies are required to fix the set  $\pi^{-1}(p)$  pointwise; equivalently, one may think of the punctured space  $\mathbb{H}^2 \setminus \pi^{-1}(p)$ . In the unmarked setting,  $\varphi_\gamma^k(\alpha)$  and  $\alpha_k$  are clearly isotopic to  $\alpha$  and  $\alpha_0$ . Since  $\tilde{F}_t$  and  $\alpha_0$  cover  $F_t$  and  $\alpha$ , respectively, it follows that  $\pi(\alpha_k) = \varphi_\gamma^k(\alpha)$ ; therefore we may use the paths  $\alpha_k \subset (\mathbb{H}^2, \pi^{-1}(p))$  to study the iterates  $\varphi_\gamma^k(\alpha) \subset (S, p)$  of  $\alpha$ .

Given explicit choices of  $\alpha$  and  $\gamma$ , it is relatively straightforward to determine  $\varphi_\gamma(\alpha)$  and  $\tilde{\varphi}_\gamma(\alpha_0)$ : simply move the marked points along their respective paths and push  $\alpha$  or  $\alpha_0$  along. An illustrative example is depicted in Figure 1. Here we consider a (non-filling) pushing



(a) A pushing curve  $\gamma$  with  $i(\gamma) = 2$ , and a simple closed curve  $\alpha \subset S_2$ . (b) Push  $p$  once around  $\gamma$  to obtain  $\varphi_\gamma(\alpha)$ .



(c) Lift to  $\mathbb{H}^2$ : The marked points  $\tilde{p}$  simultaneously slide along the lines  $\tilde{\gamma}$  and push the initial lift  $\alpha_0 = \tilde{\alpha}$ . The resulting path is  $\tilde{\varphi}_\gamma(\alpha_0)$ .

**Figure 1:** An example of point-pushing on  $S_3$  and weaving in  $\mathbb{H}^2$ .

curve  $\gamma \subset S_3$  with two self-intersection points  $q_i$  and a simple closed curve  $\alpha$  that intersects  $\gamma$  exactly once. As one can check, pushing the marked point once around  $\gamma$  transforms  $\alpha$  into the curve  $\varphi_\gamma(\alpha)$  shown in Figure 1(b). In the universal cover, all of the marked points  $\tilde{p} \in \pi^{-1}(p)$  flow simultaneously along the lines  $\tilde{\gamma}$  comprising the grid  $\pi^{-1}(\gamma)$ . As they travel, some of these points interact with the lift  $\alpha_0$  and drag it along with them. The resulting path  $\tilde{\varphi}_\gamma(\alpha_0)$ , as shown in Figure 1(c), is forced to bend around these marked points.

This example exhibits the following key features. The curve  $\varphi_\gamma(\alpha) \subset (S, p)$  is already quite complicated—the marked point is pushing nine strands of  $\varphi_\gamma(\alpha)$ , and it is difficult to keep track of which strand is which and how it got there. The structure is more transparent when one unwinds things in the universal cover; here we see that these nine strands come from different parts of  $\mathbb{H}^2$  and are being pushed in diverging directions by multiple marked points.

This essential observation is the foundation of our entire argument: On the surface there is only one marked point, but in the universal cover there are many marked points pushing the curve  $\alpha_t$  in various directions. By identifying these marked points and keeping track of their locations, we will be able to quantify the complexity of  $\varphi_\gamma^k(\alpha)$ , estimate intersection numbers, and establish a lower bound on dilatation. To formalize these ideas, we need a more careful definition of the marked points.

**Definition 2.6** (Marked point). A *marked point* in  $\mathbb{H}^2$  is a function  $\rho: \mathbb{R} \rightarrow \mathbb{H}^2$  of the form  $\rho(t) = \tilde{F}_t(\tilde{p})$ , where  $\tilde{p} \in \pi^{-1}(p)$  is any lift of the basepoint. The set of marked points is denoted by  $\mathcal{M}$ . The *location* of a marked point  $\rho \in \mathcal{M}$  at a time  $t \in \mathbb{R}$  is simply its value  $\rho(t)$ , and the set of all these locations is denoted by  $\mathcal{M}_t = \{\rho(t) \mid \rho \in \mathcal{M}\}$ .

While marked points are ostensibly geodesic paths in  $\mathbb{H}^2$ , we prefer to think of them as dynamic points that physically move with respect to time. To recall the path-like nature of a marked point  $\rho \in \mathcal{M}$ , we may simply consider its image  $\rho(\mathbb{R})$ , which is a geodesic in  $\Gamma$ .

In order to establish a precise notion of “pushing  $\alpha_t$ ” and to find marked points that have this property, it will be important to keep track of the locations of the marked points and their relative positions to each other. To this end, we construct a tree that will serve as a sort of coordinate system for  $\mathbb{H}^2$ . This tree and its properties are the business of the next subsection.

## 2.2 Uniform divergence in the coordinate tree $\mathcal{T}$

Choose a pants decomposition  $\mathcal{C}$  of  $S$ , that is, a maximal collection  $\mathcal{C} = \{c_i\}$  of homotopically distinct, disjoint, essential, simple closed curves  $c_i \subset S$ . Any such collection contains exactly  $3g - 3 + n > 0$  curves; in particular, our assumption on  $S = S_{g,n}$  ensures that  $\mathcal{C}$  is nonempty. Assuming that the  $c_i$  are geodesic, the connected components of  $\tilde{\mathcal{C}} = \pi^{-1}(\mathcal{C})$  are geodesic lines that cut  $\mathbb{H}^2$  into infinitely many components. Dual to this decomposition of  $\mathbb{H}^2$  there is a tree  $\mathcal{T} = \mathcal{T}_{\mathcal{C}}$  whose vertices  $v \in V(\mathcal{T})$  are the connected components of  $\mathbb{H}^2 \setminus \tilde{\mathcal{C}}$  and whose oriented edges  $e \in E(\mathcal{T})$  are ordered pairs  $e = (v_0, v_1)$  of vertices that share a boundary component.<sup>1</sup> This same edge with the reverse orientation will be denoted by  $\bar{e} = (v_1, v_0)$ . The unoriented edges of  $\mathcal{T}$  are in bijective correspondence with the components of  $\tilde{\mathcal{C}}$ ; accordingly, we will often suppress the distinction between edges in  $\mathcal{T}$  and these geodesics through  $\mathbb{H}^2$ . To emphasize: the vertices and edges of  $\mathcal{T}$  will often be thought of as subsets of  $\mathbb{H}^2$ .

An oriented *edge path* in  $\mathcal{T}$  is a (possibly bi-infinite) ordered list  $(e_1, \dots, e_n)$  of oriented edges  $e_i \in E(\mathcal{T})$  satisfying the condition that the terminal vertex of  $e_i$  is the initial vertex of  $e_{i+1}$ . An edge path is *geodesic* if it is without backtracking, that is, if  $e_{i+1} \neq \bar{e}_i$  for each  $i$ . The definition of  $\mathcal{T}$  implies that it is in fact a tree, meaning that there is a unique geodesic between any two vertices. The *length* of a finite edge path  $e = (e_1, \dots, e_n)$  is denoted by  $l_{\mathcal{C}}(e) = n$ ; this defines a path metric on  $\mathcal{T}$ . The action of  $G$  on  $\mathbb{H}^2$  descends to an isometric action on  $\mathcal{T}$ , and there is a natural,  $G$ -equivariant projection  $\sigma: \mathbb{H}^2 \rightarrow \mathcal{T}$  that collapses components of  $\mathbb{H}^2 \setminus \tilde{\mathcal{C}}$  and  $\tilde{\mathcal{C}}$  to vertices and edges, respectively. Since a non-elliptic isometry of  $\mathbb{H}^2$  can preserve at most one geodesic line, we see that the fixed set in  $\mathcal{T}$  of a nontrivial deck transformation  $g \in G$  contains at most a single edge.

Any oriented path  $\mu \subset \mathbb{H}^2$  that is transverse to  $\tilde{\mathcal{C}}$  projects to an edge path in  $\mathcal{T}$ . If  $\mu$  is a geodesic path, then so is  $\sigma(\mu)$ , and we use  $l_{\mathcal{C}}(\mu)$  to denote  $l_{\mathcal{C}}(\sigma(\mu))$ . The  $\mathcal{T}$ -length of a loop  $\beta \subset S$  is similarly defined by  $l_{\mathcal{C}}(\beta) = l_{\mathcal{C}}(\sigma(x\beta))$ , where  $x \in \pi^{-1}(\beta)$  is any point that projects

---

<sup>1</sup>Note that  $\mathcal{T}$  is just the Bass–Serre tree for the graph of groups description of  $\pi_1(S)$  corresponding to the pants decomposition  $\mathcal{C}$  of  $S$ ; see, for example, [SW].

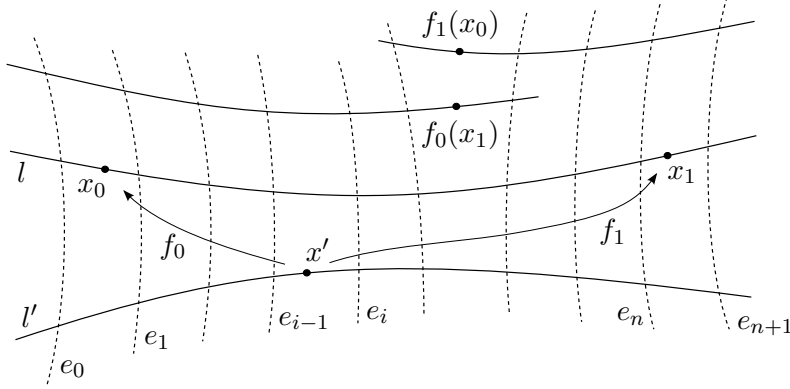


**Figure 2:** The two edge paths  $\sigma(l)$  and  $\sigma(l')$  cannot overlap too much, for otherwise the deck transformation sending  $f_0(x_1)$  to  $f_1(x_0)$  would fix two edges of  $\mathcal{T}$ .

to  $\beta$ . With this notation,  $l_{\mathcal{C}}(\gamma) = \sum_i i(\gamma, c_i)$  is the number of times the loop  $\gamma$  crosses the curves in  $\mathcal{C}$ . Since  $\gamma$  fills  $S$ , we have that  $l_{\mathcal{C}}(\gamma) \geq |\mathcal{C}| \geq 1$ .

The negative curvature of  $\mathbb{H}^2$  implies that distinct geodesics  $l, l' \subset \mathbb{H}^2$  diverge when projected to  $\mathcal{T}$  in the sense that they determine distinct edge paths. Nevertheless, these projections may agree along an arbitrarily long edge path. The following crucial lemma shows that, for geodesics in the equivariant family  $\Gamma$  defined in (2.4), divergence in  $\mathcal{T}$  happens uniformly quickly.

**Lemma 2.7** (Uniform divergence). *Let  $l, l' \in \Gamma$  be two distinct lifts of  $\gamma$ , and let  $X = \sigma(l) \cap \sigma(l')$  be the intersection of their projections to  $\mathcal{T}$ . Then  $X$  is a (possibly empty or degenerate) geodesic edge path of length  $l_{\mathcal{C}}(X) \leq l_{\mathcal{C}}(\gamma) + 1$ . In the case that  $l_{\mathcal{C}}(\gamma) \leq 2$ , this bound may be improved to  $l_{\mathcal{C}}(X) \leq l_{\mathcal{C}}(\gamma)$ .*

*Proof.* Suppose, on the contrary, that  $l_{\mathcal{C}}(X) \geq n + 2$ , where  $n = l_{\mathcal{C}}(\gamma)$ . Then  $X$  contains a subpath of the form  $(e_0, e_1, \dots, e_n, e_{n+1})$ . Writing  $e_j = (v_j, v_{j+1})$ , we choose a generic point  $x_0 \in l$  that is contained in  $v_1$  and does not project to a self-intersection point of  $\gamma$  on  $S$ . Since points in the  $G$ -orbit of  $x_0$  occur with spacing  $l_{\mathcal{C}}(\gamma) = n$  along both  $l$  and  $l'$ , we may find such points  $x_1 \in l$  and  $x' \in l'$  with  $x_1 \in v_{n+1}$  and  $x' \in v_i$  for some  $1 \leq i \leq n$ . The situation is depicted in Figure 2. Letting  $f_0, f_1 \in G$  be the deck transformations defined by  $f_j(x') = x_j$ , we see that  $g = f_1 f_0^{-1}$  acts by a hyperbolic translation along  $l$  sending  $x_0$  to  $x_1$ . Since  $f_j^{-1}(l) = l' \neq l$ , the isometry  $f_j$  does not preserve the axis  $l$  of  $g$  and therefore cannot commute with  $g$ :  $f_j g \neq g f_j$ .

The orientation on  $\gamma: [0, 1] \rightarrow S$  lifts to natural orientations on  $l$  and  $l'$  which in turn induce orientations on  $X$ . We may assume that  $l$  induces the orientation  $(e_0, \dots, e_{n+1})$  on  $X$ , so that the path  $_{x_0}\gamma$  crosses the edges  $e_1, e_2, \dots, e_n$  in order.

**Case 1:** *The geodesic  $l'$  induces the opposite orientation on  $X$ .* In this case, the path  $_{x'}\gamma$  crosses the edges  $\overline{e_{i-1}}, \overline{e_{i-2}}, \dots$  in order. Consequently, since  $f_0$  maps  $_{x'}\gamma$  equivariantly onto  $_{x_0}\gamma$ , we see that  $f_0(\overline{e_{i-1}}, \overline{e_{i-2}}, \dots, \overline{e_0}) = (e_1, e_2, \dots, e_i)$ . In particular, we have  $f_0(\overline{e_0}) = e_i$ . Reversing direction and considering the first edges crossed by the paths  $_{x_0}\bar{\gamma}$  and  $_{x'}\bar{\gamma}$ , where  $\bar{\gamma}$

denotes  $\gamma$  with the opposite orientation, we similarly find that  $f_0(e_i) = \bar{e}_0$ . As  $G = \pi_1(S)$  is torsion-free, this implies that  $f_0^2$  is a non-trivial deck transformation preserving the distinct edges  $\bar{e}_0$  and  $e_i$ —a contradiction.

**Case 2.** *The geodesics  $l$  and  $l'$  induce the same orientation on  $X$ .* We now have that  $_{x'}\gamma$  and  $_{x'}\bar{\gamma}$  project to the edge paths  $(e_i, e_{i+1}, \dots)$  and  $(\bar{e}_{i-1}, \bar{e}_{i-2}, \dots)$ , respectively. As  $f_0$  maps  $_{x'}\gamma$  equivariantly onto  $_{x_0}\gamma$ , we see that  $f_0((e_i, \dots, e_{n+1})) = (e_1, \dots, e_{n+2-i})$ . In particular  $f_0((e_n, e_{n+1})) = (e_{n+1-i}, e_{n+2-i})$ . Similarly, we have  $f_1((\bar{e}_{i-1}, \dots, \bar{e}_0)) = (\bar{e}_n, \dots, \bar{e}_{n+1-i})$ , so that  $f_1((\bar{e}_1, \bar{e}_0)) = (\bar{e}_{n+2-i}, \bar{e}_{n+1-i})$ . Therefore

$$f_0g((e_0, e_1)) = f_0((e_n, e_{n+1})) = (e_{n+1-i}, e_{n+2-i}) = f_1((e_0, e_1)).$$

Since  $f_1 = gf_0$ , this shows that the distinct deck transformations  $f_0g$  and  $gf_0$  both send  $e_0 \mapsto e_{n+1-i}$  and  $e_1 \mapsto e_{n+2-i}$ , which is impossible.

It remains to prove the stronger inequality in the case that  $n = l_C(\gamma) \leq 2$ . We proceed as above assuming only that  $X$  contains a subpath of the form  $(e_0, \dots, e_n)$ ; the setup and notation are otherwise unchanged. The arguments in Case 1 are still valid because they do not involve the edge  $e_{n+1}$ . Thus it suffices to assume that  $l$  and  $l'$  induce the same orientation on  $X$ . The case  $x' \in v_1$  then yields an immediate contradiction because  $f_0$  cannot preserve both  $e_0$  and  $e_1$ . The remaining possibility  $x' \notin v_1$  necessitates  $n = 2$  and  $x' \in v_2$ , in which case we find that  $f_1$  sends  $(\bar{e}_1, \bar{e}_0)$  to  $(\bar{e}_2, \bar{e}_1)$  and that  $f_0^{-1}$  sends  $(e_0, e_1)$  to  $(e_1, e_2)$ . It now follows that  $f_1f_0((e_1, e_2)) = f_1((e_0, e_1)) = (e_1, e_2)$ , contradicting the fact that  $f_1f_0$  is nontrivial.  $\square$

## 2.3 $\Gamma$ -chains and grid paths

The marked points travel through  $\mathbb{H}^2$  along the geodesic lines  $l \in \Gamma$ , and they pass each other at the intersections of these lines. In order to describe the locations and interactions of the marked points that push  $\alpha_t$ , we will need to consider paths in  $\mathbb{H}^2$  that travel along geodesics in  $\Gamma$  and potentially turn at their intersections. These turning paths will lead us to the desired marked points and show that many such points exist.

**Definition 2.8** (Grid path). A *grid path* is a concatenation  $\mu = \mu_1 \cdots \mu_n$  of oriented geodesic segments  $\mu_i \subset l_i \in \Gamma$  whose endpoints “match up,” that is, the terminal endpoint of  $\mu_i$  is the initial endpoint of  $\mu_{i+1}$ . The  $\mu_i$  are called the *straight segments* of  $\mu$ , and we require that adjacent segments  $\mu_i$  lie on distinct geodesics  $l_i$ .

While a grid path may backtrack in  $\mathcal{T}$  when it turns at the junction of two geodesic segments, the extent of this backtracking is universally bounded by Lemma 2.7. Therefore, by making the straight segments sufficiently long, we may effectively disregard any backtracking and ensure that the grid path progresses through  $\mathcal{T}$  at a reliable rate. The following definitions and lemma make this precise.

**Definition 2.9** ( $\Gamma$ -chain). A  $\Gamma$ -*chain* is an ordered tuple  $(l_1, \dots, l_n)$  of distinct geodesics  $l_i \in \Gamma$  which satisfy the property that  $l_i$  and  $l_j$  intersect if and only if  $|i - j| \leq 1$ .

**Definition 2.10** (Internal edge). An *internal edge* of a finite geodesic segment  $\mu \subset \mathbb{H}^2$  is simply an edge  $e \in E(\mathcal{T})$  whose removal separates  $\sigma(\mu)$  into two edge paths of length at least  $l_{\mathcal{C}}(\gamma) + 1$ . In the case that  $l_{\mathcal{C}}(\gamma) \leq 2$ , we only require these pieces to have length at least  $l_{\mathcal{C}}(\gamma)$ . In either case,  $\mu$  contains internal edges provided that  $l_{\mathcal{C}}(\mu) \geq 3l_{\mathcal{C}}(\gamma)$ .

**Lemma 2.11** (Long grid paths). *Let  $\mu = \mu_1 \cdots \mu_n$  be a grid path with endpoints  $x, y \in \mathbb{H}^2$ , and let  $l_i \in \Gamma$  be the geodesic containing  $\mu_i$ . If  $l_{\mathcal{C}}(\mu_i) \geq 3l_{\mathcal{C}}(\gamma)$  for each  $1 < i < n$ , then  $(l_1, \dots, l_n)$  is a  $\Gamma$ -chain and the  $\mathcal{T}$ -geodesic from  $\sigma(x)$  to  $\sigma(y)$  contains every internal edge of each segment  $\mu_i$ .*

*Proof.* We first prove the second claim. Note that  $\mu_i$  necessarily contains an internal edge when  $1 < i < n$ . The first and last segments  $\mu_1$  and  $\mu_n$  need not have internal edges, but the claim applies if such edges do exist. Let  $M$  denote the relevant upper bound from Lemma 2.7, so  $M$  is either  $l_{\mathcal{C}}(\gamma) + 1$  or  $l_{\mathcal{C}}(\gamma)$  depending on whether or not  $l_{\mathcal{C}}(\gamma) > 2$ . The edge path  $\sigma(\mu)$  connects  $\sigma(x)$  to  $\sigma(y)$  and would be a  $\mathcal{T}$ -geodesic except for the fact that backtracking may occur when the geodesic segments  $\sigma(\mu_i)$  are concatenated. Upon removing all such backtracking by successively cancelling edge pairs  $(\dots, e, \bar{e}, \dots)$ , we will obtain the desired  $\mathcal{T}$ -geodesic. Every edge that is removed because of backtracking at the junction of  $\mu_i$  with  $\mu_{i+1}$  must be contained in both  $\sigma(\mu_i)$  and  $\sigma(\mu_{i+1})$ . In light of Lemma 2.7, it follows that each junction  $\sigma(\mu_i)\sigma(\mu_{i+1})$  can result in at most  $M$  cancellations. Since internal edges are, by definition, separated from these junctions by at least  $M$  edges on either side, they cannot be involved in any cancellation. The claim follows.

As for the first assertion, it suffices to show that  $\sigma(l_i)$  and  $\sigma(l_j)$  are disjoint whenever  $|i - j| \geq 2$ . If this is not the case, there is a vertex  $v \in \sigma(l_i) \cap \sigma(l_j)$  for some  $i + 1 \leq j - 1$ . Consider the shortened grid path  $\mu_{i+1} \cdots \mu_{j-1}$  from  $x'$  to  $y'$ . Let  $a$  and  $b$  be internal edges of  $\mu_{i+1}$  and  $\mu_{j-1}$ , respectively; such internal edges exist because  $1 < i + 1 \leq j - 1 < n$ . Since  $a$  is separated from  $x'$  by at least  $M$  edges, the fact that  $l_{\mathcal{C}}(\sigma(l_i) \cap \sigma(\mu_{i+1})) \leq M$  implies  $a \notin \sigma(l_i)$ . We similarly have  $b \notin \sigma(l_j)$ . By inducting on  $|i - j|$ , we may furthermore assume that  $a \notin \sigma(l_j)$  and  $b \notin \sigma(l_i)$ ; this is possible because the base case  $|i - j| = 2$  allows one to choose  $a = b$ . We now see that  $\sigma(l_i) \cup \sigma(l_j)$  contains an edge path from  $\sigma(x')$  through  $v$  to  $\sigma(y')$  that avoids both  $a$  and  $b$ . Applying the second assertion to the grid path  $\mu_{i+1} \cdots \mu_{j-1}$  yields a contradiction.  $\square$

## 2.4 The tools for weaving

We return to the task of finding marked points that “push”  $\alpha_t$ , where  $\alpha_t = \tilde{F}_t(\alpha_0)$  is the image of our initial lift  $\alpha_0$  at time  $t$ . In this subsection we formalize the notion of pushing and provide the necessary tools for working with these points. The sought-after points will be described explicitly in the next subsection.

These considerations involve infinite paths in  $\mathbb{H}^2$  and their images under isotopies of  $\mathbb{H}^2$ . Notice that isotopies of  $\mathbb{H}^2$  move points a bounded distance and therefore fix the boundary at infinity  $\partial\mathbb{H}^2$  pointwise. In particular, if  $\mu: \mathbb{R} \rightarrow \mathbb{H}^2$  is path with two endpoints at infinity, then these endpoints remain fixed throughout all isotopies.

We henceforth assume that the pants decomposition  $\mathcal{C}$  is chosen to contain our simple closed curve  $\alpha \subset S$ . In this case,  $\alpha_0$  is a component of  $\tilde{\mathcal{C}}$  and corresponds to an edge of  $\mathcal{T}$ ; this edge  $\sigma(\alpha_0)$ , together with its adjacent vertices, will be denoted by  $\varepsilon_0 \subset \mathcal{T}$ .

Let  $G_{\varepsilon_0} \leq G$  be the stabilizer of  $\varepsilon_0$  in  $G$ , that is,  $G_{\varepsilon_0} = \{g \in G \mid g(\varepsilon_0) = \varepsilon_0\}$ . This is a cyclic subgroup consisting of hyperbolic isometries that act by translation along the geodesic axis  $\alpha_0 \subset \mathbb{H}^2$ . If  $\mu \subset S$  is any simple loop isotopic to  $\varphi_\gamma^k(\alpha)$  in the marked surface  $(S, p)$ , then  $\mu$  has a particular lift  $\tilde{\mu} \subset \mathbb{H}^2$  which is isotopic to  $\alpha_k$  in  $(\mathbb{H}^2, \pi^{-1}(p))$ , namely, the lift whose endpoints in  $\partial\mathbb{H}^2$  agree with the endpoints of  $\alpha_k$ , which are also the endpoints of  $\alpha_0$ . Choose any two points  $x \in \alpha_0$  and  $y \in \tilde{\mu}$ . Since  $\mu$  is isotopic to  $\alpha$  in  $S$ , the two deck transformations defined by  $x \mapsto x \cdot \alpha$  and  $y \mapsto y \cdot \mu$  are equal; indeed, every  $g \in G_{\varepsilon_0}$  preserves the lift  $\tilde{\mu}$  and acts as a translation  $y \mapsto y \cdot \mu^n$  along  $\tilde{\mu}$ . It follows that  $\tilde{\mu}$  projects to a simple closed loop  $G_{\varepsilon_0}\tilde{\mu}$  in the quotient space  $X = G_{\varepsilon_0} \backslash \mathbb{H}^2$  that bijectively covers  $\mu$  in  $S$ . Each intersection point  $y \in \mu \cap \mathcal{C}$  with a pants curve  $c_i$  then lifts to a unique intersection point of the loop  $G_{\varepsilon_0}\tilde{\mu}$  with a coset  $G_{\varepsilon_0}\tilde{c}_i \subset X$ . This has the following implication:

**Observation 2.12.** Let  $\mu \subset S$  be a simple closed curve that is isotopic to  $\varphi_\gamma^k(\alpha)$  in  $(S, p)$  (or, equivalently, in  $S \setminus \{p\}$ ), and let  $\tilde{\mu}$  be the unique lift whose endpoints agree with those of  $\alpha_k$ . Assuming  $\mu$  is transverse to  $\mathcal{C}$ , the cardinality of  $\mu \cap \mathcal{C}$  is equal to the number of edges that the loop  $G_{\varepsilon_0}\sigma(\tilde{\mu})$  crosses in the quotient graph  $G_{\varepsilon_0} \backslash \mathcal{T}$ . That is,  $|\mu \cap \mathcal{C}|$  is equal to the number of  $G_{\varepsilon_0}$ -cosets of edges that  $\tilde{\mu}$  crosses in  $\mathcal{T}$ . Therefore, in order to estimate the intersection number

$$i(\varphi_\gamma^k(\alpha), \mathcal{C}) := \sum_i i(\varphi_\gamma^k(\alpha), c_i) = \inf_\mu |\mu \cap \mathcal{C}|,$$

it suffices to vary  $\mu$  in the isotopy class of  $\varphi_\gamma^k(\alpha)$  and bound the number of cosets of edges that  $\tilde{\mu}$  crosses in  $\mathcal{T}$ .

It is now apparent that we should consider paths that are isotopic to  $\alpha_k$  and study their projections to  $\mathcal{T}$ . For a given  $t \in \mathbb{R}$  and a subset  $V \subseteq \mathcal{M}$ , let  $[\alpha_t]_V$  denote the isotopy class of the path  $\alpha_t$  in  $(\mathbb{H}^2, V_t)$ , where  $V_t = \{\rho(t) \mid \rho \in V\}$  is the set of locations of those marked points in  $V$ . Equivalently,  $[\alpha_t]_V$  is the isotopy class of  $\alpha_t$  in  $\mathbb{H}^2 \setminus V_t$ . This isotopy class is obtained by simply “forgetting” some of the marked points at time  $t$ , but one may alternately think of forgetting these points at time 0 and pushing the initial path  $\alpha_0$  by a modified isotopy that only moves those marked points in  $V$ . The resulting path is a representative of  $[\alpha_t]_V$ .

Recall that the vertices and edges of  $\mathcal{T}$  are defined to be subsets of  $\mathbb{H}^2$ ; in particular, it makes sense to say that a path  $\mu \subset \mathbb{H}^2$  intersects a vertex  $v \in V(\mathcal{T})$ . More generally, any subset  $A \subset \mathcal{T}$  may be thought of as a subset of  $\mathbb{H}^2$  by looking at the preimage  $\sigma^{-1}(A) \subset \mathbb{H}^2$ . This identification will be used implicitly in the sequel.

For a subset  $X \subseteq \mathbb{H}^2$  (or  $X \subseteq \mathcal{T}$ ), we say that  $[\alpha_t]_V$  *intersects*  $X$  if every path in the isotopy class intersects  $X$ . Otherwise, there is a representative path that avoids  $X$  and we say that  $[\alpha_t]_V$  is *disjoint from*  $X$ . Since every path that is isotopic to  $\alpha_t$  in  $(\mathbb{H}^2, \mathcal{M}_t)$  lies in the isotopy class  $[\alpha_t]_V$ , we see that if  $[\alpha_t]_V$  intersects  $X$ , then so does  $[\alpha_t]_{\mathcal{M}}$ . Furthermore,

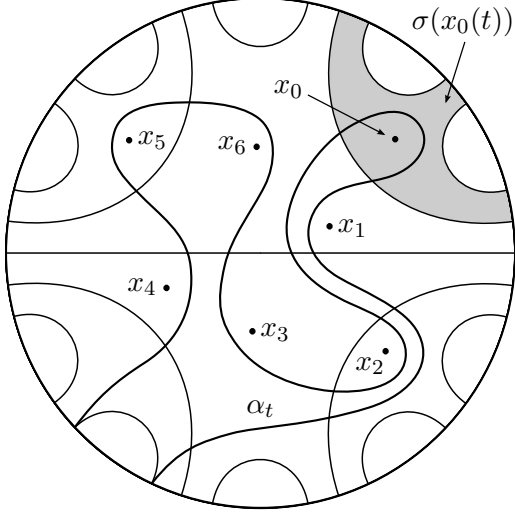


**Figure 3:** The marked point  $x_0$  constrains  $[\alpha_t]_{\{x_0, \dots, x_6\}}$  because the path  $\alpha_t$  is isotopically forced to intersect the vertex  $\sigma(x_0(t)) \in \mathcal{T}$ .

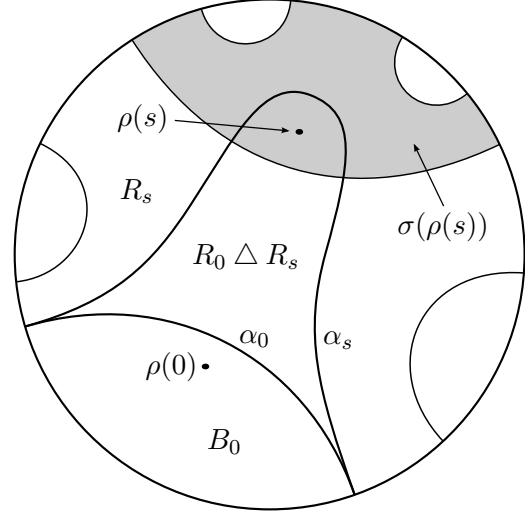


**Figure 4:** Proving Proposition 2.14: The marked point  $\rho$  necessarily constrains  $[\alpha_s]_{\{\rho\}}$ .

the endpoints of  $\alpha_0$  in  $\partial\mathbb{H}^2$  remain fixed throughout all isotopies so that  $[\alpha_t]_V$  intersects the base edge  $\varepsilon_0 \subset \mathcal{T}$  for all times  $t$  and all subsets  $V \subseteq \mathcal{M}$ . Our goal is to show that, as time progresses,  $[\alpha_t]_V$  intersects larger and larger subsets of  $\mathcal{T}$ .

**Definition 2.13** (Constraining points). Let  $V \subseteq \mathcal{M}$  be a set of marked points containing a marked point  $\rho$ , and let  $t \geq 0$  be a real number. We say that  $\rho$  *constrains*  $[\alpha_t]_V$  if  $[\alpha_s]_V$  intersects  $\sigma(\rho(s)) \in \mathcal{T}$  for all times  $s \geq t$ . In this case, every path in  $[\alpha_s]_V$  projects onto (a superset of) the unique  $\mathcal{T}$ -geodesic connecting  $\sigma(\rho(s))$  to  $\varepsilon_0$ . See Figure 3 for an illustration.

The first thing to check is that such points exist. Recall that  $\alpha_0$  was chosen specifically so that it intersects the path  ${}_{p_0}\gamma$  starting at the basepoint  $p_0 \in \mathbb{H}^2$ ; it follows that  ${}_{hp_0}\gamma = h({}_{p_0}\gamma)$  intersects  $\alpha_0 = h(\alpha_0)$  for every  $h \in G_{\varepsilon_0}$ .

**Proposition 2.14** (Initial constraining points). *For a fixed  $h \in G_{\varepsilon_0}$ , let  $\rho \in \mathcal{M}$  be the marked point whose position at time  $t$  is given by  $\rho(t) = \tilde{F}_t(h\rho_0)$ . Then  $\rho$  constrains  $[\alpha_1]_{\{\rho\}}$ .*

*Proof.* Fix a time  $s \geq 1$ . After forgetting about all other marked points and adjusting the pushing isotopy  $\tilde{F}_t$  accordingly, we may assume that  $\alpha_s$  represents an arbitrary path in the isotopy class  $[\alpha_s]_{\{\rho\}}$ . By the Jordan Curve Theorem, each path  $\alpha_t$  divides  $\mathbb{H}^2$  into two path connected components, which we denote by  $R_t$  and  $B_t$  for the “red” and “blue” sides, respectively. These names are assigned consistently in  $t$  so that they are preserved by the pushing isotopy, that is,  $\tilde{F}_t(B_0) = B_t$ . Assuming that  $\rho$  initially lies in the blue side, we have that  $\rho(t) \in B_t$  for all  $t$ . Since the path  $\rho([0, 1]) = {}_{hp_0}\gamma$  intersects  $\alpha_0$ , the marked point  $\rho$  evidently crosses over  $\alpha_0$  during the time interval  $[0, 1]$ . Recalling that  $\sigma(\rho(s)) \in \mathcal{T}$  is a subset of  $\mathbb{H}^2$ , we have that  $\rho(s) \in R_0$  and  $\sigma(\rho(s)) \subseteq R_0$  at time  $s$ ; see Figure 4.

The symmetric difference of  $R_0$  and  $R_s$  is contained in a bounded neighborhood of  $\alpha_0$  because isotopies only move points a bounded distance; on the other hand,  $\sigma(\rho(s))$  contains

points that are arbitrarily far from  $\alpha_0$ . Therefore, by avoiding the symmetric difference, it is possible to choose a point  $z \in \sigma(\rho(s)) \cap R_s$ . The fact that  $\rho(s) \in B_s$  and  $z \in R_s$  lie in opposite components of  $\mathbb{H}^2 \setminus \alpha_s$  implies that every path from  $\rho(s) \in \sigma(\rho(s))$  to  $z \in \sigma(\rho(s))$  must intersect  $\alpha_s$ . Since  $\sigma(\rho(s))$  is path connected, this shows that  $\alpha_s$  intersects  $\sigma(\rho(s))$ .  $\square$

Once there are some constraints on  $\alpha_t$ , the weaving pattern of the marked points creates more in a recursive manner. The relevant interaction occurs when a marked point  $x_1$  *passes in front of* another marked point  $x_2$ , meaning that the intersection  $x_1(\mathbb{R}) \cap x_2(\mathbb{R}) = \{y\}$  is a single point and that  $x_1$  reaches  $y$  before  $x_2$ . Thus the times defined by  $x_i(t_i) = y$  satisfy  $t_1 < t_2$ . The basic intuition is this: if  $x_1$  constrains  $\alpha_t$  while it passes in front of  $x_2$ , then it drags  $\alpha_t$  across the path in front of  $x_2$ . Since  $\alpha_t$  is now blocking its way,  $x_2$  is forced to push  $\alpha_t$  ahead as it progresses through  $\mathbb{H}^2$ .

To make this inductive step precise, we formulate it in the context of  $\mathcal{T}$ . Suppose that  $x_1$  passes in front of  $x_2$ , and let  $X = \sigma(x_1(\mathbb{R})) \cap \sigma(x_2(\mathbb{R}))$  be the intersection of their  $\mathcal{T}$ -geodesics; according to Lemma 2.7,  $X$  contains at most  $l_{\mathcal{C}}(\gamma) + 1$  edges. For a time  $s$ , consider the two rays  $x_j(\mathbb{R}_{\leq s})$ , where  $\mathbb{R}_{\leq s} = \{t \in \mathbb{R} \mid t \leq s\}$ ; we think of these rays as “tails” connecting the marked points  $x_j$  to  $\partial\mathbb{H}^2$ . We say that  $x_1$  and  $x_2$  have *diverged in  $\mathcal{T}$  at time  $s$*  if  $X$  separates each ray  $\sigma(x_i(\mathbb{R}_{\leq s}))$  into two connected components, neither of which is a single vertex. Since  $\sigma(x_2(t_2)) = \sigma(y) \in X$  and the marked points cross  $l_{\mathcal{C}}(\gamma)$  edges of  $\mathcal{T}$  per unit time, each time  $s \geq t_2 + 2$  satisfies this criterion.

Assuming this is the case, choose any two edges  $e, e' \in E(\mathcal{T})$  in opposite components of  $\sigma(x_1(\mathbb{R})) \setminus X$  and consider their relationship to the geodesic ray  $\eta = x_2(\mathbb{R}_{\leq s})$ . Thinking of  $\eta$  as a wall or a barrier, it is apparent that the only way to get from  $e$  to  $e'$  is to “go around” the marked point  $x_2(s)$  at the end of  $\eta$ . More precisely, any path  $\mu \subset \mathbb{H}^2 \setminus \eta$  that intersects both  $e$  and  $e'$  must also intersect  $\sigma(x_2(s))$ ; see Figure 5. The purpose of the next lemma is to prove that  $\eta$  enjoys this same separation property on the level of isotopy classes of paths.

**Lemma 2.15** (Tails separate). *Suppose that the marked point  $\rho$  passes in front of another marked point  $x$  and that they have diverged in  $\mathcal{T}$  by time  $s$ . Let  $V \subset \mathcal{M}$  be a finite set of marked points that contains  $x$ , and let  $\eta = x(\mathbb{R}_{\leq s})$  be the tail of  $x$ . If  $e \in E(\mathcal{T})$  is any edge in the infinite component of  $\sigma(\rho(\mathbb{R}_{\leq s})) \setminus \sigma(x(\mathbb{R}))$ , then  $\eta$  separates  $\rho(s)$  from  $e$  in the following sense: If the isotopy class  $[\alpha_s]_V$  intersects both  $\sigma(\rho(s))$  and  $e$  but is disjoint from  $\eta$ , then  $[\alpha_s]_V$  also intersects  $\sigma(x(s))$ .*

*Proof.* Let  $\eta' = x(\mathbb{R}_{\geq s})$  be the future ray of  $x$  and let  $\tilde{c} \in E(\mathcal{T})$  be the boundary component of  $\sigma(x(s))$  that intersects  $\eta$ . The fact that  $x$  and  $\rho$  have diverged in  $\mathcal{T}$  implies that  $\tilde{c}$  is disjoint from  $\sigma(\rho(\mathbb{R}))$ . Recalling that  $\tilde{c}$  is a geodesic component of  $\tilde{\mathcal{C}}$ , it follows from the Jordan Curve Theorem that  $\tilde{c}$  divides  $\mathbb{H}^2$  into two components, one containing  $\eta'$  and the other containing both  $\sigma(\rho(s))$  and  $e$ . Since every path in  $\mathbb{H}^2$  that intersects both  $\sigma(\rho(s))$  and  $\eta'$  must intersect  $\tilde{c}$  and, consequently,  $\sigma(x(s))$ , it suffices to show that  $[\alpha_s]_V$  intersects  $\eta'$ . Supposing this is not the case, there is a representative path  $\mu_0 \in [\alpha_s]_V$  that is disjoint from  $\eta'$ . The situation is illustrated in Figure 6.

Compactify  $\mathbb{H}^2 \setminus V_s$  by adding the boundary  $\partial\mathbb{H}^2 = S^1$  at infinity and removing a small open disk about each puncture point  $y \in V_s$ . The resulting space  $W$  is then a compact,

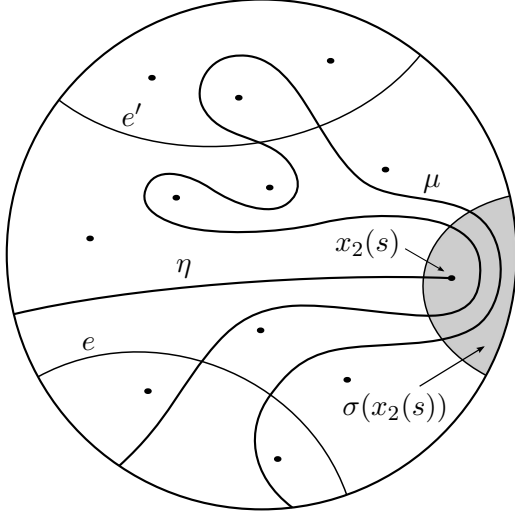


**Figure 5:**  $\eta$  separates  $e$  from  $e'$ : any path that intersects  $e$  and  $e'$  must go through  $\sigma(x_2(s))$ .

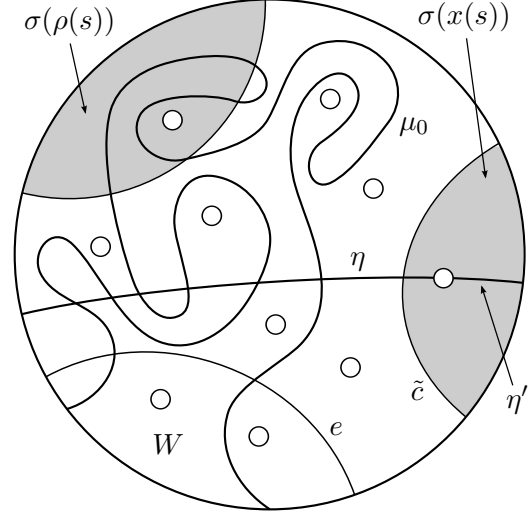


**Figure 6:** The representative arc  $\mu_0 \in [\alpha_t]_V$  is isotopically disjoint from  $\eta \cup \eta'$  in  $W$ .

genus zero surface with finitely many boundary components. An *arc* in  $W$  is a continuous injection  $\beta: [0, 1] \rightarrow W$  with  $\beta^{-1}(\partial W) = \{0, 1\}$ ; all isotopies of arcs are required to fix the boundary pointwise. The rays  $\eta$  and  $\eta'$  now define disjoint arcs in  $W$ , and  $[\alpha_s]_V$  becomes an isotopy class of arcs in  $W$  of which  $\mu_0$  is a representative arc.

Again by the Jordan Curve Theorem, the union  $\eta \cup \eta'$  separates  $W$  into two path connected components, and the choice of  $e$  ensures that  $\sigma(\rho(s))$  and  $e$  are contained in opposite components of  $W \setminus (\eta \cup \eta')$ . We produce an arc  $\mu$  that is isotopic to  $\mu_0$  but disjoint from both  $\eta$  and  $\eta'$ , contradicting the hypothesis that  $\mu \in [\alpha_s]_V$  necessarily intersects both  $\sigma(\rho(s))$  and  $e$ . To find such an arc, we invoke a basic fact from surface topology. Two transverse arcs  $a$  and  $b$  in  $W$  form a *bigon* if the two subarcs  $a_0 \subset a$  and  $b_0 \subset b$  between a pair of intersection points bound an embedded disk in  $W$ . Such a disk  $D \subset W$  provides an isotopy that pulls the subarc  $a_0$  across  $D$ , replaces it with an arc parallel to  $b_0$ , and thereby reduces the cardinality of  $a \cap b$  by 2. The *bigon criterion* is essentially a converse to this observation.

**Fact (Bigon criterion).** *Two transverse simple arcs  $a$  and  $b$  minimize the cardinality of  $a \cap b$  in their isotopy classes if and only if they do not form any bigons.*

A proof of the bigon criterion for simple closed curves is given in [FM, Proposition 1.3]; as per the discussion in [FM, §1.5], this result also holds in the context of simple arcs on a surface with boundary. Indeed, their argument goes through verbatim with straightforward modifications to account for the fact that a lift of an arc  $a$  to the universal cover does not cyclically cover  $a$  but rather covers it bijectively.

We now complete the proof. By transversality and compactness, we may assume that  $\mu_0 \cap \eta$  is either empty or a finite number of points. By assumption,  $\mu_0$  and  $\eta$  are isotopically disjoint in  $W$ , thus the bigon criterion implies that they may be made disjoint by successively pulling  $\mu_0$  across bigons. Since  $\eta$  and  $\eta'$  are disjoint, this procedure does not introduce any

intersections with  $\eta'$ . The result is an arc  $\mu \in [\alpha_s]_V$  that is disjoint from both  $\eta$  and  $\eta'$ .  $\square$

In order to apply Lemma 2.15 inductively, we need to identify marked points  $x \in \mathcal{M}$  and subsets  $V \subset \mathcal{M}$  for which the tail  $\eta = x(\mathbb{R}_{\leq s})$  is disjoint from  $[\alpha_s]_V$ . This is easily accomplished by ensuring that the marked points in  $V$  never cross the ray  $x(\mathbb{R}_{\leq t})$ .

**Lemma 2.16** (Finding disjoint tails). *Let  $V = (y_1, \dots, y_n, x) \subset \mathcal{M}$  be a finite set of marked points, and suppose that  $(y_1(\mathbb{R}), \dots, y_n(\mathbb{R}), x(\mathbb{R}))$  is a  $\Gamma$ -chain. If  $y_n$  passes in front of  $x$  and  $[\alpha_0]_V$  is disjoint from  $x(\mathbb{R})$ , then, at each time  $t \geq 0$ ,  $[\alpha_t]_V$  is disjoint from the ray  $x(\mathbb{R}_{\leq t})$ .*

The result will follow easily from the following basic principle.

**Claim.** *Let  $[s, s']$  be a time interval, and let  $U \subset \mathbb{H}^2$  be a connected open set with the property that for each  $\rho \in V$ , the image  $\rho([s, s'])$  is either contained in  $U$  or is disjoint from the closure of  $U$ . If  $[\alpha_s]_V$  is disjoint from  $U$ , then  $[\alpha_t]_V$  is disjoint from  $U$  for all  $t \in [s, s']$ .*

*Proof of Claim.* The isotopy of  $\mathbb{H}^2$  that pushes the marked points in  $V$  may be taken to be the identity away from the marked points, that is, off of an open neighborhood of  $\cup_{\rho \in V} \rho([s, s'])$ . In particular, we may assume that this isotopy is the identity on  $\partial U$  throughout the time interval  $[s, s']$ . Applying this isotopy to a representative path  $\mu \in [\alpha_s]_V$  that is disjoint from  $U$ , we see that each isotopy class  $[\alpha_t]_V$  has a representative that is disjoint from  $\partial U$  and therefore from  $U$ .  $\square$

*Proof of Lemma 2.16.* Let  $t_1, t_2 \in \mathbb{R}$  be the times defined by  $y_n(t_1) = z = x(t_2)$ , where  $\{z\} = y_n(\mathbb{R}) \cap x(\mathbb{R})$ . The hypothesis on passing is that  $t_1 < t_2$ , and we choose a point  $t_0 \in (t_1, t_2)$ . Assuming that  $t_0 > 0$ , let  $U$  be a small open neighborhood of  $x(\mathbb{R}_{\leq t_0})$  whose closure is disjoint from  $y_n(\mathbb{R})$  and  $[\alpha_0]_V$ . The chain condition implies that, for  $i < n$ , the marked point  $y_i$  avoids the closure of  $U$  throughout all of time. Since  $x$  remains inside  $U$  during the interval  $[0, t_0]$ , the above claim implies that  $[\alpha_t]_V$  is disjoint from  $U$ , and thus from  $x(\mathbb{R}_{\leq t})$ , for each time  $t \in [0, t_0]$ . In the case that  $t_0 \leq 0$ , we simply note that the hypotheses ensure that  $[\alpha_0]_V$  is disjoint from  $x(\mathbb{R}_{\leq 0})$ .

It remains to consider a time  $t \geq s_0 = \max\{t_0, 0\}$ . At time  $s_0$ ,  $y_n$  has already crossed  $x(\mathbb{R})$ ; thus there is no obstruction to sliding any intersections of  $[\alpha_{s_0}]_V$  with  $x(\mathbb{R}_{\geq s_0})$  forward along  $x(\mathbb{R})$  to obtain a representative path  $\mu \in [\alpha_{s_0}]_V$  that is disjoint from  $x(\mathbb{R}_{\leq t})$ . Enlarging  $U$  to a neighborhood  $U'$  of  $x(\mathbb{R}_{\leq t})$ , we find that  $[\alpha_{s_0}]_V$  is disjoint from  $U'$  and that all of the marked points  $y_i$  avoid  $U'$  throughout the interval  $[s_0, t]$ . A second application of the claim now shows that  $[\alpha_t]_V$  is disjoint from  $x(\mathbb{R}_{\leq t})$ .  $\square$

## 2.5 The points that push

The stage is set: we have developed the navigational tools and built up the machinery for pushing in the universal cover  $\mathbb{H}^2$ . Everything is in place to exhibit exponentially many marked points that constrain  $[\alpha_t]_{\mathcal{M}}$ .

Recall our pushing curve  $\gamma: [0, 1] \rightarrow S$ , which is a geodesic loop based at  $\gamma(0) = p$ . For each self-intersection point  $q \in S$  of  $\gamma$ , we may form the decomposition  $\gamma = \beta_q \delta_q \nu_q$ , where

$\beta_q$  is the initial segment of  $\gamma$  from  $p$  to  $q$ ,  $\delta_q$  is the subsequent loop based at  $q$ , and  $\nu_q$  is the final segment from  $q$  back to  $p$ . Skipping over the loop  $\delta_q$  at  $q$ , we form the concatenation  $\tau_q = \beta_q\nu_q$ . This is a piecewise geodesic loop based at  $p$  that goes straight in the forward direction along  $\gamma$ , turns at  $q$ , and continues along  $\gamma$  to  $p$ ; accordingly, we refer to  $\tau_q$  as the “turn at  $q$ .” More explicitly, if  $0 < t_{q1} < t_{q2} < 1$  are the two preimage points in  $\gamma^{-1}(q)$ , then  $\tau_q: [0, 1] \rightarrow S$  may be parameterized as

$$\tau_q(t) = \begin{cases} q, & t_{q1} \leq t \leq t_{q2} \\ \gamma(t), & \text{otherwise.} \end{cases}$$

Let  $\mathcal{W} = \{\gamma\} \cup \left(\bigcup_q \{\tau_q\}\right) \subset \pi_1(S, p)$  be the collection consisting of the straight loop  $\gamma$  and these  $i(\gamma)$  turns. We will find marked points that constrain  $[\alpha_t]_{\mathcal{M}}$  by following paths in  $\mathbb{H}^2$  built out of the elements in  $\mathcal{W}$ . Every turn  $\tau_q$  in  $\mathcal{W}$  lifts to a grid path in  $\mathbb{H}^2$  that initially follows along a geodesic lift  $l \in \Gamma$  and then turns onto a new geodesic lift  $l' \in \Gamma$ . Moreover, these paths concatenate nicely so that every word  $\omega_1 \cdots \omega_n$  in the letters  $\omega_i \in \mathcal{W}$  lifts to a grid path  $\mu = {}_x(\omega_1 \cdots \omega_n)$ , regardless of the starting point  $x \in \pi^{-1}(p)$ . When  $\mu$  is decomposed  $\mu = \mu_1 \cdots \mu_j$  as a grid path, the number  $j$  of straight segments is one more than the number of turns in  $\mu$ , that is,  $j - 1 = |\{i : \omega_i \neq \gamma\}|$ . In order to apply the theory we have developed, we need to consider grid paths whose straight segments define  $\Gamma$ -chains. According to Lemma 2.11, this may be accomplished by “padding” the word  $\omega_1 \cdots \omega_n$  with copies of  $\gamma$  in order to ensure that the straight segments are long enough.

**Proposition 2.17** (The points). *Let  $k \geq 1$  be an integer, and let  $h \in G_{\varepsilon_0}$  be a deck transformation that preserves the base edge  $\varepsilon_0$ . Set  $\omega_1 = \gamma$ , and choose loops  $\omega_2, \dots, \omega_k \in \mathcal{W}$ . For  $1 \leq i \leq k$ , let  $x_i \in \mathcal{M}$  be the marked point whose location at time  $5i$  is given by*

$$x_i(5i) = (hp_0) \cdot [(\gamma^2\omega_1\gamma^2) \cdots (\gamma^2\omega_i\gamma^2)].$$

*If  $V = \{x_1, \dots, x_k\} \subset \mathcal{M}$ , then  $x_k$  constrains  $[\alpha_{5k}]_V$  and, in particular,  $[\alpha_{5k}]_{\mathcal{M}}$ .*

*Proof.* For notational convenience, we let  $x_0 \in \mathcal{M}$  denote the marked point whose initial location is  $x_0(0) = hp_0$ . Notice that the marked points  $x_i$  are defined so that

$$x_{i+1}(5i+5) = ((hp_0) \cdot [(\gamma^2\omega_1\gamma^2) \cdots (\gamma^2\omega_i\gamma^2)]) \cdot (\gamma^2\omega_{i+1}\gamma^2) = x_i(5i) \cdot (\gamma^2\omega_{i+1}\gamma^2).$$

Since the marked point  $x_i$  travels from  $x_i(5i)$  to  $x_i(5i) \cdot \gamma^5$  during the time interval  $[5i, 5i+5]$ , choosing  $\omega_{i+1} = \gamma$  results in the equation  $x_{i+1}(5i+5) = x_i(5i+5)$ . As distinct marked points cannot be at the same place at the same time, this shows that choosing  $\omega_{i+1} = \gamma$  is equivalent to setting  $x_{i+1} = x_i$ .

We proceed by induction on  $k$ , starting with the case  $k = 1$  and  $V = \{x_1\}$ . The assignment  $\omega_1 = \gamma$  ensures that  $x_1 = x_0$  so that  $V = \{x_0\}$ . Proposition 2.14 now shows that  $x_1 = x_0$  constrains  $[\alpha_1]_V$  and, consequently,  $[\alpha_5]_V$ .

For  $k > 1$ , we inductively assume that the marked point  $x_{k-1}$  constrains  $[\alpha_{5(k-1)}]_{V'}$ , where  $V' = \{x_1, \dots, x_{k-1}\}$ . Since  $5(k-1) \leq 5k$  and  $V' \subseteq V = \{x_1, \dots, x_k\}$ , this implies that  $x_{k-1}$

constrains  $[\alpha_{5k}]_V$ . We must show that  $x_k$  constrains  $[\alpha_{5k}]_V$  as well. The result is immediate if  $x_k = x_{k-1}$ , so it suffices to consider the case  $\omega_k \neq \gamma$ .

Each index  $i \geq 2$  with  $\omega_i = \gamma$  results in repeated entries in the list  $x_1, \dots, x_k$ ; upon deleting all neighboring repeats, we obtain an ordered list  $y_1, \dots, y_j$  of marked points  $y_i \in \mathcal{M}$  that satisfy  $y_i \neq y_{i+1}$  and  $\{y_1, \dots, y_j\} = V$ . Here  $k-j$  is the number of indices  $i \in \{2, \dots, k\}$  for which  $\omega_i = \gamma$ .

The path  $\mu =_{hp_0} [(\gamma^2\omega_1\gamma^2) \cdots (\gamma^2\omega_k\gamma^2)]$  defines a grid path in  $\mathbb{H}^2$  that may be decomposed as a concatenation  $\mu = \mu_1 \cdots \mu_n$  of geodesic segments  $\mu_i$  along lifts  $l_i \in \Gamma$  of  $\gamma$  that satisfy  $l_i \neq l_{i+1}$ . The number  $n$  of straight segments  $\mu_i$  in this decomposition is equal to  $1+m$ , where  $m = |\{1 \leq i \leq k : \omega_i \neq \gamma\}|$  is the number of turns in  $\mu$ . Noting that  $k-j = (k-m)-1$ , we find that  $j = n$ . It is clear from the definitions that the marked points  $x_1, \dots, x_k$  travel along the straight segments of  $\mu$ . Upon reindexing them as  $y_1, \dots, y_j$ , the resulting marked point  $y_i$  travels along the geodesic  $y_i(\mathbb{R}) = l_i$  containing the segment  $\mu_i$ . Indeed, since each turn  $\tau_q$  along  $\mu$  results in both a new segment  $\mu_i$  and a distinct marked point  $y_i$ , this follows inductively from the observation that  $y_1(\mathbb{R}) = l_1$ .

The assumption  $x_k \neq x_{k-1}$  implies that  $x_k = y_j$  and  $x_{k-1} = y_{j-1}$ . The geodesics  $x_{k-1}(\mathbb{R})$  and  $x_k(\mathbb{R})$  intersect by definition, and we claim that  $x_{k-1}$  passes in front of  $x_k$ . Indeed, suppose that  $\omega_k = \tau_q = \beta_q\nu_q$  is the concatenation of the two geodesic segments  $\beta_q$  and  $\nu_q$ . It then takes  $t_{q1}$  time units for a marked point to travel across  $\beta_q$  and  $(1-t_{q2})$  time units to cross  $\nu_q$ , where  $t_{q1} < t_{q2}$  are the two preimages of  $q$  under  $\gamma$ . Since  $x_k(5k) = x_{k-1}(5k-5) \cdot \gamma^2\beta_q\nu_q\gamma^2$ , we see that

$$x_{k-1}(5k-5+2+t_{q1}) = x_k(5k-2-(1-t_{q2})).$$

Therefore  $x_{k-1}$  does pass in front of  $x_k$  because  $5k-3+t_{q1} < 5k-3+t_{q2}$ .

Each straight segment  $\mu_i$ , with  $1 < i < j$ , has length  $l_C(\mu_i) \geq 3l_C(\gamma)$  because there are at least four copies of  $\gamma$  between any two turns along  $\mu$ . Therefore  $\mu = \mu_1 \cdots \mu_j$  satisfies the hypotheses of Lemma 2.11, and it follows that  $(l_1, \dots, l_j)$  is a  $\Gamma$ -chain. Moreover, the proof of Lemma 2.11 shows that  $\sigma(l_1)$  and  $\sigma(l_j)$  are disjoint if  $j > 2$ . Since  $\sigma(\mu_1)$  contains the base edge  $\alpha_0$  of  $\mathcal{T}$ , this shows that  $l_j$  and  $\alpha_0$  are disjoint when  $j > 2$ . While  $\sigma(\mu_1) \cap \sigma(l_j)$  is nonempty when  $j = 2$ , the fact that  $\alpha_0$  intersects the initial subpath  $_{hp_0}\gamma$  of  $\mu_1 =_{hp_0}(\gamma^5 \cdots)$  implies that  $\alpha_0$  is not one of the last  $l_C(\gamma)+1$  edges of  $\sigma(\mu_1)$  and therefore cannot be contained in the intersection  $\sigma(\mu_1) \cap \sigma(l_2)$ . In any case, we find that  $[\alpha_0]_V$  is disjoint from  $y_j(\mathbb{R})$ . Since  $(y_1(\mathbb{R}), \dots, y_j(\mathbb{R}))$  is a  $\Gamma$ -chain and  $y_{j-1}$  crosses in front of  $y_j$ , Lemma 2.16 now implies that  $[\alpha_t]_V$  is disjoint from  $y_j(\mathbb{R}_{\leq t})$  for all times  $t \geq 0$ .

Fix a time  $s \geq 5k$  and consider the path  $\mu' =_{hp_0} [(\gamma^2\omega_1\gamma^2) \cdots (\gamma^2\omega_{k-1}\gamma^2)(\gamma^5 \cdots)]$  from  $hp_0$  to  $x_{k-1}(s) = y_{j-1}(s)$ . Comparing this path with  $\mu$ , we find that  $\mu'$  decomposes as a grid path  $\mu' = \mu_1 \cdots \mu_{j-2}\mu'_{j-1}$ , where  $\mu_{j-1}$  is the initial subpath of  $\mu'_{j-1}$ . Let  $e$  be an internal edge of  $\mu_{j-1}$ , in which case  $e$  must lie in the infinite component of  $\sigma(y_{j-1}(\mathbb{R}_{\leq s})) \setminus \sigma(y_j(\mathbb{R}))$ . Since  $\mu'_{j-1} \supseteq \mu_{j-1}$ ,  $e$  is also an internal edge of  $\mu'_{j-1}$ . As the two marked points  $y_j$  and  $y_{j-1}$  have diverged in  $\mathcal{T}$  by the time  $s \geq 5k$ , it now follows that the ray  $\eta = y_j(\mathbb{R}_{\leq s})$  separates  $\sigma(y_{j-1}(s))$  from  $e$  in the sense of Lemma 2.15

By our induction hypothesis, the isotopy class  $[\alpha_s]_V$  intersects  $\sigma(y_{j-1}(s))$ . It follows that every path in  $[\alpha_s]_V$  projects onto the  $\mathcal{T}$ -geodesic from  $\sigma(y_{j-1}(s))$  to the base edge  $\varepsilon_0$ . By

Lemma 2.11, this  $\mathcal{T}$ -geodesic contains the edge  $e$ , so it must be that  $[\alpha_s]_V$  intersects  $e$  as well. Applying the separation property from Lemma 2.15, we finally conclude that  $[\alpha_s]_V$  intersects  $\sigma(y_j(s))$ . This proves that  $x_k$  constrains  $[\alpha_{5k}]_V$ .  $\square$

For each  $h \in G_{\varepsilon_0}$ , we have now described  $(i(\gamma) + 1)^{k-1} = |\mathcal{W}|^{k-1}$  marked points that constrain the isotopy class  $[\alpha_{5k}]_{\mathcal{M}}$ . However, it remains to be seen that these marked points are distinct and that they project to distinct vertices in the quotient graph  $G_{\varepsilon_0} \setminus \mathcal{T}$ .

**Proposition 2.18** (Distinctness). *Let  $k \geq 1$  be an integer. For each  $h \in G_{\varepsilon_0}$  and each ordered list  $\omega = (\omega_1, \omega_2, \dots, \omega_k)$  of  $k$  elements  $\omega_i \in \mathcal{W}$  satisfying  $\omega_1 = \gamma$ , consider the point*

$$\Psi(h, \omega) = (hp_0) \cdot [(\gamma^2 \omega_1 \gamma^2) \cdots (\gamma^2 \omega_k \gamma^2)] \in \mathbb{H}^2.$$

*For each distinct choice of  $h$  and  $\omega$ , this point projects to a distinct vertex  $\sigma(\Psi(h, \omega))$  in  $\mathcal{T}$ . In particular, the cosets  $G_{\varepsilon_0} \sigma(\Psi(h, \omega))$  and  $G_{\varepsilon_0} \sigma(\Psi(h', \omega'))$  are equal if and only if  $\omega = \omega'$ .*

*Proof.* We first establish some notation. Let  $M$  denote the optimal upper bound from Lemma 2.7; thus  $M$  is either  $l_{\mathcal{C}}(\gamma) + 1$  or  $l_{\mathcal{C}}(\gamma)$  depending on whether or not  $l_{\mathcal{C}}(\gamma) > 2$ . Furthermore, in the case that  $l_{\mathcal{C}}(\gamma) \geq 3$ , we take a decomposition  $\gamma = \xi_1 \xi_2$  of  $\gamma$  into two subpaths which satisfy  $l_{\mathcal{C}}(\xi_1) = 2$  and  $l_{\mathcal{C}}(\xi_2) \geq 1$ . If  $l_{\mathcal{C}}(\gamma) \leq 2$ , we instead choose this decomposition such that  $l_{\mathcal{C}}(\xi_1) = 1$  and  $l_{\mathcal{C}}(\xi_2) \leq 1$ . Notice that  $M + 1 = l_{\mathcal{C}}(\gamma) + l_{\mathcal{C}}(\xi_1)$ .

Choose any list  $\omega$  and consider the path  $\mu = {}_{p_0}[(\gamma^2 \omega_1 \gamma^2) \cdots (\gamma^2 \omega_k \gamma^2)]$  from the basepoint  $p_0$  to  $\Psi(1, \omega)$ . This defines a grid path  $\mu = \mu_1 \cdots \mu_n$  whose straight segments  $\mu_i$  satisfy the hypotheses of Lemma 2.11. Since  $\omega_1 = \gamma$ , the first straight segment  $\mu_1$  contains the initial subpath  ${}_{p_0}\gamma^5$  and has length  $l_{\mathcal{C}}(\mu_1) \geq 5l_{\mathcal{C}}(\gamma)$ . The beginning  ${}_{p_0}\gamma$  of this path intersects the base edge  $\alpha_0 \in E(\mathcal{T})$  of  $\mathcal{T}$ ; therefore  $\sigma(\mu_1)$  must contain a geodesic edge path of the form  $(\alpha_0, b_2, \dots, b_m)$ , where  $b_m$  is an internal edge of  $\mu_1$ . Notice that we may choose  $b_m$  so that it does not depend on  $\omega$ . If  $v \in V(\mathcal{T})$  denotes the initial vertex of this edge path, then both  $\alpha_0$  and  $v$  are fixed by every element of  $G_{\varepsilon_0}$ . Lemma 2.11 now implies that the  $\mathcal{T}$ -geodesic from  $\sigma(p_0)$  to  $\sigma(\Psi(1, \omega))$  contains the edge  $b_m$ ; in particular, the  $\mathcal{T}$ -geodesic from  $v$  to  $\sigma(\Psi(1, \omega))$  must have the form

$$(\alpha_0, b_2, \dots, b_m, \dots).$$

Applying a deck transformation  $h \in G_{\varepsilon_0}$ , we see that the  $\mathcal{T}$ -geodesic from  $hv = v$  to  $h\sigma(\Psi(1, \omega)) = \sigma(\Psi(h, \omega))$  has the form  $(\alpha_0, hb_2, \dots, hb_m, \dots)$ . That is, the  $m^{\text{th}}$  edge of the  $\mathcal{T}$ -geodesic from  $v$  to  $\sigma(\Psi(h, \omega))$  is  $hb_m$ . This feature is independent of  $\omega$ . Since  $hb_m \neq h'b_m$  for distinct  $h, h' \in G_{\varepsilon_0}$ , this proves that the vertices  $\sigma(\Psi(h, \omega))$  and  $\sigma(\Psi(h', \omega'))$  are distinct when  $h \neq h'$ .

For the remainder of the proof, we may consider a fixed element  $h \in G_{\varepsilon_0}$ . Let  $\omega = (\omega_1, \dots, \omega_k)$  and  $\omega' = (\omega'_1, \dots, \omega'_k)$  be two distinct lists, and let  $j$  be the smallest index with  $\omega_j \neq \omega'_j$ . Set  $e \in E(\mathcal{T})$  to be the last edge that the path  $\eta = {}_{hp_0}[(\gamma^2 \omega_1 \gamma^2) \cdots (\gamma^2 \omega_j \gamma^2) \xi_1]$  crosses, and let  $y = (hp_0) \cdot \eta$  be the endpoint of this path. Define  $e' \in E(\mathcal{T})$  and  $y' = (hp_0) \cdot \eta'$  similarly. The bulk of our argument is devoted to proving the following claim.

**Claim.** *The  $\mathcal{T}$ -geodesic from  $\sigma(y)$  to  $\sigma(y')$  has length at least  $l_{\mathcal{C}}(\gamma) + 2$  and contains both  $\bar{e}$  and  $e'$ . This essentially means that the two geodesics connecting  $\sigma(hp_0)$  to  $\sigma(y)$  and  $\sigma(y')$  have diverged in  $\mathcal{T}$ .*

*Proof of Claim.* First consider the case that neither  $\omega_j$  nor  $\omega'_j$  is equal to  $\gamma$ . It follows that  $\omega_j = \tau_q = \beta_q \nu_q$  and  $\omega'_j = \tau_{q'} = \beta_{q'} \nu_{q'}$  for two distinct self-intersection points  $q, q'$  of  $\gamma$ . Let

$$z = (hp_0) \cdot [(\gamma^2 \omega_1 \gamma^2) \cdots (\gamma^2 \omega_{j-1} \gamma^2) (\gamma^2 \beta_q)]$$

be the point where  $\eta$  makes its final turn towards  $y$ , and let  $A = {}_z(\nu_q \gamma^2 \xi_1)$  be the geodesic from  $z$  to  $y$ . Define  $z'$  and  $A'$  similarly. The geodesic segment  $X$  from  $z$  to  $z'$  is then a subpath of a segment of the form  ${}_x\gamma$ ; as such, it has  $l_{\mathcal{C}}(X) \leq l_{\mathcal{C}}(\gamma)$ . On the other hand, the edge paths  $\sigma(A)$  and  $\sigma(A')$  both have length at least  $2l_{\mathcal{C}}(\gamma) + l_{\mathcal{C}}(\xi_1)$ , and their intersection  $\sigma(A) \cap \sigma(A')$  contains at most  $M$  edges.

As in the proof of Lemma 2.11,  $\sigma(\bar{A}XA')$  is an edge path from  $\sigma(y)$  to  $\sigma(y')$  that can be made into a  $\mathcal{T}$ -geodesic by successively cancelling edge pairs  $(\dots, d, \bar{d}, \dots)$  to remove any backtracking. The path  $\sigma(X)$  can contribute to at most  $l_{\mathcal{C}}(X)$  cancellations, and, assuming all of these edges cancel, we can then have at most  $M$  cancellations involving edges of  $\sigma(\bar{A})$  with edges of  $\sigma(A)$ . Therefore, the  $\mathcal{T}$ -geodesic  $L$  from  $\sigma(y)$  to  $\sigma(y')$  will be obtained from  $\sigma(\bar{A}XA)$  after at most  $l_{\mathcal{C}}(X) + M$  cancellations. Since each cancellation removes two edges, it follows that

$$\begin{aligned} l_{\mathcal{C}}(L) &\geq 4l_{\mathcal{C}}(\gamma) + 2l_{\mathcal{C}}(\xi_1) + l_{\mathcal{C}}(X) - 2(l_{\mathcal{C}}(X) + l_{\mathcal{C}}(M)) \\ &= 2l_{\mathcal{C}}(\gamma) - l_{\mathcal{C}}(X) + 2 \geq l_{\mathcal{C}}(\gamma) + 2. \end{aligned}$$

Furthermore, since  $\sigma(\bar{A})$  and  $\sigma(A')$  each contain at least  $2l_{\mathcal{C}}(\gamma) + l_{\mathcal{C}}(\xi_1) \geq l_{\mathcal{C}}(X) + M + 1$  edges, we see that the first edge of  $\sigma(\bar{A})$  and the last edge of  $\sigma(A')$  do not cancel. As these edges are exactly  $\bar{e}$  and  $e'$ , the claim holds when neither  $\omega_j$  nor  $\omega'_j$  is equal to  $\gamma$ .

The argument for the case  $\omega_j \neq \omega'_j = \gamma$  is similar: Define  $z$  as above and again let  $A = {}_z(\nu_q \gamma^2 \xi_1)$  be the geodesic from  $z$  to  $y$ . The geodesic from  $z$  to  $y'$  is then given by  $A' = {}_z(\delta_q \nu_q \gamma^2 \xi_1)$ . Since these are both segments along geodesics in  $\Gamma$ , the concatenation  $\sigma(\bar{A})\sigma(A')$  can result in at most  $M$  cancellations. The resulting  $\mathcal{T}$ -geodesic has length at least

$$4l_{\mathcal{C}}(\gamma) + 2l_{\mathcal{C}}(\xi_1) - 2l_{\mathcal{C}}(M) \geq 2l_{\mathcal{C}}(\gamma) + 2$$

and still contains the initial and terminal edges  $\bar{e}$  and  $e'$ . This proves the claim.  $\square$

We now complete the proof of Proposition 2.18. To prove that  $\Psi(h, \omega)$  and  $\Psi(h, \omega')$  lie in distinct vertices of  $\mathcal{T}$ , it suffices to show that the  $\mathcal{T}$ -geodesic between these vertices is nondegenerate. To ease the notation, set  $x = \Psi(h, \omega)$  and set  $x' = \Psi(h, \omega')$ . First suppose that  $j = k$ , in which case we have  $y = x \cdot \xi_1$  and  $y' = x' \cdot \xi_1$ . Together with the above claim, the triangle inequality then implies that

$$d(\sigma(x), \sigma(x')) \geq l_{\mathcal{C}}(\gamma) + 2 - 2l_{\mathcal{C}}(\xi_1) \geq 1,$$

where  $d$  is the path metric in  $\mathcal{T}$ . In the case that  $j < k$ , we instead consider the path  $\mu = {}_{hp_0}[(\gamma^2 \omega_1 \gamma^2) \cdots (\gamma^2 \omega_k \gamma^2)]$  from  $hp_0$  to  $x$ . This is a grid path whose straight segments satisfy the hypotheses of Lemma 2.11. Let  $\mu_i$  be the straight segment of  $\mu$  containing the

edge  $e$ . Then  $\mu_i$  contains a subpath of the form  $\gamma^2\xi_1\xi_2\gamma$ , where  $e$  is the last edge that the  $\xi_1$  factor crosses. It is now evident that  $e$  separates  $\mu_i$  into two edge paths of lengths at least  $2l_{\mathcal{C}}(\gamma)$  and  $l_{\mathcal{C}}(\gamma) + l_{\mathcal{C}}(\xi_2) \geq M$ . Therefore, the definition of  $\xi_2$  ensures  $e$  is an internal edge of  $\mu_i$ . Lemma 2.11 now implies that the  $\mathcal{T}$ -geodesic from  $\sigma(hp_0)$  to  $\sigma(x)$  contains  $e$  and, similarly, that  $\mathcal{T}$ -geodesic from  $\sigma(hp_0)$  to  $\sigma(x')$  contains  $e'$ . Writing these geodesic edge paths as  $(b_1, \dots, b_n, e, a_1, \dots, a_m)$  and  $(b'_1, \dots, b'_{n'}, e', a'_1, \dots, a'_{m'})$ , and combining them with the geodesic  $(\bar{e}, d_1, \dots, d_l, e')$  from  $\sigma(y)$  to  $\sigma(y')$ , we find that

$$(\bar{a}_m, \dots, \bar{a}_1, \bar{e}, d_1, \dots, d_l, e', a'_1, \dots, a'_{m'})$$

is a nondegenerate, non-backtracking edge path from  $\sigma(x)$  to  $\sigma(x')$ .  $\square$

## 2.6 The point of pushing: proof of the lower bound

Now that we have found distinct cosets of marked points that constrain  $[\alpha_t]_{\mathcal{M}}$ , it is a simple matter to count intersection numbers and bound the dilatation  $\lambda_\gamma$ . We first state the following corollary to the above propositions.

**Corollary 2.19** (Intersection numbers). *Let  $\gamma \subset S$  be a filling loop that represents a primitive element of  $\pi_1(S)$ , let  $\alpha$  be an essential simple closed curve on  $S$ , and let  $\mathcal{C} = \{c_i\}$  be a pants decomposition of  $S$  that contains  $\alpha$ . For all integers  $k \geq 1$ , the iterates  $\varphi_\gamma^{5k}(\alpha)$  of  $\alpha$  under the point-pushing homeomorphism  $\varphi_\gamma$  satisfy*

$$i(\varphi_\gamma^{5k}(\alpha), \mathcal{C}) = \sum_i i(\varphi_\gamma^{5k}(\alpha), c_i) \geq (i(\gamma) + 1)^{k-1}.$$

*Proof.* After modifying each curve by an isotopy to make it geodesic, we may assume that  $\gamma$  and  $\alpha$  satisfy Assumptions 2.3 and that  $\mathcal{C}$  satisfies the assumptions of §2.2. It follows that all of the marked points described in Proposition 2.17 constrain  $[\alpha_{5k}]_{\mathcal{M}}$ . Let  $\mu \subset S$  be any simple closed curve that is isotopic to  $\varphi_\gamma^{5k}(\alpha)$  in  $(S, p)$ , and let  $\tilde{\mu} \subset (\mathbb{H}^2, \pi^{-1}(p))$  be the lift of  $\mu$  whose endpoints on  $\partial\mathbb{H}^2$  agree with those of  $\alpha_0$ . We assume that  $\mu$  is transverse to the curves in  $\mathcal{C}$ . Since  $\tilde{\mu}$  is in the isotopy class  $[\alpha_{5k}]_{\mathcal{M}}$ , its projection  $\sigma(\tilde{\mu})$  to  $\mathcal{T}$  is an edge path that necessarily visits all of the vertices described by Proposition 2.18. Since these project to  $(i(\gamma) + 1)^{k-1}$  distinct vertices in the quotient graph  $G_{\varepsilon_0} \setminus \mathcal{T}$ , it is apparent that  $\sigma(\tilde{\mu})$  projects to a closed loop in  $G_{\varepsilon_0} \setminus \mathcal{T}$  that crosses at least this many edges. Observation 2.12 now implies that

$$|\mu \cap \mathcal{C}| \geq (i(\gamma) + 1)^{k-1}.$$

Since  $\mu$  is an arbitrary representative in the isotopy class of  $\varphi_\gamma^{5k}(\alpha)$ , this proves the claim.  $\square$

In light of the connection between dilatation and intersection numbers (Theorem 2.2), this inequality easily implies a lower bound on the dilatation of  $\varphi_\gamma$ . Furthermore, it provides for an immediate proof of Kra's theorem that  $\mathcal{P}(\gamma)$  is pseudo-Anosov if and only if  $\gamma$  fills  $S$  (Theorem 1.2). Both of these results are combined into the following statement. We note that our proof of Kra's theorem is similar in spirit to the short proof given by Farb and Margalit in [FM, Theorem 13.5].

**Theorem 2.20** (The lower bound). *Let  $S = S_{g,n}$  be a surface satisfying  $3g + n > 3$ , and let  $\mu: [0, 1] \rightarrow S$  be a closed curve on  $S$ . The mapping class  $\mathcal{P}(\mu)$  is pseudo-Anosov if and only if  $\mu$  fills  $S$ ; in this case the dilatation  $\lambda_\mu$  of  $\mathcal{P}(\mu)$  satisfies the inequality*

$$\lambda_\mu \geq \sqrt[5]{i(\mu) + 1}$$

*with the following exceptions: If  $S = S_{0,4}$  or  $S_{1,2}$  and  $\mu$  is the square of a primitive element in  $\pi_1(S)$ , then the lower bound is only  $\lambda_\mu \geq \sqrt[5]{i(\mu)}$ . If  $S = S_{1,1}$  and  $\mu$  is the second, third, or fourth power of a primitive element, then the lower bound is only  $\lambda_\mu \geq \sqrt[5]{(i(\mu) + 1)/2}$ .*

*Proof.* If  $\mu$  does not fill  $S$ , then we may find an essential simple closed curve  $\eta \subset S$  that is disjoint from  $\mu$ . It then follows from the definition of the point-pushing homomorphism that we may choose a representative of  $\mathcal{P}(\mu)$  that fixes  $\eta$  pointwise. Therefore  $\mathcal{P}(\mu)$  is not pseudo-Anosov because it fixes the isotopy class of  $\eta$ .

On the other hand, if  $\mu$  fills  $S$ , then we may decompose  $\mu$  as a power  $\mu = \gamma^m$  of some primitive filling curve  $\gamma \in \pi_1(S)$ . Let  $\varphi_\gamma$  denote a representative homeomorphism for  $\mathcal{P}(\gamma)$  and let  $\alpha$  be any essential closed curve on  $S$ . After choosing a pants decomposition  $\mathcal{C}$  as in Corollary 2.19, it follows that  $i(\varphi_\gamma^{5k}(\alpha), \mathcal{C}) \geq (i(\gamma) + 1)^{k-1}$  for all  $k \geq 1$ . In particular, the sequence  $i(\varphi_\gamma^{5k}(\alpha), \mathcal{C})$  is not periodic, so no iterate of  $\varphi_\gamma$  fixes the isotopy class of  $\alpha$ . As  $\alpha$  was chosen arbitrarily, this proves that  $\mathcal{P}(\gamma)$  and  $\mathcal{P}(\mu) = \mathcal{P}(\gamma)^m$  are both pseudo-Anosov. Furthermore, upon manipulating the inequality from Corollary 2.19, we find that

$$\left( \frac{(i(\gamma) + 1)^{1/5}}{\lambda_\gamma} \right)^{5k} \leq (i(\gamma) + 1) \frac{i(\varphi_\gamma^{5k}(\alpha), \mathcal{C})}{\lambda_\gamma^{5k}} = (i(\gamma) + 1) \sum_{c_i \in \mathcal{C}} \frac{i(\varphi_\gamma^{5k}(\alpha), c_i)}{\lambda_\gamma^{5k}}.$$

Theorem 2.2 implies that the rightmost expression has a finite limit. Therefore the leftmost expression remains bounded as  $k$  tends to infinity, which is only possible if  $\lambda_\gamma \geq (i(\gamma) + 1)^{1/5}$ . This proves the theorem when  $\mu = \gamma$  is a primitive element of  $\pi_1(S)$ .

It remains to bound the dilatation  $\lambda_\mu = \lambda_\gamma^m$  in the case that  $m \geq 2$ . Isotope  $\gamma$  to attain the minimum intersection number  $i(\gamma) > 0$  in Definition 1.4. By building a single closed curve out of  $m$  offset copies of this loop, we obtain a representative for  $\mu = \gamma^m$  that has  $m^2 i(\gamma) + (m - 1)$  transverse self intersections. This gives an upper bound

$$i(\mu) + 1 \leq m^2 i(\gamma) + m \tag{2.21}$$

on the self-intersection number of  $\mu$ . To relate this to the dilatation of  $\mathcal{P}(\mu)$ , we need to consider several inequalities involving the numbers  $i(\gamma)$  and  $m$ . Firstly, the inequality

$$m^2 k + m \leq (k + 1)^m \tag{2.22}$$

holds for all integers  $m \geq 2$  and  $k \geq 3$ . Secondly, thinking of  $\gamma \subset S$  as a four-valent graph, we have that

$$-i(\gamma) = \chi(\gamma) \leq \chi(S_{g,n}) = 2 - 2g - n, \tag{2.23}$$

where this inequality is strict in the case that  $S$  is closed. The following three cases now account for all surfaces  $S_{g,n}$  satisfying  $3g + n > 3$ .

**Case 1:**  $\chi(S) \leq -3$  or  $S = S_{2,0}$ . In this case (2.23) implies that  $i(\gamma) \geq 3$  (note that  $S_{2,0}$  is closed). Combining (2.21) and (2.22) then yields the desired inequality

$$\lambda_\mu = \lambda_\gamma^m \geq (i(\gamma) + 1)^{m/5} \geq (m^2 i(\gamma) + m)^{1/5} \geq \sqrt[5]{i(\mu) + 1}.$$

**Case 2:**  $S = S_{0,4}$  or  $S = S_{1,2}$ . In this case (2.23) only ensures that  $i(\gamma) \geq 2$ . When  $k = 2$ , the inequality (2.22) remains valid provided that  $m \geq 3$ . In such cases, we obtain the bound  $\lambda_\mu \geq (i(\mu) + 1)^{1/5}$  as above. When  $m = 2$ , the modified inequality  $2^2 k + 2 - 1 \leq (k + 1)^2$  holds provided  $k \geq 2$ . Combining this with (2.21), we find that

$$\lambda_\mu = \lambda_\gamma^2 \geq (i(\gamma) + 1)^{2/5} \geq (2^2 i(\gamma) + 2 - 1)^{1/5} \geq \sqrt[5]{i(\mu)}$$

in the case that  $\mu$  is the square of a primitive element of either  $\pi_1(S_{0,4})$  or  $\pi_1(S_{1,2})$ .

**Case 3:**  $S = S_{1,1}$ . The Euler characteristic now guarantees that  $i(\gamma) \geq -\chi(S_{1,1}) = 1$ . When  $k = 1$ , (2.22) still holds provided that  $m \geq 5$ ; therefore we may conclude the general bound  $\lambda_\mu \geq (i(\mu) + 1)^{1/5}$  in these cases. For  $2 \leq m \leq 4$ , we instead have the inequality  $(m^2 k + m)/2 \leq (k + 1)^m$ , which holds for all  $k \geq 1$ . Together with (2.21), this shows that

$$\lambda_\mu = \lambda_\gamma^m \geq (i(\gamma) + 1)^{m/5} \geq \left( \frac{m^2 i(\gamma) + m}{2} \right)^{m/5} \geq \sqrt[5]{\frac{i(\mu) + 1}{2}}$$

in the case that  $\mu$  is the second, third, or fourth power of a primitive element in  $\pi_1(S_{1,1})$ .  $\square$

**Remark 2.24.** Although we have formulated this result in the context of punctured surfaces, our arguments apply equally well to compact surfaces with boundary. Furthermore, these two contexts are readily seen to be equivalent: If  $\bar{S}$  is a compact surface with interior  $S$  and basepoint  $p \in S$ , then restricting to  $S \subset \bar{S}$  induces a natural surjection  $\text{Mod}(\bar{S}, p) \rightarrow \text{Mod}(S, p)$  that commutes with  $\mathcal{P}$ . As elements of  $\text{Mod}(\bar{S}, p)$  are required to fix  $\partial\bar{S}$  pointwise, the kernel of this map is a free abelian group generated by Dehn twists about the components of  $\partial\bar{S}$ . These twists act trivially on the set  $\mathcal{S}$  of isotopy classes of essential, simple closed curves on  $\bar{S}$ . Since pseudo-Anosov dilatation can be detected by the action on  $\mathcal{S}$  (c.f. Theorem 2.2), it follows that the the surjection  $\text{Mod}(\bar{S}, p) \rightarrow \text{Mod}(S, p)$  preserves dilatation and that Theorem 1.6 lifts to  $\text{Mod}(\bar{S}, p)$ .

### 3 An invariant pretrack

Train tracks are an invaluable tool in the study of pseudo-Anosov homeomorphisms, and they will play an essential role in in our investigation. While it is a nontrivial matter to find an invariant train track for an arbitrary pseudo-Anosov map (there is, however, an algorithm due to Bestvina and Handel [BH]), §3.2 describes a simple method for constructing invariant pretracks for pseudo-Anosov elements of the the point-pushing subgroup. We will use this construction to establish the upper bounds in Theorems 1.6, 1.10, and 1.12. We begin our discussion by recalling the relevant train track theory, which is developed more thoroughly in [PH, Mos, Pen1, PP].

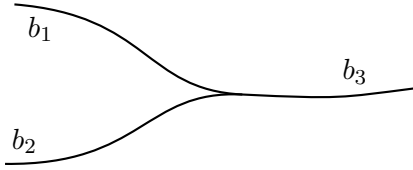


Figure 7: A switch.

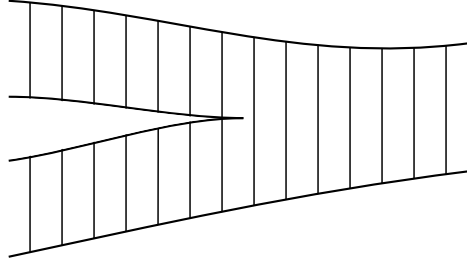


Figure 8: The local tie neighborhood.

### 3.1 Preliminary train track theory

A *pretrack* on  $S = S_{g,n}$  is a nonempty, smooth, closed 1-complex  $\tau \subset S$ , whose edges are called *branches* and whose vertices are called *switches*, with the property that all branches incident on a given switch  $v \in \tau$  share a common tangent line  $L_v \leq T_v S$  at  $v$ ; in this way, the branches incident at  $v$  are divided into two sides depending on whether their tangent vectors at  $v$  are parallel or antiparallel. The local picture around a switch is shown in Figure 7. The closure of a component of  $S \setminus \tau$  is naturally a surface with cusps on its boundary, and we define the Euler index of a such a surface to be the Euler characteristic minus  $1/2$  for each boundary cusp. For instance, a  $k$ -gon, that is, a topological disk with  $k$  cusps on its boundary, has Euler index  $\frac{2-k}{2}$ .

A *train track* on  $S$  is simply a pretrack whose complimentary components all have negative Euler index. This amounts to ruling out complimentary nullgons, monogons, bigons, smooth annuli, and once-punctured nullgons. In the context of a marked surface  $(S, p)$ , the marked point  $p$  counts as a puncture and will be treated as such. We will use the term “track” to refer to both pretracks and train tracks. A track  $\tau$  *fills* the surface if each component of  $S \setminus \tau$  is a topological disk or a once-punctured disk.

A *weight function* on a track  $\tau$  is an assignment of a nonnegative real number to each branch of  $\tau$  in such a way that the net weights incident on either side of each switch agree. For instance, if the weight  $w_i$  is assigned to branch  $b_i$  in Figure 7, then these weights must satisfy the equation  $w_1 + w_2 = w_3$ . The set of weight functions on  $\tau$  is denoted by  $E_\tau$ ; it is a convex cone in  $\mathbb{R}^B$ , where  $B$  is the set of branches in  $\tau$ .

Let  $\mathcal{MF}(S)$  denote the space of equivalence classes of measured foliations on  $S$ ; see [FLP] for the theory of measured foliations. Because of the train track condition on complimentary components, there is natural injection  $\rho: E_\tau \rightarrow \mathcal{MF}(S)$  from the set of weights on a filling train track  $\tau$  onto a convex cone  $V_\tau \subseteq \mathcal{MF}(S)$  consisting of those measured foliations which are “carried” by  $\tau$  [PP, pp. 360–361]. As every measured foliation is carried by some train track, the cones  $V_\tau$  are often regarded as parameterized coordinate patches in  $\mathcal{MF}(S)$ . A pretrack which fails to be a train track only due to the existence of complimentary bigons will be called a *bigon track*. The natural function  $\rho: E_\tau \rightarrow V_\tau$  still makes sense for a bigon track, but it may fail to be injective [Pen2, p. 183].

The tubular neighborhood  $N$  of a track  $\tau$  is naturally fibered by “ties” which are transverse to the track, as in Figure 8. If  $\sigma$  is another track on  $S$ , then  $\tau$  *carries*  $\sigma$ , denoted

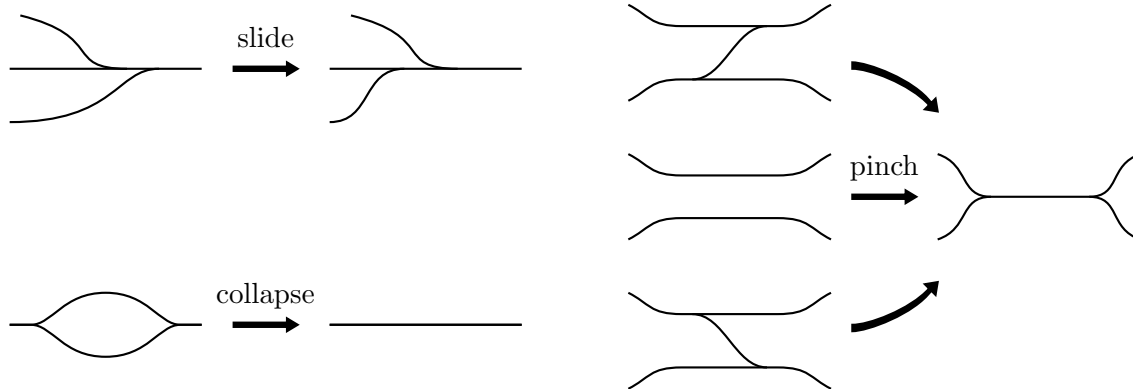


**Figure 9:** The elementary carrying moves.

$\sigma \prec \tau$ , if  $\sigma$  may be smoothly isotoped into  $N$  while remaining transverse to the ties. Such an isotopy  $\Phi_t: S \rightarrow S$  with  $\Phi_1(\sigma) \subset N$  is called a *supporting map* for the carrying; it defines a corresponding *incidence matrix*  $M = (M_{ij})$  as follows: For each branch  $b_i$  of  $\tau$  choose a distinguished fiber  $x_i \subset N$  over an interior point of  $b_i$ . Then, for each branch  $c_j$  of  $\sigma$ , set  $M_{ij} = |\Phi_1^{-1}(x_i) \cap c_j|$  to be the number of times  $\Phi_1(c_j)$  crosses the distinguished tie  $x_i$ . Although the incidence matrix  $M$  depends on the carrying  $\Phi_t$ , it nevertheless induces a canonical linear transformation  $M: E_\sigma \rightarrow E_\tau$  from the set of weight functions on  $\sigma$  to the set of weight functions on  $\tau$ . In the case that  $\sigma$  and  $\tau$  are filling train tracks, the carrying  $\sigma \prec \tau$  implies that  $V_\sigma \subseteq V_\tau$ , and any incidence matrix  $M$  describes the corresponding transition function between these parameterizations of  $V_\sigma$  [PP, p. 362].

Because of the switch conditions, a weight function  $\mu \in E_\tau$  may be specified by its values on a proper subset  $B' \subset B$  of the branches of  $\tau$ ; for example, in the situation of Figure 7, the weight  $\mu(b_3)$  is determined by the values of  $\mu(b_1)$  and  $\mu(b_2)$ . This means that the natural projection  $\mathbb{R}^B \rightarrow \mathbb{R}^{B'}$  is injective on  $E_\tau \subset \mathbb{R}^B$ . If  $E'_\tau \subset \mathbb{R}^{B'}$  denotes image of  $E_\tau$ , then inverting this projection gives a linear bijection  $A_\tau: E'_\tau \rightarrow E_\tau$ . In the case of a carrying  $\sigma \prec \tau$  with incidence matrix  $M$ , we can make use of these bijections and instead consider the  $|B'_\tau| \times |B'_\sigma|$  matrix  $M' = A_\tau^{-1} M A_\sigma$ . This smaller matrix gives a linear transformation  $M': E'_\sigma \rightarrow E'_\tau$  that contains all of the information of the carrying. To ease calculations, we will work with incidence matrices of this smaller form.

In addition to isotopy, we will make use of three elementary moves on a track  $\tau$  which produce a new track  $\tau'$  that carries  $\tau$ . The moves are illustrated in Figure 9, and they consist of: sliding one switch past another, collapsing a bigon, or pinching branches together in the manner illustrated. For each move there is a natural choice of supporting map for the carrying  $\tau \prec \tau'$  whose corresponding incidence matrix has the obvious effect on weights.

If  $f \in \text{Mod}(S)$  is a pseudo-Anosov mapping class and  $\tau$  is a track on  $S$ , then the image  $f(\tau)$  is well-defined up to isotopy. We say that  $\tau$  is an *invariant track* for  $f$  if  $f(\tau) \prec \tau$ . If, additionally,  $\tau$  is a filling train track or filling bigon track, then any incidence matrix  $M$  for the carrying  $f(\tau) \prec \tau$  describes the induced map  $f_*: \mathcal{MF}(S) \rightarrow \mathcal{MF}(S)$  in the coordinate chart  $\rho: E_\tau \rightarrow V_\tau$ , that is, we have  $f_*(\rho(\mu)) = \rho(M\mu)$  for any weight function

$\mu \in E_\tau$  [Pen1, p. 444]. Projectively, the unstable measured foliation  $\mathcal{F}_+$  of  $f$  is an attracting fixed point for the action of  $f_*$  on  $\mathcal{MF}(S)$  [FLP, Exp. 12]; it follows that the coordinate chart  $V_\tau$  contains sequences that converge projectively to  $\mathcal{F}_+$ . Since  $V_\tau$  is closed, this implies that  $\mathcal{F}_+$  is contained in  $V_\tau$  and necessarily corresponds to an eigenvector of  $M$ . In particular, the dilatation of  $f$  is an eigenvalue of the incidence matrix  $M$ .

A square integer matrix  $A$  is *Perron–Frobenius* if it has nonnegative entries and some iterate  $A^k$  has strictly positive entries. In this case, the eigenvalue of  $A$  with maximum modulus is positive real and its corresponding eigenvector has strictly positive entries [Gan, Ch XIII §2 Theorem 2]. It follows that the modulus of any eigenvalue of a Perron–Frobenius matrix is bounded above by the largest row-sum of the matrix. Applying this classical result to the case of a Perron–Frobenius incidence matrix  $M$ , we may conclude the following key lemma.

**Lemma 3.1.** *Let  $f$  be a pseudo-Anosov mapping class, and suppose that  $\tau$  is a filling train track or bigon track that is invariant under  $f$ . If  $M$  is a Perron–Frobenius incidence matrix for the carrying  $f(\tau) \prec \tau$ , then the dilatation of  $f$  is bounded above by the largest row-sum of  $M$ .*

### 3.2 Invariant tracks for point-pushing homeomorphisms

In this subsection we describe a simple procedure for producing a pretrack from a curve; this construction will be used in §4 and §5 to analyze explicit examples and prove the upper bounds in Theorems 1.6, 1.10 and 1.12. Let  $\gamma: [0, 1] \rightarrow S$  be a smooth curve on  $S$  with  $\gamma(0) = \gamma(1) = p$ . We say that such a loop is *generic* if it is simple except for finitely many transverse double-intersection points in the interior of  $\gamma$  (i.e., not at  $p$ ). If  $\gamma$  is generic and  $q \in S$  is a self-intersection point of  $\gamma$ , we let  $t_{q1}$  and  $t_{q2}$  denote the two preimages of  $q$  under  $\gamma$ , that is, we have  $\gamma^{-1}(q) = \{t_{q1}, t_{q2}\}$  with  $0 < t_{q1} < t_{q2} < 1$ .

Notice that a generic loop  $\gamma \subseteq S$  is naturally a smooth, closed 1-complex, and that  $\gamma$  only fails to be a pretrack because the intersection points are transverse rather than tangential. Thus we can build a pretrack that is intrinsically related to  $\gamma$  by simply adjusting this 1-complex around its intersection points to ensure that it satisfies the tangential condition at switches.

Locally around an intersection point  $q$ , the curve  $\gamma$  cuts  $S$  into four quadrants which have corners incident at  $q$  and boundaries given by arcs of  $\gamma$ . The quadrant whose two boundary edges agree with the tangent vectors  $\gamma'(t_{q1})$  and  $\gamma'(t_{q2})$  is the *outbound quadrant*, and catty-corner to this is the *inbound quadrant*; the situation is depicted in Figure 10(a).

We now describe how to adjust the 1-complex  $\gamma$  around  $q$  to obtain a pretrack. The path  $\gamma$  crosses  $q$  twice, first at time  $t_{q1}$  and then at  $t_{q2}$ . For a sufficiently small  $\varepsilon > 0$ , we consider the four nearby points  $a_i^\pm = \gamma(t_{qi} \pm \varepsilon)$  on the edges of  $\gamma$  incident at  $q$ . Add three short, curved segments connecting the three pairs of points  $(a_1^-, a_2^+)$ ,  $(a_1^+, a_2^-)$ , and  $(a_1^+, a_2^+)$ ; this has the effect of cutting off the corner of every quadrant except for the inbound quadrant. Removing the segment of  $\gamma$  between  $a_1^-$  and  $a_1^+$ , we obtain the local pretrack illustrated in Figure 10(b); it has a trigon located at  $q$ , the inbound quadrant has a cusp, and the other

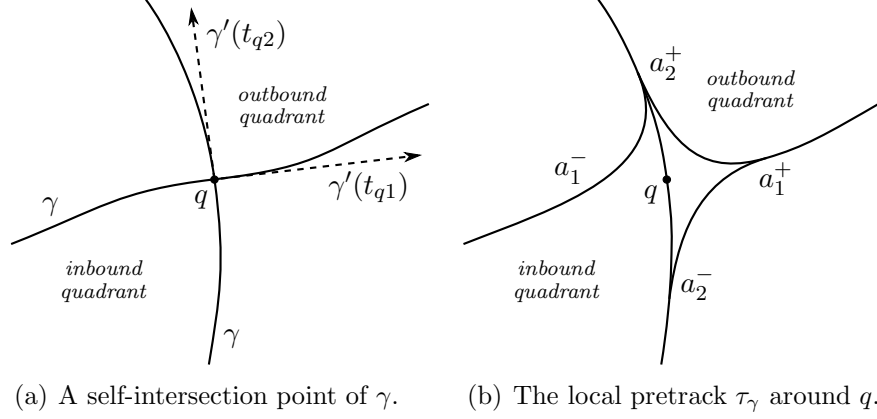


**Figure 10:** Constructing a pretrack  $\tau_\gamma$  from a generic curve  $\gamma$ .

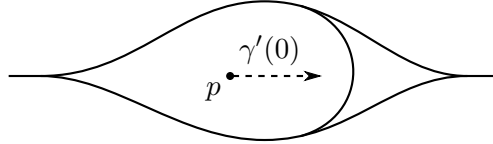


**Figure 11:** Adjusting for the basepoint: the eye of the pretrack  $\tau_\gamma$ .

quadrants have smooth corners. Notice that this 1-complex is still tangent to  $\gamma'(t_{q2})$  but is no longer tangent to  $\gamma'(t_{q1})$ .

After making these adjustments at each self-intersection point, we obtain a pretrack on the surface  $S$ . The last step is to create a track on  $S \setminus \{p\}$ . Consider the branch that passes through  $p$  and split it (e.g., at  $\gamma(1 - \varepsilon)$  and  $\gamma(0 + \varepsilon)$ ) into a bigon around  $p$ . Finally, as illustrated in Figure 11, add a smooth arc across the front of the bigon separating it into a trigon and a monogon containing  $p$ . We refer to this section of track as the *eye* of the track.

**Definition 3.2** (Induced pretrack). Let  $\gamma: [0, 1] \rightarrow S$  be a generic closed curve on the surface  $S$ . The corresponding pretrack, as constructed above, is called the *pretrack induced by  $\gamma$*  and will be denoted by  $\tau_\gamma$ . See Figures 14 and 15 for examples of such pretracks.

**Proposition 3.3** (Invariance of the induced pretrack). *Let  $\gamma: [0, 1] \rightarrow S$  be a generic loop representing a nontrivial element of the fundamental group  $\pi_1(S, p)$ . Then the induced pretrack  $\tau_\gamma$  is left invariant by the mapping class  $\mathcal{P}(\gamma) = [\varphi_\gamma]$ .*

*Proof.* Observe that the pretrack  $\tau_\gamma$  depends on the choice of basepoint  $p \in S$ . For  $t \in [0, 1]$ , we may choose a reparameterization  $\hat{\gamma}$  of  $\gamma$  based at the point  $\hat{\gamma}(0) = \gamma(t)$ , and we let  $\tau_t = \tau_{\hat{\gamma}}$  denote the corresponding pretrack. This new track differs from  $\tau_\gamma$  in two important ways: Firstly, the eye of the track is now located at  $\gamma(t)$  instead of at  $p = \gamma(0)$ . Secondly, the order of traversal at a self-intersection point  $q$  might have changed; this would have the effect of reversing the orientation of the local picture around  $q$ —the inbound and outbound quadrants would be unchanged but the segment connecting  $a_2^-$  and  $a_2^+$  would be replaced by a segment joining  $a_1^-$  and  $a_1^+$  (see Figure 10(b)). In this case we say that the branch containing  $q$  has

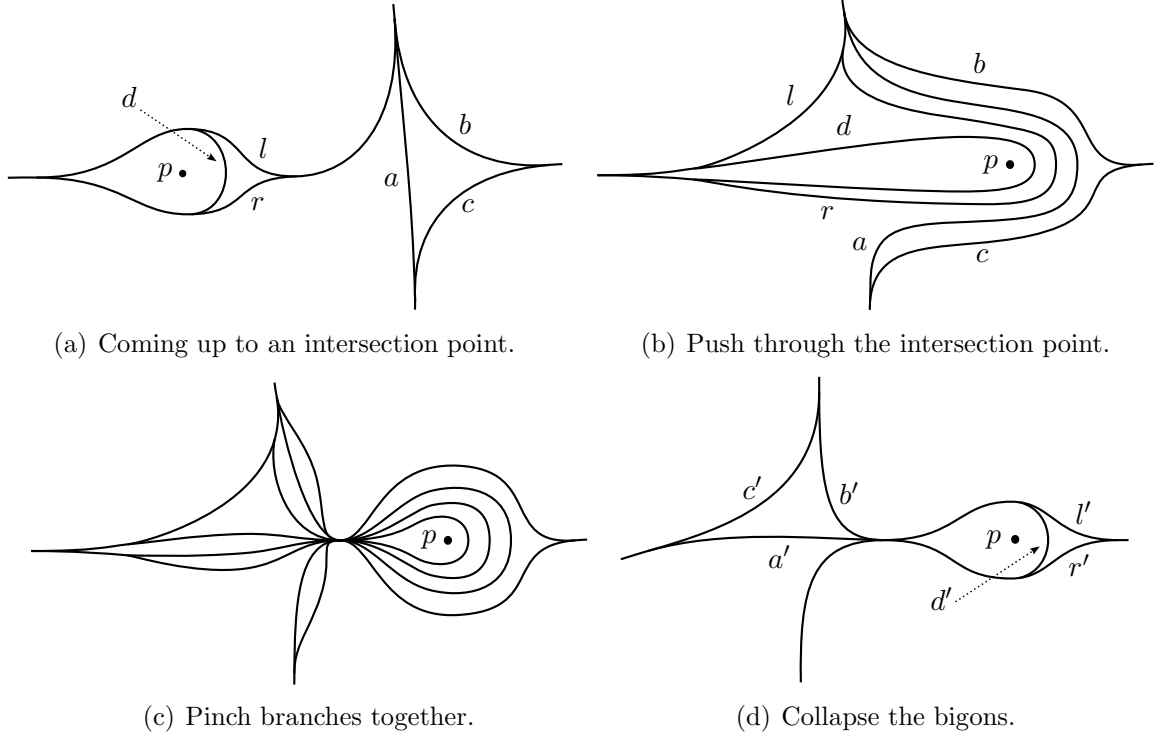


**Figure 12:** Proving that  $\tau_\gamma$  carries  $\mathcal{P}(\gamma)(\tau_\gamma)$ : navigating a self-intersection point of  $\gamma$ .

“flipped” in order to satisfy the condition that it is always transverse to the direction of travel for  $\hat{\gamma}$ 's *first* intersection with  $q$ .

Before proceeding with the proof, we highlight the key idea: pushing across a self-intersection point has the effect of moving the eye and flipping the branch containing that point. Since one full loop around  $\gamma$  crosses each intersection point twice, each branch flips twice and there is no net effect. To make this precise, we argue as follows.

Recall from (1.1) that the point-pushing homeomorphism  $\varphi_\gamma$  is obtained at the end of an isotopy  $F_t: S \rightarrow S$  that pushes the point  $p$  around  $\gamma$ . Let  $[s, s'] \subseteq [0, 1]$  be a time interval during which  $F_t$  either pushes  $p$  along an edge of  $\gamma$  or pushes  $p$  through a self-intersection point of  $\gamma$ . We will prove that if  $F_t(\tau_\gamma) \prec \tau_t$  for  $t = s$ , then the same is true when  $t = s'$ . Since  $[0, 1]$  may be covered by finitely many of these intervals, it will then follow that  $\varphi_\gamma(\tau_\gamma) = F_1(\tau_\gamma) \prec \tau_1 = \tau_\gamma$ .

Strictly speaking, we should start with the track  $F_s(\tau_\gamma)$  and apply the isotopy over the interval  $[s, s']$  to obtain  $F_{s'}(\tau_\gamma)$ . Instead, we will use the given carrying  $F_s(\tau_\gamma) \prec \tau_s$  and start with the track  $\tau_s$ . We then apply the isotopy to  $\tau_s$  and obtain a new track  $\sigma$ . Since we could have alternately taken note of the steps in the carrying and simply performed them after completing the isotopy, we see that  $F_{s'}(\tau_\gamma) \prec \sigma$ . Thus it suffices to show  $\sigma \prec \tau_{s'}$ .

We first suppose that  $F_t$  pushes  $p$  along an edge of  $\gamma$  during the interval  $[s, s']$ . This isotopy may be adjusted so that it drags the eye of  $\tau_s$  along with  $p$  and does not affect the rest of the surface. The resulting track at the end of the time interval is  $\tau_{s'}$ .

It remains to examine the case that  $F_t$  pushes  $p$  through a self-intersection point  $q$  during the interval  $[s, s']$ . At time  $t = s$  we have the track  $\tau_s$ , and the initial situation is as depicted in Figure 12(a). Pushing  $p$  through  $q$  results in the track  $\sigma$  illustrated in Figure 12(b). After pinching several branches together as in Figure 12(c), we may collapse the the resulting bigons to obtain the track  $\sigma'$  shown in Figure 12(d). Note that  $\sigma \prec \sigma'$ . A comparison of  $\tau_s$  and  $\sigma'$  shows that pushing through  $q$  has the effect of moving the eye to  $\gamma(s')$  and flipping the branch containing  $q$ . Since changing the starting point from  $\gamma(s)$  to  $\gamma(s')$  switches the order of traversal at  $q$ —the direction we just pushed is the *second* direction of traversal if we start at  $\gamma(s')$ — $\sigma'$  evidently satisfies the defining characteristics of  $\tau_{s'}$ .  $\square$

The proof of Proposition 3.3 exhibits an explicit carrying  $\varphi_\gamma(\tau_\gamma) \prec \tau_\gamma$ , and it is straightforward to determine the corresponding incidence matrix. Notice that any weight function is locally determined by its values on the six branches that are labeled in Figure 12(a). We identify these distinguished branches in the following way. In the eye of the pretrack,  $d$  is the branch immediately in front of the marked point, while  $l$  and  $r$  form the left and right sides (in the direction of travel) of the trigon at the front of the eye. In the local picture around a self-intersection point  $q$ ,  $a_q$  is the branch containing  $q$ ,  $b_q$  is the curved branch through the outbound quadrant, and  $c_q$  is the curved branch forming the other side of this trigon.

Suppose that  $w$  is a weight function on  $\tau_\gamma$ , and let  $q_1, \dots, q_n$  denote the  $n = i(\gamma)$  self-intersection points of  $\gamma$ . We say that  $w_e = (w(d), w(l), w(r))$  is the weight vector at the eye, and that  $w_i = (w(a_{q_i}), w(b_{q_i}), w(c_{q_i}))$  is the weight vector at  $q_i$ . The weight function is then completely determined by its weight vectors  $w_e, w_1, \dots, w_n$ .

By keeping track of the weights throughout the carrying illustrated in in Figure 12, one finds that pushing the marked point through  $q_i$  transforms the weight vector  $(w_e, w_1, \dots, w_n)$  according to the block matrix

$$A_i^{\text{right}} = \begin{pmatrix} \begin{pmatrix} 1 & 0 & 1 \\ 0 & 0 & 0 \\ 0 & 0 & 0 \end{pmatrix} & \cdots & \begin{pmatrix} 1 & 0 & 0 \\ 0 & 1 & 0 \\ 0 & 0 & 1 \end{pmatrix} & \cdots & 0 \\ \vdots & \ddots & \vdots & & \vdots \\ \begin{pmatrix} 2 & 0 & 1 \\ 0 & 0 & 1 \\ 0 & 1 & 0 \end{pmatrix} & \cdots & \begin{pmatrix} 0 & 0 & 0 \\ 1 & 1 & 0 \\ 0 & 0 & 0 \end{pmatrix} & \cdots & 0 \\ \vdots & & \vdots & \ddots & \vdots \\ 0 & \cdots & 0 & \cdots & I \end{pmatrix} \quad \text{or} \quad A_i^{\text{left}} = \begin{pmatrix} \begin{pmatrix} 1 & 1 & 0 \\ 0 & 0 & 0 \\ 0 & 0 & 0 \end{pmatrix} & \cdots & \begin{pmatrix} 1 & 0 & 0 \\ 0 & 0 & 1 \\ 0 & 1 & 0 \end{pmatrix} & \cdots & 0 \\ \vdots & \ddots & \vdots & & \vdots \\ \begin{pmatrix} 2 & 1 & 0 \\ 0 & 1 & 0 \\ 0 & 0 & 1 \end{pmatrix} & \cdots & \begin{pmatrix} 0 & 0 & 0 \\ 1 & 1 & 0 \\ 0 & 0 & 0 \end{pmatrix} & \cdots & 0 \\ \vdots & & \vdots & \ddots & \vdots \\ 0 & \cdots & 0 & \cdots & I \end{pmatrix}$$

depending on whether the inbound quadrant is on the right (as in Figure 12) or left side of  $p$ . Here  $A_i^{\text{right}}$  and  $A_i^{\text{left}}$  are each the identity matrix except for the four indicated blocks in the  $e$  and  $i$  positions. The full incidence matrix for the carrying is then an appropriate product of these matrices.

**Corollary 3.4** (Incidence matrix). *Suppose that  $\gamma$  crosses its  $n$  intersection points in the order  $q_{i_1}, q_{i_2}, \dots, q_{i_{2n}}$  and that the handedness of the  $j^{\text{th}}$  crossing is  $\mathcal{O}_j \in \{\text{right}, \text{left}\}$ . Let  $M_\gamma: E_{\tau_\gamma} \rightarrow E_{\tau_\gamma}$  be the linear transformation induced by the carrying  $\varphi_\gamma(\tau_\gamma) \prec \tau_\gamma$  described in Proposition 3.3. Then the action of  $M_\gamma$  on a weight vector  $(w_e, w_1, \dots, w_n)$  is given by the matrix product*

$$M_\gamma = A_{i_{2n}}^{\mathcal{O}_{2n}} \cdots A_{i_1}^{\mathcal{O}_1}.$$

**Remarks 3.5.** It is an obvious drawback that  $\tau_\gamma$  is only a pretrack and not, in general, a train track. There is a beautiful algorithm, due to Bestvina and Handel [BH], that will find an invariant train track for any pseudo-Anosov mapping class. However, in the case of a point-pushing map, it is not clear how the resulting track depends on the pushing curve. The point of our construction is that  $\tau_\gamma$  depends visibly on  $\gamma$ , and, as seen in Corollary 3.4, the corresponding incidence matrix depends quantifiably on the self-intersection number  $i(\gamma)$ . Thus  $\tau_\gamma$  provides a connection between  $i(\gamma)$  and the dilatation  $\lambda_\gamma$ . It would be interesting if our construction could be modified to produce a train track while maintaining these key features. We make two comments to this effect.

Firstly, whether or not a complimentary component of  $\gamma \subset S$  satisfies the train track condition for  $\tau_\gamma$  depends only on the pattern of directions in which  $\gamma$  traverses its boundary edges. By studying the problematic patterns and adjusting for them accordingly, it may be possible to find a formulaic modification of  $\tau_\gamma$  that is always a train track. The author considered this approach and is able to make appropriate adjustments for most bad types of complimentary regions; however, these local fixes do not always piece together to give a global train track.

Secondly, when  $\tau_\gamma$  is not a train track, it is often possible to find an invariant train track in the following way. Start with an essential, simple closed curve  $\sigma \subset S$ , and begin to push it around the loop  $\gamma$ . As things become more complicated, we may consider  $\sigma$  as track and use carrying moves from Figure 9 to simplify the picture whenever it seems expedient. Proceeding in this way with the sole objective of simplification will soon result in a track that exhibits the structure of  $\tau_\gamma$ . However, since bad complimentary regions can only result from certain pinching moves, a careful selection of carryings will ensure that the train track property is preserved. Thus, with some luck and perseverance, this procedure may eventually stabilize and result in an invariant train track for  $\mathcal{P}(\gamma)$ . In practice, this method is likely to produce a train track for any particular pushing curve. However, it is not clear in general how to select the carryings to guarantee that the process will always stabilize and yield an invariant train track.

## 4 The largest dilatations

Having established a general lower bound on the dilatation of a point-pushing homeomorphism, we now turn our attention to upper bounds. In this section we use the train track theory developed in §3 to bound  $\lambda_\gamma$  from above and complete the proof of Theorem 1.6.

### 4.1 The image of a loop

As in the proof of the lower bound, we will estimate dilatation by studying the action on simple closed curves and counting intersection numbers. Rather than lifting to the universal cover, as we did in §2, we will use train tracks to analyze curves directly on the surface. We begin with some general observations.

A simple closed curve is a smooth, closed 1-complex that naturally has the structure of a pretrack. Thus it makes sense to talk about simple closed curves being carried by a track. Let  $f \in \text{Mod}(S, p)$  be a pseudo-Anosov map, and suppose that  $\tau$  is an invariant track for  $f$ . We then have the  $|B| \times |B|$  incidence matrix  $M$  for the carrying  $f(\tau) \prec \tau$ , where  $B = \{b_i\}$  is the set of edges of  $\tau$ . If  $\alpha \subset S$  is a simple closed curve that is carried by  $\tau$ , then the carrying  $\alpha \prec \tau$  defines a  $|B| \times 1$  incidence matrix that we think of as weight vector  $v \in E_\tau$ . Since  $\tau$  is invariant under  $f$ , it follows that  $\tau$  carries  $f^k(\alpha)$ , and that the weight vector for the carrying  $f^k(\alpha) \prec f^k(\tau) \prec \tau$  is given by  $u = M^k v$ . This means that the curve  $f^k(\alpha)$  has an isotopic representative that is contained in the tie neighborhood of  $\tau$  and intersects the central tie over  $b_i$  exactly  $u(b_i)$  times. Conversely, such a representative for  $f^k(\alpha)$  may be constructed directly from the weight vector  $u$ : For each edge  $b_i$  of  $\tau$ , place  $u(b_i)$  disjoint segments running parallel to  $b_i$ . Because  $u \in E_\tau$  satisfies the switch conditions, the endpoints incident at each switch match up in pairs to produce a simple closed curve that is isotopic to  $f^k(\alpha)$ .

Now suppose that  $\eta \subset S$  is another simple closed curve. After adjusting  $\eta$  by an isotopy, we may assume that its intersections with  $\tau$  are all transverse and contained in the interiors of the branches  $b_i$ . Corresponding to this setup, we then have the  $1 \times |B|$  intersection matrix  $N = (N_{1j})$  given by  $N_{1j} = |\eta \cap b_j|$ . If  $a \subset S$  is the simple closed curve constructed from the weight vector  $u = M^k v$  as above, it follows that the cardinality of  $\eta \cap a$  is given by the dot product  $Nu$ . In particular, for all integers  $k \geq 0$ , the matrix products

$$NM^k v = Nu = |\eta \cap a| \geq i(\eta, f^k(\alpha)) \quad (4.1)$$

give convenient upper bounds on the intersection numbers of  $f^k(\alpha)$  and  $\eta$ .

## 4.2 An upper bound on dilatation

We now carry out such an estimate in the case of a point-pushing pseudo-Anosov map. Let  $\gamma: [0, 1] \rightarrow S$  be a filling curve on an oriented surface  $S = S_{g,n}$  that satisfies  $3g+n > 3$ . After adjusting  $\gamma$  by an isotopy, we may assume it is generic and that it realizes the minimum self-intersection number  $i(\gamma) > 0$  in Definition 1.4. It follows from Kra's theorem that the point-pushing homeomorphism  $\varphi_\gamma$  is pseudo-Anosov, and we consider its induced invariant pretrack  $\tau_\gamma$  as constructed in Definition 3.2. In order to apply the above discussion and relate intersection numbers to dilatation, we'll need to find an essential, simple closed curve that is carried by  $\tau_\gamma$ .

Suppose that  $i(\gamma) = n$ , and let  $q_1, \dots, q_n \in S$  be the  $n$  self-intersection points of  $\gamma$ . The path  $\gamma: [0, 1] \rightarrow S$  crosses each of these points twice, and they are ordered according to their first crossing times. Thus  $q_n$  need not be the intersection point that is crossed last, but rather it is the intersection point that is reached last. Using  $q_n \in \gamma$  as a break point, we form the decomposition  $\gamma = \alpha\delta\beta$ , where  $\alpha$  is the initial portion of  $\gamma$  from  $p = \gamma(0)$  to  $q_n$ ,  $\delta$  is the subsequent loop based at  $q_n$ , and  $\beta$  is the final segment from  $q_n$  back to  $p = \gamma(1)$ .

**Claim 4.2.** *The subloop  $\delta \subset \gamma$  is a simple closed curve that is carried by  $\tau_\gamma$ .*

*Proof.* For each  $1 \leq i \leq n$ , let  $0 < t_{i1} < t_{i2} < 1$  be the two preimages of  $q_i$  under  $\gamma$ . Thus  $\delta$  is the restriction of  $\gamma$  to the interval  $[t_{n1}, t_{n2}]$ . The ordering on the self-intersection

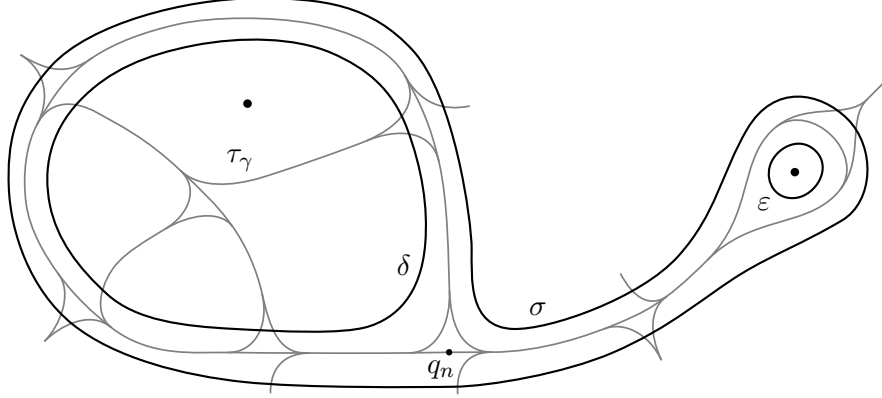


**Figure 13:** The track  $\tau_\gamma$  carries both  $\delta$  and  $\sigma$ ; at least one of these curves is essential.

points implies that  $t_{i1} < t_{n1}$  for all  $i < n$ . Therefore  $\delta$  is simple because it crosses each self-intersection point of  $\gamma$  at most once.

To prove that  $\delta \prec \tau_\tau$ , we must isotope  $\delta$  into the tie neighborhood of  $\tau_\gamma$  while keeping  $\delta$  transverse to the ties. We first argue that this condition already holds everywhere along  $\delta$  except near its basepoint  $q_n$ . This is clear away from the self-intersection points of  $\gamma$ , so consider the situation near a self-intersection point  $q_i$ . There is nothing to prove unless  $\delta$  crosses  $q_i$ , in which we have  $t_{n1} < t_{i2} < t_{n2}$ . Therefore  $\delta$  crosses  $q_i$  while travelling in the  $\gamma'(t_{i2})$  direction. Since, by Definition 3.2,  $\tau_\gamma$  contains a branch through  $q_i$  that is tangent to this direction, it follows that  $\delta$  is tangent to  $\tau_\gamma$  and that the carrying condition does hold near  $q_i$ .

It remains to adjust  $\delta$  near its basepoint  $q_n$  so that the carrying condition is satisfied. Notice that  $\delta$  leaves  $q_n$  going in the direction  $\gamma'(t_{n1})$  and returns travelling in the direction  $\gamma'(t_{n2})$ . These two edges of  $\gamma$  do not bound the inbound quadrant at  $q_n$ , so they are not separated by a cusp of  $\tau_\gamma$ . Using the notation of Figure 10, we find that one may isotope  $\delta$  so that it starts at the point  $a_1^+$ , leaves in the direction  $\gamma'(t_{n1})$ , travels once around  $\delta$  to the point  $a_2^-$ , and then follows the curved branch of  $\tau_\gamma$  back to  $a_1^+$ . The resulting curve, as illustrated in Figure 13, satisfies the carrying condition and proves that  $\delta \prec \tau_\gamma$ .  $\square$

**Lemma 4.3.** *There exists an essential, simple closed curve  $\sigma \subset S$  that is carried by  $\tau_\gamma$ .*

*Proof.* Any nullhomotopy of  $\delta$  would provide a homotopy between  $\gamma = \alpha\delta\beta$  and  $\alpha\beta$  that reduces the self-intersection number of  $\gamma$ . Since this is not possible,  $\delta$  is nontrivial. If  $\delta$  is also essential, then we are done by Claim 4.2. Otherwise,  $\delta$  is puncture-parallel and we construct an essential curve as follows.

The definition of  $q_n$  ensures that the restriction of  $\gamma$  to  $(t_{n1}, 1]$  crosses each self-intersection point  $q_i$  at most once. Therefore  $\beta = \gamma|_{[t_{n2}, 1]}$  is a simple path from  $q_n$  to  $p$  whose interior is disjoint from  $\delta$ . Note also that  $\beta$  is everywhere tangent to  $\tau_\gamma$  for the same reason that  $\delta$  is. Let  $\varepsilon \subset S$  be a simple closed curve around the marked point  $p$ ; for example,  $\varepsilon$  may be chosen to be the boundary of a small neighborhood of  $p$ . Using  $\beta$  as a guide, form the connect sum

$\sigma = \delta \# \varepsilon$  of  $\delta$  with  $\varepsilon$ . More precisely, remove an interval from each loop and glue in two parallel copies of  $\beta$  to form a single closed curve that is homotopic to  $\delta\beta\varepsilon\bar{\beta}$ . As illustrated in Figure 13, the structure of the pretrack near  $q_n$  and  $p$  ensures that  $\sigma$  is carried by  $\tau_\gamma$ . Furthermore,  $\sigma$  is simple because it is the union of four simple segments whose interiors are disjoint.

Recalling that the marked point  $p$  counts as a puncture, we see that  $\delta$  and  $\varepsilon$  are both puncture-parallel, separating curves. Therefore  $\sigma$  separates  $S$  into two components, one of which is a twice-punctured disk. Since  $S$  is neither  $S_{0,2}$  nor  $S_{0,3}$ , the other component of  $S \setminus \sigma$  cannot be a disk or a once-punctured disk. This proves that  $\sigma$  is essential.  $\square$

Now that we have found an essential, simple closed curve that is carried by  $\tau_\gamma$ , we may proceed to estimate intersection numbers and bound the dilatation  $\lambda_\gamma$ . Let  $B = \{b_i\}$  be the set of edges of  $\tau_\gamma$ , and let  $M$  be the  $|B| \times |B|$  incidence matrix for the carrying  $\varphi_\gamma(\tau_\gamma) \prec \tau_\gamma$  given in Proposition 3.3. Take  $\sigma \subset S$  to be the essential curve from Lemma 4.3, and let  $v \in E_{\tau_\gamma}$  be the  $|B| \times 1$  weight vector associated to the carrying  $\sigma \prec \tau_\gamma$ .

Let  $B' \subset B$  be the set of  $3(i(\gamma) + 1)$  distinguished branches defined after the proof of Proposition 3.3, and let  $E'_{\tau_\gamma} \subset \mathbb{R}^{B'}$  be the image of  $E_{\tau_\gamma}$  under the projection  $P: \mathbb{R}^B \rightarrow \mathbb{R}^{B'}$ . Since any weight vector is determined by its values on these edges, there is a linear bijection  $Q: E'_{\tau_\gamma} \rightarrow E_{\tau_\gamma}$  that inverts  $P$  (see the discussion in §3.1). This map may be realized, in a non-unique way, by a  $|B| \times |B'|$  matrix whose  $i^{\text{th}}$  row expresses a weight function's value on  $b_i$  as a linear combination of its values on the branches  $b' \in B'$ . Since the action of  $\varphi_\gamma$  on  $E'_{\tau_\gamma}$  is given by the  $|B'| \times |B'|$  incidence matrix  $M_\gamma$  in Corollary 3.4, we evidently have that  $M = QM_\gamma P$ .

Let  $v' = Pv$  denote the projection of  $v$  to  $E'_{\tau_\gamma}$ . This may be expressed as a vector  $v' = (v'_1, \dots, v'_l)$ , where  $l = |B'|$ . The entries in  $v'$  are nonnegative integers, and we let  $r = \max_i \{v'_i\} \geq 0$  denote the largest entry in  $v'$ . According to Corollary 3.4,  $M_\gamma$  is a product of  $2 \cdot i(\gamma)$  matrices of the form  $A_i^{\text{right}}$  or  $A_i^{\text{left}}$ ; as such, it cannot be too big.

**Lemma 4.4.** *If  $D$  is a product of  $k \geq 0$  matrices of the form  $A_i^{\text{right}}$  or  $A_i^{\text{left}}$  given in Corollary 3.4, then every entry of the vector  $Dv'$  is bounded above by  $3^k r$ .*

*Proof.* If  $A = (A_{ij})$  is any matrix of the specified form, then each row of  $A$  has sum at most 3. Assuming inductively that the claim holds for any given  $k$ -fold product  $D$ , we find that

$$(ADv')_i = \sum_j A_{ij} (Dv')_j \leq \sum_j A_{ij} 3^k r = 3^k r \sum_j A_{ij} \leq 3^k r \cdot 3.$$

Therefore the claim also holds for the  $(k + 1)$ -fold product  $AD$ .  $\square$

We now give a general upper bound on the dilatation  $\lambda_\gamma$ . Together with Theorem 2.20, the following result completes the proof of Theorem 1.6.

**Theorem 4.5** (The upper bound). *Let  $S = S_{g,n}$  be a surface satisfying  $3g + n > 3$ , and let  $\gamma: [0, 1] \rightarrow S$  be a filling loop. Then the dilatation  $\lambda_\gamma$  of the mapping class  $\mathcal{P}(\gamma)$  is bounded above by  $9^{i(\gamma)}$ .*

*Proof.* Retaining the notation of the preceding discussion, we see that for  $k \geq 0$  the weight vector associated to the carrying  $\varphi_\gamma^k(\sigma) \prec \tau_\gamma$  is given by the matrix product

$$M^k v = Q M_\gamma^k v'.$$

Let  $\eta \subset S$  be any essential, simple closed curve that is transverse to the track  $\tau_\gamma$  and disjoint from the switches. We may then form the  $1 \times |B|$  intersection matrix  $N = (N_{1j})$  whose entries are given by  $N_{1j} = |\eta \cap b_j|$ . It now follows from (4.1) that the intersection numbers  $i(\varphi_\gamma^k(\sigma), \eta)$  are bounded above by the following matrix products

$$i(\varphi_\gamma^k(\sigma), \eta) \leq N M^k v = N Q M_\gamma^k v'.$$

Let  $d$  denote the sum of the entries in the  $1 \times |B|$  matrix  $NQ$ . By Corollary 3.4,  $M_\gamma^k$  is a product of  $2k \cdot i(\gamma)$  matrices of the form  $A_i^{\text{right}}$  or  $A_i^{\text{left}}$ . Therefore, we may apply Lemma 4.4 and conclude that

$$i(\varphi_\gamma^k(\sigma), \eta) \leq \sum_j (NQ)_j (M_\gamma^k v')_j \leq 3^{2k i(\gamma) r} \sum_j (NQ)_j = dr 3^{2k i(\gamma)}.$$

Dividing by the dilatation, we see that the inequality

$$\frac{i(\varphi_\gamma^k(\sigma), \eta)}{\lambda_\gamma^k} \leq dr \left( \frac{9^{i(\gamma)}}{\lambda_\gamma} \right)^k$$

holds for all integers  $k \geq 0$ . Since  $\sigma$  and  $\eta$  are both essential, simple closed curves, Theorem 2.2 implies that the left hand side has a positive limit as  $k$  tends to infinity. It follows that right hand side is bounded away from zero, which necessitates  $\lambda_\gamma \leq 9^{i(\gamma)}$ .  $\square$

**Remark 4.6.** It seems unlikely that this upper bound is optimal. When  $\tau$  is a reasonable train track, the matrix products in (4.1) actually grow like  $i(f^k(\alpha), \eta)$  and  $\lambda_f^k$ . However, if  $\tau$  has complimentary monogons, then the loops constructed from the weight vectors  $M^k v$  will be very inefficient representatives of  $f^k(\alpha)$ , and the dot products  $N M^k v$  will drastically overestimate the intersection numbers  $i(f^k(\alpha), \eta)$ . Indeed, in order to minimize the cardinality of  $f^k(\alpha) \cap \eta$ , one would need to straighten the representative loop  $f^k(\alpha)$  by pulling its strands across the complimentary monogons.

In the case of a pushing curve  $\gamma \subset S$  with very high self-intersection number, Euler characteristic considerations imply that  $\tau_\gamma$  will have on the order of  $\chi(S) + i(\gamma)/2$  complimentary monogons and nullgons. Consequently, we expect that our upper bound is far from sharp when  $i(\gamma)$  is large.

**Remark 4.7.** The above remark illustrates why the pretrack  $\tau_\gamma$  is not able to provide a general lower bound on the dilatation  $\lambda_\gamma$ . Namely, without the train track condition on complimentary components, the pretrack  $\tau_\gamma$  does not aid in calculating the infimum in the Definition 2.1 of intersection number. The pretrack  $\tau_\gamma$  does provide an upper bound on  $\lambda_\gamma$  precisely because one can bound  $i(\varphi_\gamma^k(\alpha), \eta)$  from above without taking infimums.

The following simple argument shows that any general upper bound must be at least on the order of  $\exp(i(\gamma)^{1/2})$ . Let  $\mu \subset S$  be any filling curve on  $S$  and let  $\lambda = \lambda_\mu$  be the dilatation of the pseudo-Anosov mapping class  $\mathcal{P}(\mu)$ . For example,  $\mu$  may be chosen to fill  $S$  efficiently so that  $i(\mu)$  is relatively small. Powers  $\gamma = \mu^k$  of  $\mu$  may then be represented by closed loops that are built by concatenating  $k$  offset copies of  $\mu$ . These offset copies contribute  $k^2$  intersection points for each self-intersection point of  $\mu$ , so we have the upper bound

$$i(\gamma) = i(\mu^k) \leq k^2 i(\mu) + (k - 1) \leq 2k^2 i(\mu).$$

Since the dilatation of  $\mathcal{P}(\gamma)$  is given by  $\lambda_\gamma = \lambda^k$ , the above inequality implies that

$$\lambda_\gamma = \lambda^k \geq \lambda^{\sqrt{i(\gamma)/2i(\mu)}} = \left( \lambda^{1/\sqrt{2i(\mu)}} \right)^{\sqrt{i(\gamma)}}.$$

In particular, there are infinite families of point-pushing pseudo-Anosovs  $\mathcal{P}(\gamma)$  whose dilatations grow faster than  $\exp(C(i(\gamma))^{1/2})$ . Therefore, fixing the self-intersection number  $i(\gamma)$ , we see that the optimal upper bound on  $\lambda_\gamma$  must lie somewhere between  $\exp(C(i(\gamma))^{1/2})$  and  $\exp(Ci(\gamma))$ .

## 5 Bounds on least dilatations

It remains to consider the least dilatations attained in the point-pushing subgroup  $\text{PP}(S)$ . In this section, we use the tools of §3 to examine two concrete examples on the closed surface  $S_g$  of genus  $g$ . These calculations will prove Theorems 1.10 and 1.12.

### 5.1 A low-dilatation example

Recall from (1.8) that  $L(\text{PP}(S)) = \inf \{\text{spec}(\text{PP}(S))\}$  is the least element in the spectrum of all entropies of point-pushing pseudo-Anosov homeomorphisms on the surface  $S$ . Our goal in this subsection is to bound the least dilatation  $L(\text{PP}(S_g))$  on the closed surface of genus  $g$  and to estimate its asymptotic dependence on genus. More precisely, we prove the following.

**Theorem 1.10.** *For the closed surface  $S_g$  of genus  $g \geq 2$ , we have*

$$\frac{1}{5} \log(2g) \leq L(\text{PP}(S_g)) < g \log(11).$$

In light of Kra's Theorem 1.2, the inequalities in (1.9) and Theorem 1.6 together imply that  $\log(\lambda_\gamma) \geq \frac{1}{5} \log(2g)$  for every pseudo-Anosov  $\mathcal{P}(\gamma) \in \text{PP}(S_g)$ . This establishes the first inequality. To bound  $L(\text{PP}(S_g))$  from above, it suffices to consider an example.

**Example 5.1.** Consider the surface  $S_2$  of genus 2, and let  $\gamma_0: [0, 1] \rightarrow S_2$  be the closed curve illustrated in Figure 14(a). Notice that  $\gamma_0$  has three self-intersection points and that  $S_2 \setminus \gamma_0$  is a single topological disk. Applying Definition 3.2 to  $\gamma_0$  produces the invariant pretrack  $\tau_{\gamma_0}$  shown in Figure 14(b). Since the complimentary components of  $\tau_{\gamma_0}$  consist of five trigons and one punctured monogon,  $\tau_{\gamma_0}$  is, in fact, a train track.

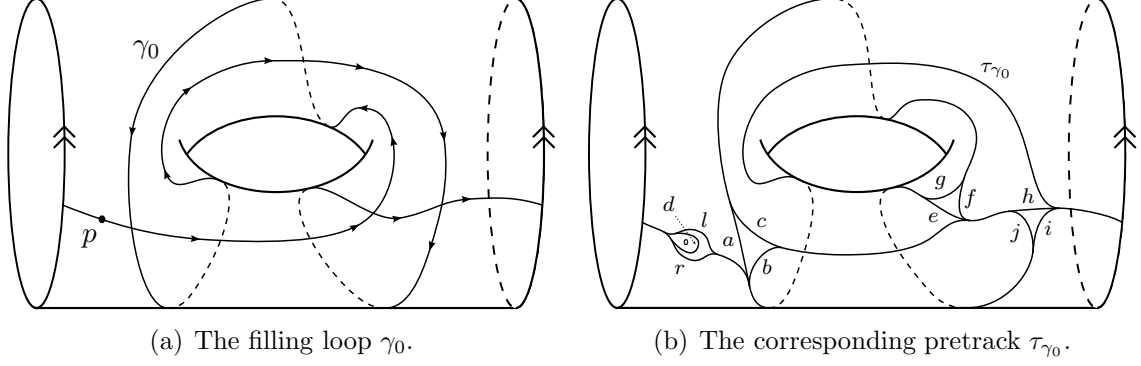


**Figure 14:** A point-pushing example on  $S_2$  (the left and right boundaries are identified).

Assigning weights as indicated in Figure 14(b) determines a weight function on  $\tau_{\gamma_0}$ . If  $v_e = (d, l, r)$  denotes the vector of weights around the eye and  $v = (a, b, c, e, f, g, h, i, j)$  denotes the vector of weights at the intersection points of  $\gamma_0$ , then Corollary 3.4 implies that the mapping class  $\mathcal{P}(\gamma_0) \in \text{Mod}(S_2, p)$  transforms the weight vector  $(v_e, v)$  according to the block matrix

$$\begin{pmatrix} A & B \\ C & D \end{pmatrix} = \begin{pmatrix} \begin{pmatrix} 11 & 8 & 2 \\ 0 & 1 & 0 \\ 0 & 0 & 1 \end{pmatrix} & \begin{pmatrix} 5 & 0 & 5 & 4 & 4 & 0 & 1 & 0 & 1 \\ 1 & 1 & 0 & 0 & 0 & 0 & 0 & 0 & 0 \\ 0 & 0 & 0 & 0 & 0 & 0 & 1 & 1 & 0 \end{pmatrix} \\ \begin{pmatrix} 2 & 2 & 0 \\ 2 & 2 & 0 \\ 0 & 0 & 0 \\ 6 & 4 & 2 \\ 2 & 2 & 0 \\ 0 & 0 & 0 \\ 10 & 8 & 2 \\ 6 & 4 & 2 \\ 0 & 0 & 0 \end{pmatrix} & \begin{pmatrix} 2 & 0 & 2 & 2 & 1 & 0 & 0 & 0 & 0 \\ 1 & 1 & 0 & 0 & 1 & 0 & 0 & 0 & 0 \\ 0 & 0 & 0 & 0 & 0 & 1 & 0 & 0 & 0 \\ 2 & 0 & 2 & 2 & 2 & 0 & 2 & 0 & 1 \\ 2 & 0 & 2 & 1 & 1 & 0 & 0 & 0 & 1 \\ 0 & 0 & 0 & 0 & 0 & 0 & 0 & 1 & 0 \\ 6 & 0 & 5 & 3 & 3 & 0 & 2 & 0 & 2 \\ 2 & 0 & 3 & 3 & 3 & 0 & 1 & 1 & 0 \\ 0 & 1 & 0 & 0 & 0 & 0 & 0 & 0 & 0 \end{pmatrix} \end{pmatrix}. \quad (5.2)$$

The surface  $S_g$  of genus  $g$  is a natural  $(g - 1)$ -fold, cyclic cover of  $S_2$ , which one may visualize as follows: Take  $g - 1$  copies of the torus with two boundary components, as in Figure 14(a), and glue them end-to-end to form a ring; the result is a rotationally symmetric surface with  $g - 1$  genera cyclically arranged around one central genus. The covering map  $S_g \rightarrow S_2$  is the quotient by the  $\mathbb{Z}/(g - 1)\mathbb{Z}$  rotational symmetry. We now lift  $\gamma_0^{g-1} \in \pi_1(S_2)$  to a filling loop  $\gamma$  on  $S_g$  and consider the corresponding mapping class  $\mathcal{P}(\gamma) \in \text{PP}(S_g)$ . As illustrated in Figure 15, the induced invariant pretrack  $\tau_\gamma$  is a train track that cuts  $S_g$  into a single punctured monogon and  $4g - 3$  trigons—one at each of the  $3g - 3$  self-intersection points of  $\gamma$ , one for each of the  $g - 1$  components of  $S_g \setminus \gamma$ , and one surrounding the punctured monogon. Although the mapping class  $\mathcal{P}(\gamma)$  is not a lift of  $\mathcal{P}(\gamma_0)$ , we note that  $\gamma \subset S_g$  is precisely the preimage of  $\gamma_0 \subset S_2$  and that  $\tau_\gamma$  is essentially just the preimage of  $\tau_{\gamma_0}$ .

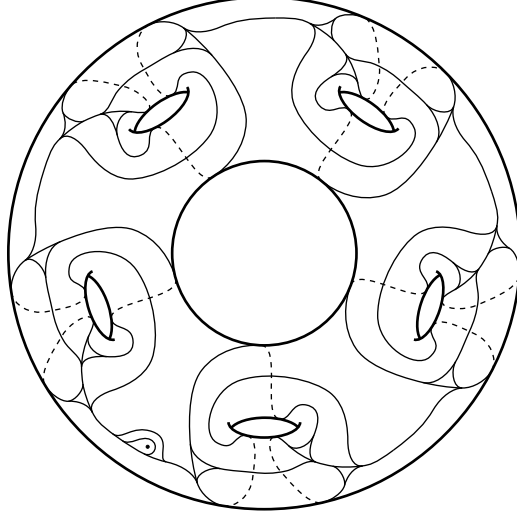


**Figure 15:** The invariant train track  $\tau_\gamma$  for  $\mathcal{P}(\gamma) \in \text{Mod}(S_g, p)$ .

We now calculate the action of  $\mathcal{P}(\gamma)$  on the weight vector

$$w = (v_e, v_1, v_2, \dots, v_{g-1}), \quad \text{where} \quad v_i = (a_i, b_i, c_i, e_i, f_i, g_i, h_i, i_i, j_i)$$

records the weights along the  $i^{\text{th}}$  copy of  $\gamma_0$  and  $v_e = (d, l, r)$  records the weights in the eye of the track. Pushing the marked point along the  $i^{\text{th}}$  copy of  $\gamma_0$  transforms the weight vectors  $v_e$  and  $v_i$  according to (5.2) and leaves the other vectors  $v_j$  unchanged. Therefore, the full action of  $\mathcal{P}(\gamma)$  on the weight vector  $w$  is given by the block matrix product

$$\begin{pmatrix} A & 0 & 0 & \cdots & B \\ 0 & I & 0 & \cdots & 0 \\ 0 & 0 & I & \cdots & 0 \\ \vdots & \vdots & \vdots & \ddots & \vdots \\ C & 0 & 0 & \cdots & D \end{pmatrix} \cdots \begin{pmatrix} A & 0 & B & \cdots & 0 \\ 0 & I & 0 & \cdots & 0 \\ C & 0 & D & \cdots & 0 \\ \vdots & \vdots & \vdots & \ddots & \vdots \\ 0 & 0 & 0 & \cdots & I \end{pmatrix} \begin{pmatrix} A & B & 0 & \cdots & 0 \\ C & D & 0 & \cdots & 0 \\ 0 & 0 & I & \cdots & 0 \\ \vdots & \vdots & \vdots & \ddots & \vdots \\ 0 & 0 & 0 & \cdots & I \end{pmatrix}. \quad (5.3)$$

Multiplying this out, we see that the incidence matrix for the carrying  $\mathcal{P}(\gamma)(\tau_\gamma) \prec \tau_\gamma$  is

$$M_\gamma = \begin{pmatrix} A^{g-1} & A^{g-2}B & A^{g-3}B & \cdots & A^2B & AB & B \\ C & D & 0 & \cdots & 0 & 0 & 0 \\ CA & CB & D & \cdots & 0 & 0 & 0 \\ \vdots & \vdots & \vdots & \ddots & \vdots & \vdots & \vdots \\ CA^{g-3} & CA^{g-4}B & CA^{g-5}B & \cdots & CB & D & 0 \\ CA^{g-2} & CA^{g-3}B & CA^{g-4}B & \cdots & CAB & CB & D \end{pmatrix}. \quad (5.4)$$

An elementary calculation shows that the first row and first column of  $M_\gamma^3$  have strictly positive entries. This implies that  $M_\gamma^6$  has strictly positive entries and, consequently, that  $M_\gamma$

is a Perron–Frobenius matrix. According to Lemma 3.1, it now follows that the dilatation  $\lambda_\gamma$  of  $\mathcal{P}(\gamma)$  is bounded above by the largest row sum of  $M_\gamma$ . Using the fact that

$$A^n = \begin{pmatrix} 11^n & 8q(n) & 2q(n) \\ 0 & 1 & 0 \\ 0 & 0 & 1 \end{pmatrix}, \quad \text{where} \quad q(n) = \sum_{j=0}^{n-1} 11^j = \frac{11^n - 1}{11 - 1} \leq \frac{1}{10} 11^n, \quad (5.5)$$

a direct comparison of the relevant matrix blocks shows that the first row of  $M_\gamma$  has the largest sum. Indeed, since the first row of  $A^{n-1}B$  sums to  $20q(n)$ , we may easily calculate the first row sum of  $M_\gamma$  and conclude that

$$\begin{aligned} \lambda_\gamma &\leq 11^{g-1} + 10q(g-1) + \sum_{j=1}^{g-1} 20q(j) \\ &\leq 11^{g-1} + 11^{g-1} + 2 \sum_{j=1}^{g-1} 11^j \\ &= 2(11^{g-1}) + 2\left(\frac{11^g - 1}{11 - 1} - 1\right) \\ &< \frac{2}{5} 11^g. \end{aligned}$$

Since  $\mathcal{P}(\gamma) \in \text{PP}(S_g)$ , this example shows that

$$L(\text{PP}(S_g)) \leq \log(\lambda_\gamma) < g \log(11)$$

and completes the proof of Theorem 1.10. □

## 5.2 Least dilatation vs. self-intersection number

In keeping with the theme that the geometric structure of  $\gamma$  controls the dynamical complexity of  $\mathcal{P}(\gamma)$ , we now refine our investigation of least dilatations to account for the dependence on self-intersection number. Accordingly, we restrict our attention to the filtration

$$\text{PP}_k(S) = \{\mathcal{P}(\gamma) \mid \gamma \in \pi_1(S) \text{ with } i(\gamma) = k\}$$

of  $\text{PP}(S)$  and strive to understand the least pseudo-Anosov dilatation achieved by pushing around a curve with prescribed self-intersection number. While Theorem 1.6 gives general upper and lower bounds on the whole spectrum  $\text{spec}(\text{PP}_k(S))$ , the following theorem establishes a better upper bound on the least dilatation in  $\text{PP}_k(S_g)$  and proves that, asymptotically,  $L(\text{PP}_k(S_g))$  grows like  $\log(k)$ .

**Theorem 1.12.** *Let  $S_g$  be a closed surface of genus  $g \geq 3$ . For any integer  $k \geq 3g - 1$ , we have that*

$$\frac{1}{5} \log(k + 1) \leq L(\text{PP}_k(S_g)) < \log(k) + g \log(11).$$

This lower bound is a direct consequence of Theorem 1.6; the upper bound results from the following family of examples.

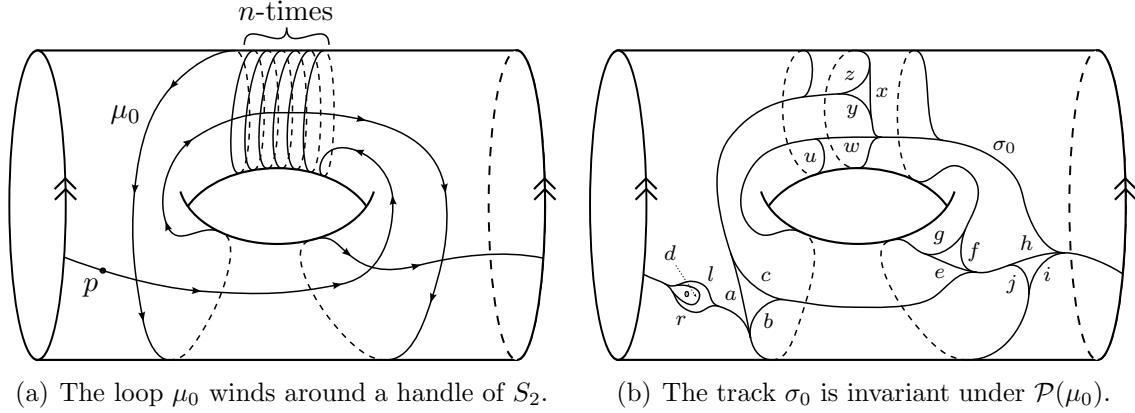


**Figure 16:** A more complicated example on  $S_2$ .

**Example 5.6.** For fixed numbers  $n \geq 2$  and  $g \geq 3$ , we will construct a filling curve on  $S_g$  whose self-intersection number depends on  $n$ . As in Example 5.1, our construction uses the cyclic covering  $S_g \rightarrow S_2$  and the filling curve  $\gamma_0 \subset S_2$  shown in Figure 14(a). To adjust the self-intersection number, we, also consider the modified loop  $\mu_0: [0, 1] \rightarrow S_2$  illustrated in Figure 16(a)— $\mu_0$  is identical to  $\gamma_0$  except in that it winds around a handle of  $S_2$  an additional  $n$  times; as such, it has self-intersection number  $i(\mu_0) = n + 3$ .

The winding structure of  $\mu_0$  creates complimentary monogons in the corresponding pre-track  $\tau_{\mu_0} \subset S_2$ , so we need to work harder to find an invariant train track for  $\mathcal{P}(\mu_0)$ . Guided by the general procedure discussed at the end of §3.2, we instead consider the track  $\sigma_0 \subset S_2$  depicted in Figure 16(b); it cuts  $S_2$  into six trigons, two bigons, one monogon, and one punctured monogon. Notice that  $\sigma_0$  has the same basic structure of  $\tau_{\gamma_0}$  from Figure 14(b), but with additional branches to deal with the winding in  $\mu_0$ .

**Claim 5.7.** *The track  $\sigma_0 \subset S_2$  is invariant under  $\mathcal{P}(\mu_0)$ , that is,  $\mathcal{P}(\mu_0)(\sigma_0) \prec \sigma_0$ .*

*Proof.* The proof is in the same spirit as Proposition 3.3: as the marked point travels along  $\mu_0$ , it pushes the track  $\sigma_0$  out of its way while we continually use isotopy and carrying moves (c.f. Figure 9) to simplify the picture. After pushing the marked point once around  $\mu_0$ , the resulting track will be identical to  $\sigma_0$ .

Let  $C \subset S_2$  be a compact cylinder containing all of the extra winding in the path  $\mu_0$  so that the paths  $\gamma_0$  and  $\mu_0$  and tracks  $\tau_{\gamma_0}$  and  $\sigma_0$  both agree on  $X = S_2 \setminus C$ . It follows that, while the marked point is in  $X$ , we may apply the same simplifying moves as in the carrying  $\mathcal{P}(\gamma_0)(\tau_{\gamma_0}) \prec \tau_{\gamma_0}$  from Proposition 3.3. Namely, when the marked point travels along an edge of  $\mu_0 \cap X$ , the eye of the track simply slides along the corresponding branch of  $\sigma_0 \cap X$ , and when the marked point pushes through a self-intersection point in  $X$ , we perform the usual carrying from Figure 12.

The only difficulty, then, is to navigate the portions of  $\mu_0$  that lie in  $C$ ; once this is done, the claim will follow. Notice that, in its journey around  $\mu_0$ , the marked point interacts with  $C$  exactly twice. The first time, it winds  $n$  times around  $C$  as it progresses from the right boundary component to the left; the second time, the marked point simply traverses  $C$  from

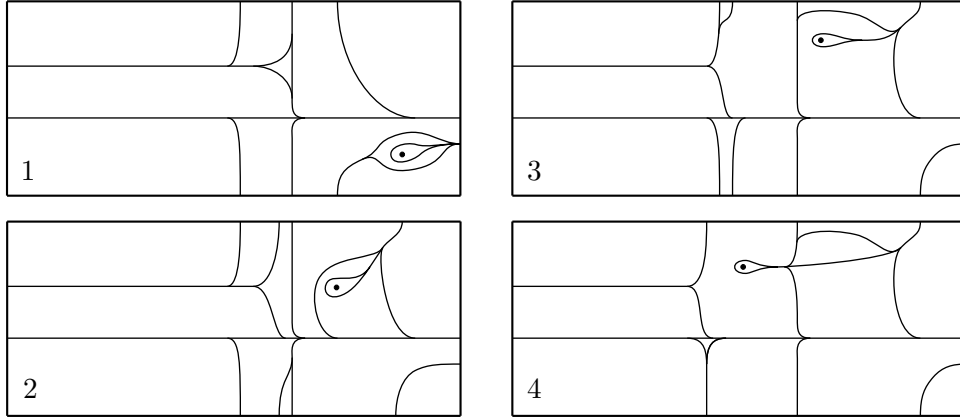


**Figure 17:** The carrying moves for navigating a winding path – part 1.

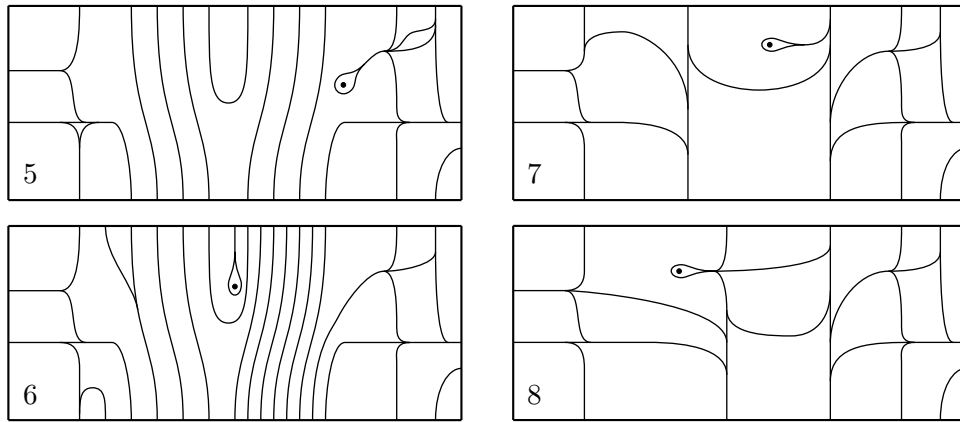


**Figure 18:** The carrying moves for navigating a winding path – part 2.

left to right. The necessary carryings for these sections are a bit involved, so we demonstrate them explicitly in a sequence of 17 snapshots spanning Figures 17 through 20. In the figures, the cylinder  $C$  is depicted as a rectangle with top and bottom edges identified.

The first time the marked point crosses  $C$  is illustrated in Figures 17 through 19. Frame 1 shows the initial situation after the marked point, surrounded by the eye of the track, enters  $C$  from the right. In frames 2 and 3, the marked point passes around the back of  $C$ , and we use a handful of slide moves to pull branches of the track apart. In frame 4, the marked point pushes through a branch of the track, which we then pinch and collapse onto the monogon containing the marked point.

The next step is for the marked point to wind around  $C$ ; however, the long horizontal branch of the track is blocking the way. In frame 5, we clear a path for the marked point by twisting this branch around  $C$  so that, in frame 6, the marked point is able to wind  $n$  times around  $C$  by moving along the space between these twistings. In frame 7, we pinch many of these branches together and collapse the resulting bigons. The marked point then pushes through another branch of the track in frame 8.

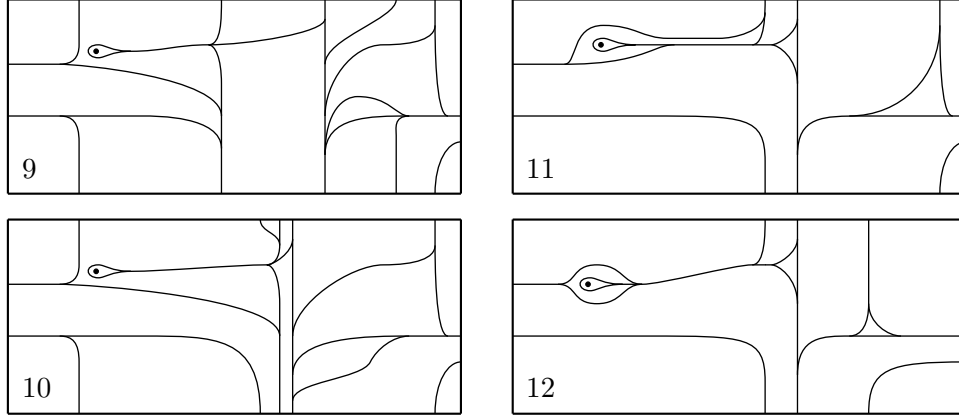


**Figure 19:** The carrying moves for navigating a winding path – part 3.

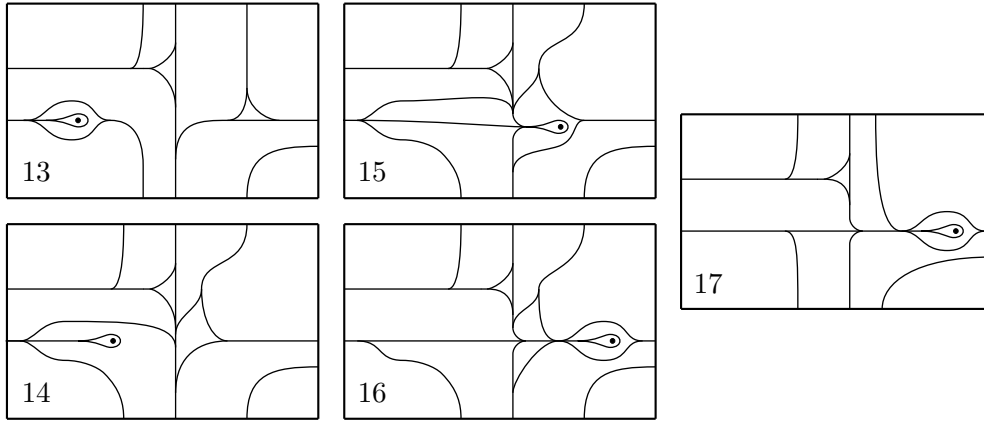


**Figure 20:** The carrying moves for navigating a winding path – part 4.

All that remains is to repackage the branches into an orderly configuration. In frame 9, we collapse two bigons and use slide moves to pull apart some of the branches on right side of  $C$ . In frames 10 and 11, we collapse two more bigons and use slides to combine several branches together. Frame 12 shows the eye of the track reformed and ready to exit through the left boundary component of  $C$ .

The second time the marked point crosses  $C$  is illustrated in Figure 20, with the initial configuration depicted in frame 13. In frame 14, we use slide moves to pull apart branches and make room for the marked point to move forward. In frame 15, the marked point pushes through the vertical branch, and in frame 16, a bigon is collapsed while branches are pinched to form an eye around the marked point. Upon collapsing two more bigons, frame 17 shows the eye of the track ready to exit  $C$ , leaving the branches in  $C$  exactly how they started in frame 1. This completes the proof that  $\mathcal{P}(\mu_0)(\sigma_0) \prec \sigma_0$ .  $\square$

As in Example 5.1, a weight function on  $\sigma_0$  is determined by the weight vectors

$$v_e = (d, l, r) \quad \text{and} \quad v = (a, b, c, e, f, g, h, i, j, u, w, x, y, z)$$

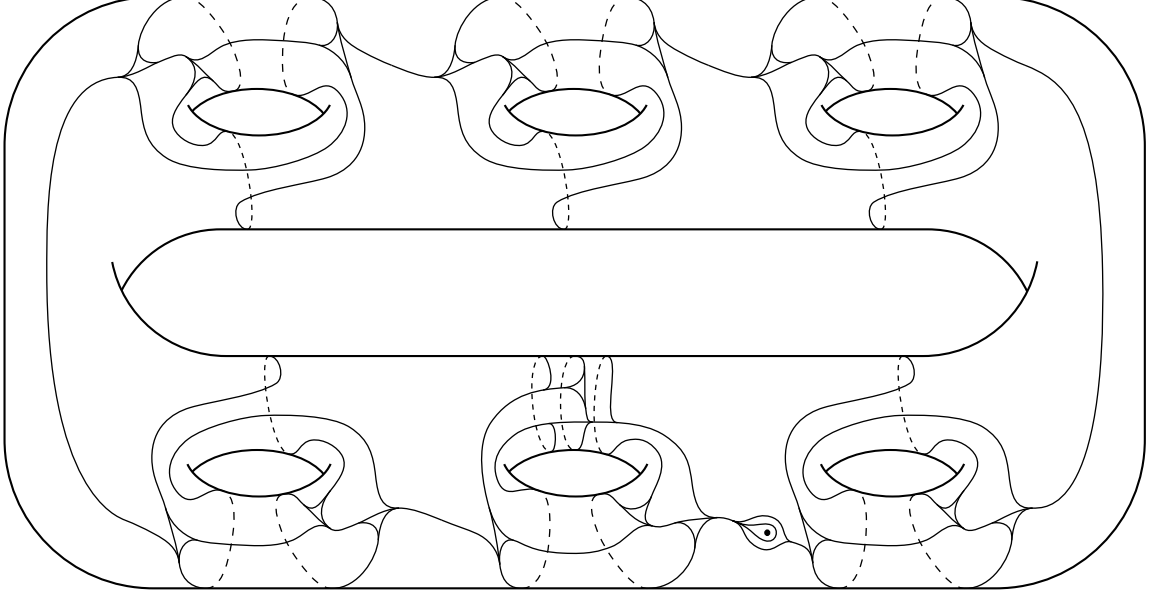


**Figure 21:** The bigon track  $\sigma$  is invariant under  $\mathcal{P}(\mu) \in \text{Mod}(S, p)$ .

that are indicated in Figure 16(b). By carefully keeping track of these weights throughout the carryings in Figures 12 and 17–20, one finds that pushing the marked point around  $\mu_0$  transforms the weight vector  $(v_e, v)$  according to the block matrix

$$\begin{pmatrix} \tilde{A} & \tilde{B} \\ \tilde{C} & \tilde{D} \end{pmatrix} = \begin{pmatrix} \begin{pmatrix} 6n+11 & 6n+11 & 0 \\ 0 & 0 & 0 \\ 0 & 0 & 0 \end{pmatrix} & \begin{pmatrix} 6n+8 & 3 & 6n+5 & 6n+4 & 6n+3 & 0 & 1 & 0 & 1 & 3 & 9n-4 & 6n+4 & 9n-1 & 9n-7 \\ 0 & 0 & 0 & 0 & 0 & 1 & 0 & 0 & 0 & 0 & 0 & 0 & 0 & 0 \\ 0 & 0 & 0 & 0 & 0 & 1 & 0 & 1 & 1 & 0 & 0 & 1 & 2 & 1 & 1 \end{pmatrix} \\ \begin{pmatrix} 2 & 2 & 0 \\ 2 & 2 & 0 \\ 0 & 0 & 0 \\ 4n+6 & 4n+6 & 0 \\ 2 & 2 & 0 \\ 0 & 0 & 0 \\ 4n+10 & 4n+10 & 0 \\ 4n+6 & 4n+6 & 0 \\ 0 & 0 & 0 \\ 0 & 0 & 1 \\ 6 & 5 & 0 \\ 2n-2 & 2n-2 & 0 \\ 0 & 0 & 0 \\ 2 & 3 & 0 \end{pmatrix} & \begin{pmatrix} 2 & 0 & 2 & 2 & 2 & 0 & 0 & 0 & 0 & 1 & 2n & 2 & 2n & 2n-2 \\ 1 & 1 & 0 & 0 & 0 & 0 & 0 & 0 & 0 & 1 & 0 & 0 & 0 & 0 \\ 0 & 0 & 0 & 0 & 0 & 0 & 0 & 0 & 0 & 0 & 0 & 0 & 1 & 1 \\ 4n+4 & 2 & 4n+2 & 4n+2 & 4n+2 & 0 & 2 & 0 & 1 & 2 & 6n-2 & 4n+4 & 6n & 6n-4 \\ 2 & 0 & 2 & 1 & 1 & 0 & 0 & 0 & 1 & 0 & 0 & 0 & 0 & 0 \\ 0 & 0 & 0 & 0 & 0 & 0 & 0 & 1 & 0 & 0 & 0 & 0 & 0 & 0 \\ 4n+8 & 2 & 4n+5 & 4n+3 & 4n+3 & 0 & 2 & 0 & 2 & 2 & 6n-2 & 4n+4 & 6n & 6n-4 \\ 4n+4 & 2 & 4n+3 & 4n+3 & 4n+3 & 0 & 1 & 1 & 0 & 2 & 6n-2 & 4n+4 & 6n & 6n-4 \\ 0 & 1 & 0 & 0 & 0 & 0 & 0 & 0 & 0 & 0 & 0 & 0 & 0 & 0 \\ 0 & 0 & 0 & 0 & 0 & 0 & 0 & 0 & 0 & 0 & 0 & 0 & 0 & 0 \\ 3 & 1 & 2 & 2 & 2 & 0 & 0 & 0 & 0 & 2 & 2n & 2 & 2n & 2n-2 \\ 2n-2 & 0 & 2n-2 & 2n-2 & 2n-2 & 0 & 0 & 0 & 0 & 0 & n-1 & 2n-1 & n-1 & n-1 \\ 0 & 0 & 0 & 0 & 0 & 0 & 0 & 0 & 0 & 0 & n-1 & 0 & n & n-1 \\ 3 & 1 & 2 & 2 & 2 & 0 & 0 & 0 & 0 & 0 & n & 2 & n+1 & n \end{pmatrix} \end{pmatrix}. \quad (5.8)$$

We are now ready to construct the example. Using the cyclic cover,  $S_g \rightarrow S_2$ , the loop  $\gamma_0^{g-2} \mu_0 \in \pi_1(S_2)$  lifts to a filling loop  $\mu \subset S_g$ . Alternately, if  $T$  denotes the torus with two boundary components, then  $S_g$  may be attained by glueing  $g - 1$  copies of  $T$  together to form a ring, and  $\mu \subset S_g$  may be constructed by concatenating copies of the arc  $\gamma_0 \subset T$  along the first  $g - 2$  copies of  $T$  with the arc  $\mu_0 \subset T$  on the last copy of  $T$ . Note that  $i(\mu) = 3(g - 1) + n$ . Similarly, we may build an invariant track  $\sigma \subset S_g$  for  $\mathcal{P}(\mu) \in \text{Mod}(S_g, p)$  by concatenating  $g - 2$  copies of  $\tau_{\gamma_0} \subset T$  with one copy of  $\sigma_0 \subset T$ . As shown in Figure 21,  $\sigma$  is a bigon track that cuts  $S_g$  into  $(2 + 3(g - 1) + (g - 3) + 1)$  trigons, four bigons, and one punctured monogon (each of the  $g - 1$  pieces of  $\sigma$  contributes three trigons, the copy of  $\sigma_0$  contributes two additional trigons and two bigons, the eye contributes a trigon and a punctured monogon, and the junctions between the pieces form either bigons or trigons).

The track  $\sigma$  allows us to estimate the dilatation of  $\mathcal{P}(\mu)$  as follows. The action of  $\mathcal{P}(\mu)$  on the weight space of  $\sigma$  is determined by a matrix product that is analogous to the one in (5.3). Using (5.8) together with (5.4), we find that the incidence matrix  $M_\mu$  for the carrying  $\mathcal{P}(\mu)(\sigma) \prec \sigma$  is given by the block matrix product

$$\begin{pmatrix} \tilde{A} & 0 & 0 & \cdots & 0 & \tilde{B} \\ 0 & I & 0 & \cdots & 0 & 0 \\ 0 & 0 & I & \cdots & 0 & 0 \\ \vdots & \vdots & \vdots & \ddots & \vdots & \vdots \\ 0 & 0 & 0 & \cdots & I & 0 \\ \tilde{C} & 0 & 0 & \cdots & 0 & \tilde{D} \end{pmatrix} \begin{pmatrix} A^{g-2} & A^{g-3}B & A^{g-4}B & \cdots & AB & B & 0 \\ C & D & 0 & \cdots & 0 & 0 & 0 \\ CA & CB & D & \cdots & 0 & 0 & 0 \\ \vdots & \vdots & \vdots & \ddots & \vdots & \vdots & \vdots \\ CA^{g-3} & CA^{g-4}B & CA^{g-5}B & \cdots & CB & D & 0 \\ 0 & 0 & 0 & 0 & 0 & 0 & I \end{pmatrix},$$

which multiplies to give

$$M_\mu = \begin{pmatrix} \tilde{A}A^{g-2} & \tilde{A}A^{g-3}B & \tilde{A}A^{g-4}B & \cdots & \tilde{A}AB & \tilde{A}B & \tilde{B} \\ C & D & 0 & \cdots & 0 & 0 & 0 \\ CA & CB & D & \cdots & 0 & 0 & 0 \\ \vdots & \vdots & \vdots & \ddots & \vdots & \vdots & \vdots \\ CA^{g-3} & CA^{g-4}B & CA^{g-5}B & \cdots & CB & D & 0 \\ \tilde{C}A^{g-2} & \tilde{C}A^{g-3}B & \tilde{C}A^{g-4}B & \cdots & \tilde{C}AB & \tilde{C}B & \tilde{D} \end{pmatrix}.$$

As before, one may show that  $M_\mu$  is Perron–Frobenius by checking that the first row and first column of  $M_\mu^3$  have strictly positive entries. Lemma 3.1 then implies that the dilatation of  $\mathcal{P}(\mu)$  is bounded above by the sum of the entries in the largest row of  $M_\mu$ , which is evidently the first. Making use of (5.5), we see that the first row of  $\tilde{A}A^j$  has sum  $(6n+11)(11^j+10q(j)+1)$  and that the first row of  $\tilde{A}A^jB$  sums to  $(6n+11)(20q(j+1)+2)$ . Since the first row of  $\tilde{B}$  sums to  $57n+20$ , we find that the first row of  $M_\mu$  has total sum

$$\begin{aligned} & (6n+11)(11^{g-2}+10q(g-2)+1) + (57n+20) + \sum_{j=1}^{g-2} (6n+11)(20q(j)+2) \\ & \leq (57n+20) + (6n+11) \left[ 11^{g-2} + 11^{g-2} + 1 + \left( \sum_{j=1}^{g-2} 2 \cdot 11^j \right) + 2(g-2) \right] \\ & \leq (57n+10n) + (6n+6n) \left[ 2(11^{g-2}) + 2 \left( \frac{11^{g-1}-1}{11-1} - 1 \right) + 2g-3 \right] \\ & \leq (67n) + (12n) \left[ \frac{2}{11}11^{g-1} + \frac{2}{10}11^{g-1} + \frac{2}{11}11^{g-1} \right] \\ & \leq (11^{g-1}n) + (12n) \left[ \frac{3}{5}11^{g-1} \right] \\ & < n11^g. \end{aligned}$$

Since  $i(\mu) = 3(g-1) + n \geq n$ , it follows that  $\lambda_\mu < i(\mu)11^g$ . This construction shows that for each  $k \geq 3g-1$  in the statement of Theorem 1.12, we may take  $n = k - 3(g-1) \geq 2$  and

produce a filling curve  $\mu \subset S_g$  with  $i(\mu) = k$  whose corresponding mapping class  $\mathcal{P}(\mu)$  has dilatation at most  $k11^g$ . Since  $\mathcal{P}(\mu) \in \text{PP}_k(S_g)$  this shows that

$$L(\text{PP}_k(S_g)) < \log(k) + g \log(11)$$

and completes the proof of Theorem 1.12. □

## References

- [AY] Pierre Arnoux and Jean-Christophe Yoccoz. Construction de difféomorphismes pseudo-Anosov. *C. R. Acad. Sci. Paris Sér. I Math.*, 292(1):75–78, 1981.
- [Ber] Lipman Bers. An extremal problem for quasiconformal mappings and a theorem by Thurston. *Acta Math.*, 141(1-2):73–98, 1978.
- [BH] M. Bestvina and M. Handel. Train-tracks for surface homeomorphisms. *Topology*, 34(1):109–140, 1995.
- [Bir] Joan S. Birman. *Braids, links, and mapping class groups*. Princeton University Press, Princeton, N.J., 1974. Annals of Mathematics Studies, No. 82.
- [FLM] Benson Farb, Christopher J. Leininger, and Dan Margalit. The lower central series and pseudo-Anosov dilatations. *Amer. J. Math.*, 130(3):799–827, 2008.
- [FLP] Albert Fathi, François Laudenbach, and Valentin Poénaru. *Travaux de Thurston sur les surfaces*, volume 66 of *Astérisque*. Société Mathématique de France, Paris, 1979. Séminaire Orsay, With an English summary.
- [FM] Benson Farb and Dan Margalit. *A Primer on mapping class groups*. To appear in Princeton Mathematical Series. Princeton Univ. Press, 2009. Version 3.1. <http://www.math.utah.edu/~margalit/primer/>.
- [Gan] F. R. Gantmacher. *The theory of matrices. Vol. 2*. Translated by K. A. Hirsch. Chelsea Publishing Co., New York, 1959.
- [Hir] Eriko Hironaka. Small dilatation pseudo-anosov mapping classes coming from the simplest hyperbolic braid, 2009. Preprint arXiv:0909.4517.
- [Iva] N. V. Ivanov. Coefficients of expansion of pseudo-Anosov homeomorphisms. *Zap. Nauchn. Sem. Leningrad. Otdel. Mat. Inst. Steklov. (LOMI)*, 167(Issled. Topol. 6):111–116, 191, 1988.
- [Kra] Irwin Kra. On the Nielsen-Thurston-Bers type of some self-maps of Riemann surfaces. *Acta Math.*, 146(3-4):231–270, 1981.
- [LT] Erwan Lanneau and Jean-Luc Thiffeault. On the minimum dilatation of pseudo-anosov homeomorphisms on surfaces of small genus, 2009. Preprint arXiv:0905.1302.

- [Mos] Lee Mosher. Train track expansions of measured foliations, 2003. In preparation. [http://andromeda.rutgers.edu/~mosher/arationality\\_03\\_12\\_28.pdf](http://andromeda.rutgers.edu/~mosher/arationality_03_12_28.pdf).
- [MP] Justin Malestein and Andrew Putman. On the self-intersections of curves deep in the lower central series of a surface group, 2009. Preprint arXiv:0901.2561.
- [Pen1] R. C. Penner. Bounds on least dilatations. *Proc. Amer. Math. Soc.*, 113(2):443–450, 1991.
- [Pen2] Robert C. Penner. A construction of pseudo-Anosov homeomorphisms. *Trans. Amer. Math. Soc.*, 310(1):179–197, 1988.
- [PH] R. C. Penner and J. L. Harer. *Combinatorics of train tracks*, volume 125 of *Annals of Mathematics Studies*. Princeton University Press, Princeton, NJ, 1992.
- [PP] Athanase Papadopoulos and Robert C. Penner. A characterization of pseudo-Anosov foliations. *Pacific J. Math.*, 130(2):359–377, 1987.
- [SW] Peter Scott and Terry Wall. Topological methods in group theory. In *Homological group theory (Proc. Sympos., Durham, 1977)*, volume 36 of *London Math. Soc. Lecture Note Ser.*, pages 137–203. Cambridge Univ. Press, Cambridge, 1979.
- [Thu] William P. Thurston. On the geometry and dynamics of diffeomorphisms of surfaces. *Bull. Amer. Math. Soc. (N.S.)*, 19(2):417–431, 1988.

Department of Mathematics  
University of Chicago  
5734 University Ave.  
Chicago, IL 60637  
E-mail: [sdowdall@math.uchicago.edu](mailto:sdowdall@math.uchicago.edu)